Maria Fernanda Colo Giannini

The influence of phytoplankton pigments composition and dominant cell size on fluorescence-derived photo-physiological parameters and implications for primary production rates

Thesis submitted to the Oceanographic Institute of the University of São Paulo as partial fulfillment of the requirements for the degree of Doctor of Science in Oceanography, area of Biological Oceanography

Supervisor: Prof[a] Dr[a] Aurea Maria Ciotti

SÃO PAULO
2016

University of São Paulo

Oceanographic Institute

The influence of phytoplankton pigments composition and dominant cell size on fluorescence-derived photo-physiological parameters and implications for primary production rates

Maria Fernanda Colo Giannini

Thesis submitted to the Oceanographic Institute of the University of São Paulo as partial fulfillment of the requirements for the degree of Doctor of Science in Oceanography, area of Biological Oceanography

(Versão corrigida)

Evaluated in ____/____/____

_____	_____
Prof(a). Dr(a).	Grade
_____	_____
Prof(a). Dr(a).	Grade
_____	_____
Prof(a). Dr(a).	Grade
_____	_____
Prof(a). Dr(a).	Grade
_____	_____
Prof(a). Dr(a).	Grade

Table of contents

Acknowledgements

Firstly, I would like to thank FAPESP (Fundação de Amparo à Pesquisa do Estado de São Paulo) for funding most of this study and for being an important research supporter in Brazil. Also, I want to thank CAPES (Coordenação de Aperfeiçoamento de Pessoal de Nível Superior) for the scholarship provided during the first year of this study.

I would like to express my special thanks to my supervisor and excellent scientist, Drª Aurea Ciotti, who has been mentoring and guiding my academic steps for several years, without hesitating to share her extensive knowledge and expertise, besides offering her sincere friendship and support during this long journey. I am forever grateful for all your dedication in this important stage of my career.

I want to enormously thank the technician staff of CEBIMar, especially Zeilto e Elso, without their help and especially their everyday happiness, this study would not have the same success. In the same manner, the academic and administration staff support was great and essential for the good and smooth progress of this project.

I would like to thank my wonderful labmates and friends from Laboratório Aquarela, Amabile, Camilla, Deborah, André, Bianca, Ana Carolina, Alexandre, Ana Luiza and Carla, for the invaluable help during field work, laboratorial analysis, scientific discussions, strong motivational support or simply for holding my stress during the final and hardest period of the doctorate, I can not imagine better labmates! I also express my enourmous gratitude to other friends from São Sebastião, specially to my lovely housemates Mariana, Katia e Paula, who were the main people to help me keeping my mental and psicological health, always cheering my days up. You girls are simply amazing!

My sincere thanks also goes to Dr. David Suggett, who provided me an opportunity to join his team as intern, and who gave access to the laboratory and research

facilities. His support was precious to successfully conclude this research. I thank also his team (David, Caitlin, Sam, Lisa and Max) and other dear friends from University of Technology (Sydney), Marco, Rendy, Tonantzin, Paloma, Ann Marie and Rachel.

I am very grateful for the help of my lovely family, especially my mom, dad and my brother, who are the most importante people for me and that have been the biggest supporters of my choices. I want to thank them especially for understanding my absence most of the time during the period of my PhD, being always present even by far. Also I want to express a great thank to my cousins Lari e Me for all the love, and for their design skills and help.

Abstract

Phytoplankton chlorophyll-a fluorescence, measured *in situ*, can be applied as a tool to estimate primary production in the ocean over a large range of temporal and spatial scales. This non-invasive technique allows for fast assessments of photo-physiological parameters in contrast to the traditional methodologies (^{14}C uptake and O_2 evolution). The main photo-physiological parameters derived by the available instruments are yields, and as such, require careful interpretation. The comprehension of the main sources of variability of the photochemical and the light absorption efficiencies in marine phytoplankton has increased in the past years, largely by studies using monospecific cultures. In natural communities, however, the development of primary production models based on chlorophyll-a fluorescence remain limited as they are simultaneously subjected to a wide range of environmental and biological factors. This study will test the hypothesis that photo-physiological models for primary production estimates can be improved when key phytoplankton features, such as the pigments composition and dominant cell size, are taking into account. The approach was to contrast the photo-physiological parameters derived from measurements in distinct oceanographic regions, as well as those derived in a specific environment with presented different nutrient concentration according to the time of sampling. In addition, we showed for monospecific cultures, how the photo-physiological parameters are quantitatively related to the production of carbon under the interactive effects of taxonomic composition and cell size. The proportions of photosynthetic and photoprotective pigments present in the communitywere related to the bulk photochemical efficiency and the cross-section of light absorption, but varied among oceanographic regionsand the depthof the water column. A parameterization of fluorescence-derived primary production rates, using four dominant size classes, was derived for natural phytoplankton communities under different nutrients conditions in a coastal environment, showing that the parameters differed among size classes above a threshold of nutrient concentration. The direct conversion rates between fluorescence-derived primary production and carbon assimilation rates, computed for two distinct phytoplankton cell sizes grown in controlled laboratorial conditions, showed that cell size strongly influences the efficiency of light absorption and photochemistry, however species-specific responses in photosynthetic energy allocation dominated the differences observed in how absorbed light is utilized to carbon assimilation, i.e., in the electron requirements for carbon assimilation. The results highlighted the importance of the tight coupling of nutrients availability and phytoplankton communities, as well as for measurements of chlorophyll-a fluorescence in the ocean and primary production models. This work presents a novel contribution to the increasing efforts to apply fluorescence-based techniques to understand and parameterize primary production estimates in marine systems, especially at highly dynamic environments.

Key-words: Chlorophyll-a fluorescence; Phytoplankton photosynthesis; Photosystem II (PSII) efficiency; Primary production

Resumo (Português)

A fluorescência da clorofila-a do fitoplâncton, medida *in situ*, pode ser uma ferramenta para estimar produção primária no oceano em grande escala temporal e espacial. Esta técnica não-invasiva permite análises rápidas de parâmetros foto-fisiológicos ao contrário de metodologias tradicionais (assimilação de ^{14}C e produção de O_2). Os principais parâmetros foto-fisiológicos de instrumentos disponíveis hoje tratam-se de eficiências, e como tal, requerem cuidados em serem interpretados. A compreensão das principais fontes de variabilidade da eficiência fotoquímica e de absorção de luz no fitoplâncton marinho tem aumentado nos últimos anos, em sua maioria em cultivos monoespecíficos. Em comunidades naturais, entretanto, o desenvolvimento de modelos de produção primária baseados na fluorescência da clorofila-a ainda é limitado uma vez que estão sujeitos à uma ampla gama de fatores ambientais e biológicos. Esse estudo testa a hipótese de que modelos foto-fisiológicos para estimar produção primária podem ser aprimorados considerando-se características fundamentais do fitoplâncton, como a composição de pigmentos e tamanho celular dominante. A estratégia foi contrastar parâmetros foto-fisiológicos derivados de medidas em regiões oceanográficas distintas, assim como medidas em um ambiente específico com diferentes concentrações de nutrientes ao longo do período amostrado. Adicionalmente, apresentamos através de cultivos monoespecíficos, como parâmetros foto-fisiológicos são quantitativamente relacionados à produção de carbono e os efeitos interativos da composição taxonômica e tamanho celular nessa relação. A proporção de pigmentos fotossintéticos e fotoprotetores da comunidade foram relacionados à eficiência fotoquímica e seção transversal de absorção de luz, porém variaram de acordo com a região oceanográfica e profundidade na coluna d'água. Uma parameterização de taxas de produção primária derivadas da fluorescência, usando quatro classes de tamanho dominantes, foi proposta para comunidades naturais de fitoplâncton sob condições de nutrientes diferentes em um ambiente costeiro, mostrando que os parâmetros diferiram entre as classes de tamanho acima de um limiar de concentração de nutrientes. As taxas de conversão diretas entre produção primária derivada da fluorescência e taxas de assimilação de carbono, computadas para dois tamanhos de fitoplâncton crescidos em condições controladas em laboratório, mostraram que tamanho celular influencia as eficiências de absorção de luz e fotoquímica, porém respostas espécie-específicas na alocação de energia fotossintética dominaram as diferenças observadas em como a luz absorvida é utilizada para assimilação de carbono, ou seja, na razão de elétrons exigidos para assimilação de carbono. Os resultados destacam a importância do acoplamento da disponibilidade de nutrientes com a comunidade fitoplanctônica, assim como das medidas de fluorescência da clorofila-a no oceano e nos modelos de produção primária. Este trabalho apresenta uma contribuição inédita nos esforços crescentes em aplicar técnicas baseadas na fluorescência para entender e parameterizar estimativas de produção primária nos sistemas marinhos, especialmente em ambientes altamente dinâmicos.

Palavras-chave: Fluorescência da clorofila-a; Fotossíntese; Eficiência do fotossistema II (PSII); Produção primária

List of Figures

Chapter 1

Chapter 2

Chapter 3

Chapter 4

List of Tables

Chapter 2

Chapter 3

Chapter 4

List of symbols and acronyms

Symbols or Acronyms	Description
RC	Reaction Center
RCI, RCII	Reaction Centers I and II
PSI, PSII	Photosystems I and II
LHCII:	Light Harvesting Complex II
Q_A	Quinone A
GPP	Gross Primary Production
NPP	Net Primary Production
DCM	Deep chlorophyll maximum
$Ø_H$	Quantum yield of energy dissipation
$Ø_P$	Quantum yield of photosynthesis
$Ø_F$	Quantum yield of fluorescence
qP	Photochemical quenching
NPQ	Non-photochemical quenching
F_0	Basal or Minimal fluorescence
F_m	Maximal fluorescence
Φ_{PSII}^{max}; F_v/F_m	Maximal photosynthetic efficiency
σ_{PSII}	Functional absorption cross-section of PSII
Φ_{PSII}'; F_q'/F_m'	Effective photosynthetic efficiency
Φ_{RC}	Quantum yield of electron transfer (=1)
ETR	Electron transfer rates
ETR^{vol}	ETR per cell unit volume
Ek	Light saturation parameter
α_{ETR}	Light utilization efficiency
PSC	Total Photosynthetic Carotenoids
PPC	Total Photoprotective Carotenoids
$S_{(f)}$	Size factor based on absorption spectra (Ciotti et al 2002)
f_pico	Small size fraction of phytoplankton (Uitz et al 2006)
ΣAP	Total accessory pigments
$\overline{SI(chl)}$	Community size index based on fractionated chlorophyll
n_{PSII}	Number of functional reaction centers
PSU	Photosystem size unit
a_{ph}	Phytoplankton absorption coefficient
a^{chl}_{ph}	Chlorophyll-a specific absorption coefficient
OD	Optical density
POC	Particulate organic carbon
PON	Particulate organic nitrogen
K_C; ϕe:c	Electron requirement for carbon fixation
JVPSII	Volume-based ETR

CHAPTER 1

General Introduction

1. Methods for estimating primary production in the oceans

Primary production rates by the marine phytoplankton provide CO_2 fixation, O_2 production and the synthesis of organic matter through the photosynthetic process (Falkowski and Raven 2007) for the largest portion of the global marine environments (Field et al. 1998; Longhurst 1998). In its simplest formulation, the photosynthesis can be described as:

$$H_2O + CO_2 + \text{light (photons)} \rightarrow CH_2O \text{ (organic matter)} + O_2$$

where light is absorbed by the photosynthetic pigments in the light harvesting antenna complex of phytoplankton cells which is then directed to the chlorophyll-a molecules present on the reaction centers (RC) of photosystem II (PSII). The efficiency with which the light energy is absorbed and directed to the photosynthetic process depend on a number of environmental constrains, such as nutritional and physiological states of the cells (Cleveland et al. 1989; Geider et al. 1993), irradiance fields (Long et al. 1994; Oxborough and Baker 2000) and water temperature (Kiefer and Mitchell 1983).

O_2 evolution and CO_2 fixation are described as the end products of photosynthesis are the most common methods to quantify primary production rates, both representing different biochemical reactions although tightly coupled (Ryther 1956; Williams & Jenkinson 1982; Bender et al. 1987; Laws 1991) and are to date the most common methods to measure primary production. Other methods to quantify the end products of photosynthesis have been applied, based on stable isotope additions, using the labelled ^{13}C and ^{18}O as tracers (see Regaudie-de-Gioux et al. 2014). The

different methods and measurement protocols, such as incubation time, will provide rates of gross or net primary production. The gross primary production (GPP) is the total photosynthesis, while the net production (NPP) is the total photosynthesis minus the respiration rates.

The standard method to estimate primary production in the ocean is to measure the uptake of radioactive ^{14}C (Steeman-Nielsen 1952), which is sensitive in areas where phytoplankton biomass is low, especially in the open oceans. Oxygen production methods are less sensitive and require longer incubations (Bender et al. 1999) but can differentiate GPP from NPP, while ^{14}C uptake estimates GPP or something in between GPP and NPP, depending on incubation time. However, both the ^{14}C uptake and the O_2 production methods require incubation of samples for a certain period of time, generating methodological constraints driven by confinement of the samples in containers and consequently, alterations in the microorganisms composition and in the physiological status of phytoplankton (Eppley 1980; Bender et al. 1987; Grande et al. 1989; Marra 2002). Samples contamination by trace metals can be another issue, mainly associated with ^{14}C stock solutions and the surfaces of the containers (Fitzwater et al. 1982). Furthermore, there are still limitations regarding the results analysis, mostly associated with the uncertainties in the respiration and other metabolic rates (Bender et al. 1999; Williams et al. 2002). The respiration during incubation periods can effectively recycle fixed CO_2 depending on the incubation time, thus preventing the accurate discrimination of gross from net primary production rates (Marra 2002; Regaudie-de-Gioux et al. 2014).

2. Fluorescence-derived primary production

To overcome some of the challenges associated with conventional measurements of primary production rates in the oceans, non-invasive techniques

(incubation-free) based on variations in the active fluorescence of chlorophyll-a have been developed (Kolber & Falkowski, 1993). The active fluorescence method quantifies the fluorescence emission by PSII during the photosynthetic process (Genty et al. 1989; Falkowski et al. 1986).

The photosynthetic apparatus in marine phytoplankton is composed of two photosynthetic units (PSI and PSII) distributed in the thylakoid membrane, inside the chloroplasts of the photosynthetic organisms (Figure 1). These units are responsible for the photochemical reactions that fix the carbon and oxidize the water molecules to produce the oxygen. These reactions are linked to the transference of electrons.

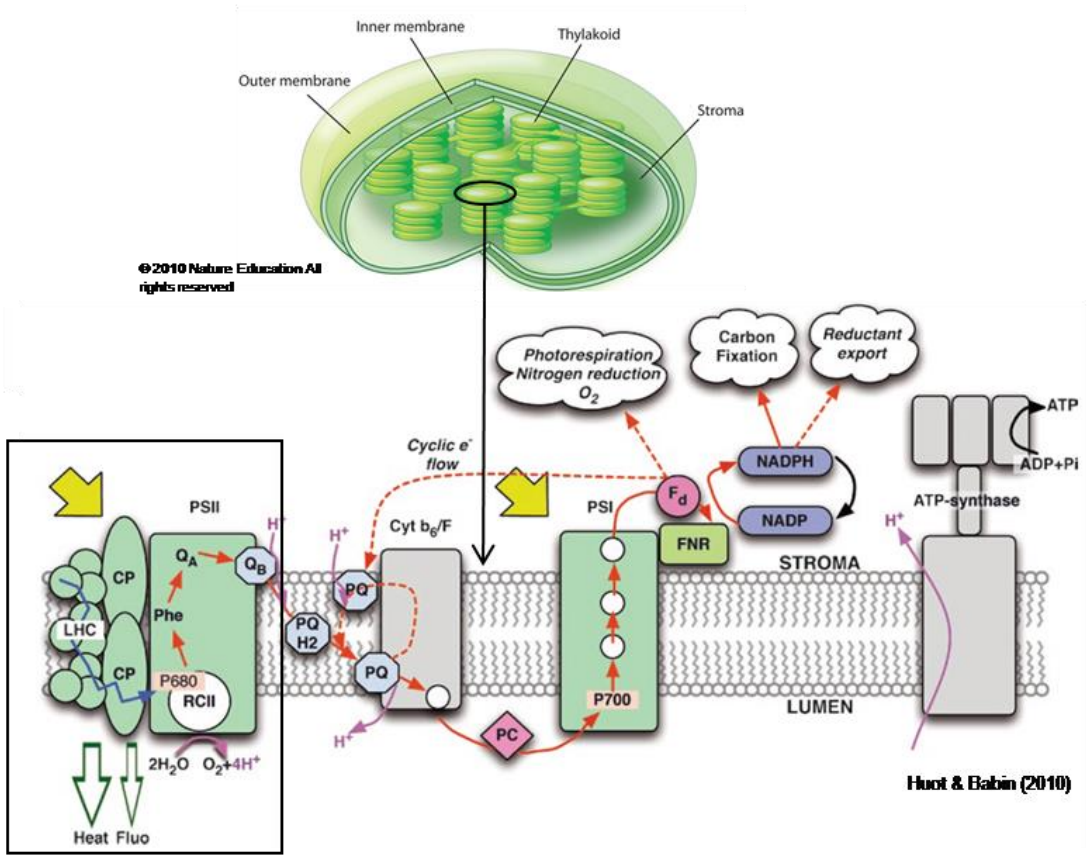

Figure 1. Distribution of thylakoids inside the chloroplasts (above) highlighting the photosynthetic chain occuring in the membrane of the thylakoids (below). The black retangle indicates the PSII associated with the light harvesting antenna complex and the reactions centers (RCII), where the initial step of the electron transport chain occurs. The yellow arrows indicate where the light is absorbed by the thylakoids membrane and the red arrows are the pathways of the electron during the photosynthetic chain until the energy generation for the CO2 fixation at the Calvin cycle. More details of the reactions are in the text (Figure adapted from Huot and Babin 2010).

The PSII contain the light harvesting complex (LHCII), which are antenna pigment complexes, and the reaction centers (RCII), which is composed of a core complex of proteins and chlorophylls and it is where the first step of electron transfer occurs. When the chlorophyll-a molecules of the RCII receive the energy from light absorption, an electron is donated to a primary electron acceptor, the Quinone A (Q_A) molecule, where the linear electron flow begins (see red arrows in Figure 1).

The linear electron flow generates a proton gradient (H^+) between the exterior of the thylakoid (stroma) and the interior of the thylakoid (lumen), through a series of reduction and oxidation reactions. The H^+ gradient across the thylakoid membrane is responsible for generating energy (ATP), through the ATP-synthase, also part of the thylakoid membrane (Figure 1). Further in the photosynthetic chain, the PSI is responsible for donating the electron to the end electron acceptor (ferrodoxin – Fd) that with the ferrodoxin-NADP reductase (FNR) reduces NADP to NADPH. The ATP and NADPH produced are energy sources to the carbon fixation in the Calvin cycle.

When a chlorophyll-a molecule in the antenna pigments complex absorbs photons, magnesium (Mg) atoms of the chlorophyll are excited from a lower (ground) to a higher (excited) energy state. When the chlorophyll-a molecule returns to its ground state, the energy released has two possible pathways (Figure 2): i. dissipation by heat, ii. transfer by inductive resonance to the adjacent molecules towards the reaction centers to be directed to the photochemical process and iii. re-emission of photons by a process called as fluorescence (Falkowski and Raven 2007; Govindjee 2004). The proportions of absorbed photons that are directed to each of the three competing pathways are represented by the quantum yield of energy dissipation ($Ø_H$), photosynthesis ($Ø_P$) and fluorescence ($Ø_F$), respectively (Figure 2a). The quantum yields are, thus, directly related to the probability of the three distinct processes to occur (Govindjee 1995;

Papageorgiou and Govindjee 2004). When the energy is directed to the photosynthetic activity, the fluorescence is reduced by the so-called photochemical quenching (qP), while the non-photochemical quenching (NPQ) refers to the energy dissipation by heat.

Assuming the quantum yields for energy dissipation as constant, the quantum yields for photosynthesis and fluorescence will be high and low, respectively, in darkness or very low light, as the PSII molecules are open and available to receive photons (Figure 2b). As light intensity increases, the Q_A molecules become reduced and the PSII close accordingly, increasing the quantum yields of fluorescence. When all the PSII are closed, the subsequent photons absorbed are then re-emitted as fluorescence, until a maximum fluorescence quantum yield is reached (Figure 2c). Note that the dissipation by heat has to be considered constant for this simple model to work. However, the relationship between chlorophyll fluorescence and photochemistry becomes non-linear as a suite of heat losses mechanisms will come into play when cells are exposed to high light (Papageorgiou and Govindjee 2004; Lin et al. 2016).

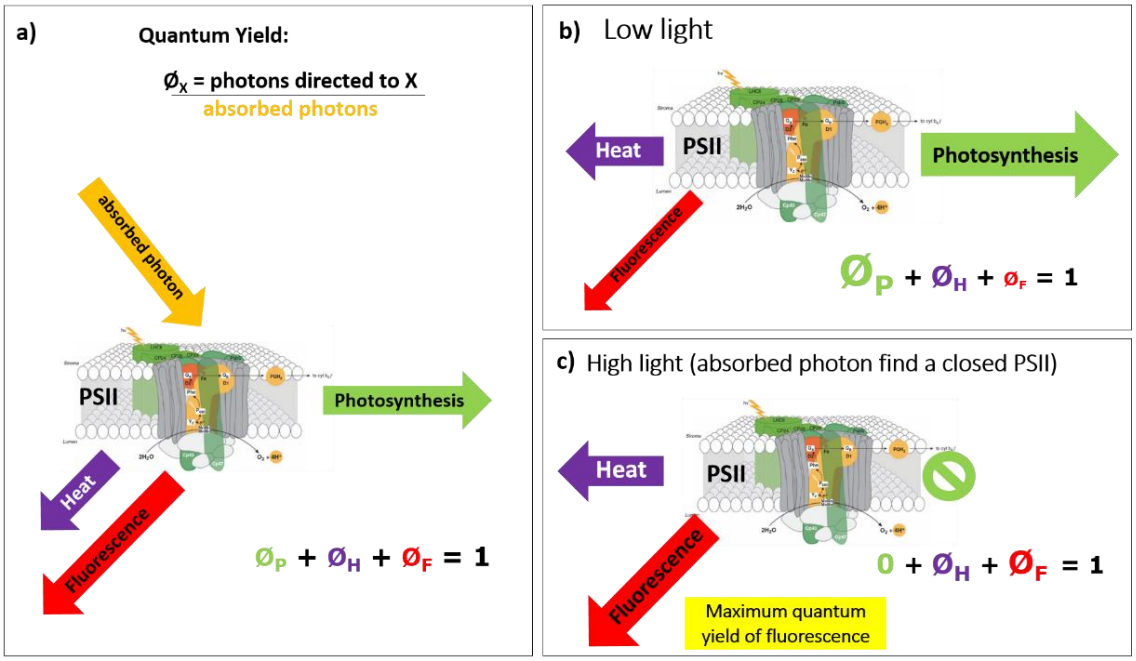

Figure 2. Three competing pathways of the absorbed photons by the PSII: photosynthesis ($Ø_P$), fluorescence ($Ø_F$) and heat dissipation ($Ø_H$). a) the probability of a photon to be directed to each of the paths are the same; b) the probability of a photon to be directed to photosynthesis is higher, due to the low light or dark-acclimation of the cells and c) the probability of fluorescence increases as light increases until all the PSII are closed (no photosynthesis) and the fluorescence are maximal. The arrows thickness is proportional to the relative contribution of each process.

The simple model of competing quantum yields assumes that the fluorescence quantum yield, or fluorescence efficiency, varies inversely to the photochemical efficiency, depending on the proportion of open reactions centers (Kiefer and Reynolds 1992), defined as the fluorescence path dynamics. Therefore, changes in fluorescence quantum yields provide information on the photosynthetic process (Kolber and Falkowski 1993), and that is the principle applied in the available commercial fluorometers. The instruments are designed to measuring the fluorescence from PSII derived from the induction of a maximal fluorescence and provide photo-physiological parameters that are related to the proportion of "closed" reaction centers during photosynthesis (Kolber and Falkowski, 1993; Suggett et al. 2003; Oxborough et al. 2012).

The fluorescence technique uses the emission of a saturating light (usually in the blue wavelength) that is strong enough to promote the variable fluorescence in a

time scale of μs, reducing all Q_A, thus saturating the photochemical path and promoting the maximal fluorescence. In darkness, when all the PSII are open and available to conduct photons to the photosynthesis, the fluorescence emitted by these molecules is minimal or basal, which is represented by F_0. As incident light increases, the fluorescence increases up to a maximum value, designated F_m, when all the PSII are closed. The variable fluorescence (F_v) is the difference between F_m and F_0 ($F_v = F_m - F_0$) and the ratio F_v/F_m is a measurement of how efficient the cells saturate the photochemical capacity and reaches the maximal fluorescence yield (Lazar 1999; Maxwell and Johnson, 2000). In ambient light, the ratio between F_v and F_m is defined as the effective photochemical efficiency (or F_q'/F_m'), and will be smaller than the maximum observed in cells dark-acclimated samples, as the pool of open PSII to receive photons is smaller. Other parameter that is derived from the variable fluorescence methods is related to the efficiency to which the energy captured by incident light is converted to electron transfer process in PSII, defined as the functional absorption cross-section of PSII (σ_{PSII}) (Kolber and Falkowski 1993).

The Kolber and Falkowski (1993) model estimates the electron transfer rate (ETR) in phytoplankton cells, which is considered as an alternative tool to estimate primary production in aquatic environments (Suggett et al. 2010). A detailed explanation of how ETR is calculated from photo-physiological parameters, and how it relates to carbon fixation and primary production rates, will be given in chapters 3 and 4 of this document. The most commonly used active fluorometers in oceanography are single turnover Fast Repetition Rate-type fluorometer (FRRf) (Kolber et al. 1998), and their derivatives, such as the Fluorescence Induction and Relaxation System (FIRe) (Gorbunov and Falkowski 2005). The protocols for exciting and measuring variable fluorescence are distinct among instruments, however they provide very similar photo-

physiological responses. The correct interpretation of the results provided by the different instruments and protocols are not straightforward and deserve caution (Huot and Babin 2010). A number of studies are still required before variable fluorescence techniques become the standard primary production methods in the oceans, especially for natural phytoplankton communities.

3. Hypothesis and goals

The present work is based on the general hypothesis that the photo-physiological model for primary production estimates can be parameterized and improved considering key phytoplankton features. Considering that the environmental conditions impose a large impact on the phytoplankton communities and thus in the photo-physiology, this work comprises a large dataset with contrasting oceanographic regimes. The central objective was then to contribute for a better understanding of the chlorophyll-a fluorescence technique and its main sources of variation, as well as to propose parameterizations according to the phytoplankton community structure, such as cell size classes and their pigments composition. In addition, we have shown how the variable fluorescence can be converted in carbon-based primary production estimates, and the interactive effects of taxonomy and cell size on this conversion. Thus, the specific objectives were approached in the following chapters:

Chapter 2: To describe the photo-physiological parameters (F_v/F_m and σ_{PSII}) of natural phytoplankton communities across distinct oceanographic regimes and trophic status at a large portion of the subtropical Atlantic Ocean, with emphasis on the relationships between such photo-physiological parameters and the pigment ratios of the phytoplankton community. We hypothesize that the use of pigments ratios would significantly improve the description and interpretation of F_v/F_m and σ_{PSII} across different oceanographic regimes as these ratios represent not only biomass and

taxonomy, but also the interactions among taxonomy and acclimation processes, which will reflect in the bulk signal of the community photo-physiology.

Chapter 3: to examine the relationship between the dominant size of natural phytoplankton communities and variability of photo-physiological parameters, i.e. F_v/F_m and σ_{PSII}, simultaneously considering different ambient nutrients conditions. The sampling design allowed discrimination of the effects of different levels of nutrient availability from cell size on the parameterization of fluorimetric photo-physiology models.

Chapter 4: to examine for the first time whether cell size influences photo-physiological performance and light harvesting properties, specifically the direct comparison of ETR and carbon fixation, as well as allocation of inorganic assimilated carbon into organic cell compounds, testing the consistency across different phytoplankton taxonomical groups with well-documented differences in photosynthetic physiology.

CHAPTER 2

Relationships between photophysiological fluorescence-derived parameters and the composition of phytoplankton pigments observed in distinct oceanographic processes in the subtropical South Atlantic

1. Introduction

In the ocean, phytoplankton growth responds to a large dynamic range of limitation by resources (Falkowski 1994) and biological interactions that are, at first order, governed by the dynamics of the environment (Cullen et al. 2002). Oceanic processes of varied temporal and spatial scales determine light and nutrient availability that not only alter phytoplankton abundances and species composition but also control their activities and consequently role on biogeochemical cycles (Gargett and Marra 2002). Over the scales of main oceanographic processes, therefore, it is of equal importance to measure the variability of phytoplankton abundances (Longhurst et al. 1995) and their photosynthetic performances (Huot et al. 2007a).

Spatial and temporal variability of phytoplankton abundance can be inferred from satellite images derived from ocean color sensors over large horizontal scales (O'Reilly et al. 1998), while small-scale variability of phytoplankton abundance is usually estimated by simple fluorimeters (Lorenzen 1966). Both ocean color and fluorimetric approaches easily estimate chlorophyll concentrations as a proxy for phytoplankton abundance, which despite of its important prediction power for photosynthetic parameters (Huot et al. 2007b) cannot account alone for primary production rates, especially over large scales (e.g., Saba et al. 2011). Primary production classic techniques are expensive and time-consuming limiting, thus, temporal and spatial coverage (see Regaudie-de-Gioux et al. 2014).

Instruments that provide near-real time estimates of photosynthetic performance of natural phytoplankton communities have been available for many years. These non-invasive techniques are based on measurements of variable fluorescence and its relationship with the electrons transfer rates (ETR, with units of mol e^- $(molPSII)^{-1}$ h^{-1}, where PSII is the photosystem unit of the cells), during the photosynthesis (Kolber and Falkowski 1993). Key parameters derived from variable fluorescence measurements include the maximal photochemical efficiency (F_v/F_m), directly related with the photosynthetic performance, and the functional absorption cross-section (σ_{PSII}), which is a function of the light harvesting efficiency and utilization by the bulk phytoplankton community. However, the complexity of fluorescence by phytoplankton (Lazár 1999) in addition to the different protocols available (Huot and Babin 2010), makes the interpretation of results derived from variable fluorescence far from straightforward (Suggett et al. 2010). It is important to note that variable fluorescence originates almost exclusively from the chlorophyll molecules present in the photosystems.

When the variable fluoresce technique is applied to phytoplankton cultures grown in laboratory, the observed values for F_v/F_m and σ_{PSII} have been associated with taxonomic composition, cell size (Suggett et al. 2009) and modes of nutrient supply (Parkhill et al. 2001). In natural phytoplankton communities, F_v/F_m and σ_{PSII} also vary with taxonomic composition and cell size but can also respond strongly to photo-acclimation and photo-adaptation (Moore et al. 2006), especially in nutrient-limited environments (Moore et al. 2008; Suggett et al. 2009). Because of that, the relationships between the photo-physiological parameters and natural communities may also vary remarkably with depth. A common observed feature in stratified oceans is the deep chlorophyll maximum (DCM) layer, which is maintained by a number of distinct processes that range from enhanced growth driven by nutrients to selection of photo-

adapted and photo-aclimated populations, from eutrophic to oligotrophic environments respectively (Cullen 2015). Thus, the photo-physiological parameters of distinct phytoplankton communities are expected to vary between surface and the DCM, but not predictably across a range of trophic status.

For a given oceanographic process that provide a gradient of nutrient supply, and therefore, a gradient of trophic status composed of different phytoplankton communities (see discussion in Ciotti et al. 1999), we hypothesized that observed values of F_v/F_m and σ_{PSII} will resemble that presented by Suggett et al. (2009), with F_v/F_m increasing from oligotrophic to eutrophic areas, while σ_{PSII} decreases, as communities will change dominance from small to larger cells. These gradient of cell size is expected to alter the efficiency for light absorption as well (Ciotti et al. 2002), which will tend to decrease with increasing cell size. Ciotti et al. (in preparation) have shown that the variability observed in pigment packaging at the surface is much higher than that observed in the DCM across large trophic gradients in the Atlantic and Pacific.

There are no universal metrics for a given phytoplankton community and common approaches simplify the taxonomy of natural communities according with dominance of major groups given by either microscopy-cytometry or pigment profiles. A selection of diagnostic marker pigments (Claustre 1994) can be used to indicate major taxonomical groups present (Mackey 1996, Jeffrey et al. 2011) or to assign dominance of phytoplankton size fractions (e.g. Vidussi et al. 2001; Uitz et al. 2006). Indeed, when present in substantial proportions, a diagnostic pigment provides a robust tool indicating the presence of a given taxonomic group. However, some of the pigments excluded from these procedures could help to explain the variability observed in photophysiological parameters.

In ocean, where phytoplankton are subject to highly dynamic environmental conditions, the taxonomical classification from pigments into specific groups might be precluded by the variability of cellular pigment proportions as a response of physiological state (Henriksen et al. 2002). Pigments concentration, and especially their proportion to chlorophyll-a concentration, may indicate nutrient-limited growth (Goerick and Montoya 1998; Henriksen et al. 2002) and photoacclimation processes (Macintyre et al. 2002). Detection of chlorophyll-a degradation products can also be used as bulk physiological index, such as the proportion of chlorophyllide originated from senescence (Jefrey 1974, Wright et al. 2010), but no information of the extent to which F_v/F_m and σ_{PSII} can be explained by phytoplankton pigment composition, without a priori classification into specific taxonomic groups, is available. We hypothesize that the use of pigments ratios would significantly improve the description and interpretation of F_v/F_m and σ_{PSII} across different oceanographic regimes as these ratios represent not only biomass and taxonomy, but also the interactions among taxonomy and acclimation processes, which will reflect in the bulk signal of the community photo-physiology.

The objectives of the present work are characterizing the photo-physiology of phytoplankton communities using chlorophyll-a fluorescence-derived parameters (F_v/F_m and σ_{PSII}) in different oceanographic processes of the subtropical South Atlantic Ocean, contrasting the observations from surface and from DCM. The photo-physiological parameters were related to pigment ratios across distinct oceanographic regimes and trophic status. The relationships found between photo-physiology and individual pigments were compared to those observed between other physiological indexes, based on pigments, such as the sum of total photosynthetic (PSC) and photo-protective carotenoids (PPC) (Barlow et al. 2002), size fractions in the community (Uitz et al. 2006) and an index of degradation products (Wright et al. 2010). In addition, the effects

of an index for pigments packaging, or size factor ($S_{(f)}$; Ciotti et al. 2002) on the photo-physiology was evaluated.

2. Methods

2.1. Study Area

Contrasting oceanographic regions were sampled during the spring and early summer of 2011 in the Southern Atlantic Ocean, as part of the CO_2 South Atlantic Subtropical project. The cruise attended a multidisciplinary study focused on better understanding phytoplankton dynamics and ocean-atmospheric fluxes of carbon. The cruise left Rio Grande, Brazil (32°1'S; 52°5'W) on October 24 2011 and crossed the 35˚S meridian to Cape Town, Africa, returning to Rio de Janeiro, Brazil (22°55"S; 43°9'W) in December 23 2011. The 35˚S transect was chosen due to the reports of important CO_2 input from the atmosphere are (Takahashi et al. 2009; Khatiwala et al. 2009) combined to the lack of *in situ* data of this sector of the South Atlantic Ocean. The dynamic range of oceanographic conditions is expected to provide conditions of diverse phytoplankton communities with contrasting pigment compositions and photosynthetic activities.

The surface water masses in this sector of the Atlantic Ocean are forced by the atmospheric systems associated with the South Equatorial and Circumpolar Currents (Peterson and Stramma 1991) that defines the mean latitudinal position of the Subtropical Front (STF) in response to the expansion and contraction of the South Atlantic Subtropical Gyre (McClain et al. 2004). During austral spring and summer, high phytoplankton standing stocks are observed along the STF (suggested by ocean color imagery - Tilstone et al. 2009) consistent with net CO_2 fluxes from the atmosphere. Studies also suggest increase in primary production rates in this region related to the increase in photosynthetic rates (e.g. Maranan and Holligan 1999).

Notable features associated with the STF are mesoescale eddies, which disturbs the vertical position of the picnocline and can either promote input from nutrients from bellow stimulating phytoplankton growth (McGillicuddy et al. 2007) or transport surface waters bellow (Omand et al. 2015).

The observations were carried out over four distinct areas: i) a section across the continental margin near the plume of La Plata river ($n_{(surface)}$= 7 and $n_{(DCM)}$= 8), ii) a longitudinal section across the South Atlantic Subtropical Front (STF) ($n_{(surface)}$= 55 and $n_{(DCM)}$= 41), iii) a section across the upwelling near Benguela ($n_{(surface)}$= 9 and $n_{(DCM)}$= 5), and iv) a section across the South Atlantic Subtropical Gyre ($n_{(surface)}$= 20 and $n_{(DCM)}$= 17) (Figure 1). Details about sectors i to iii can be found in Lencina-Avila et al (2016).

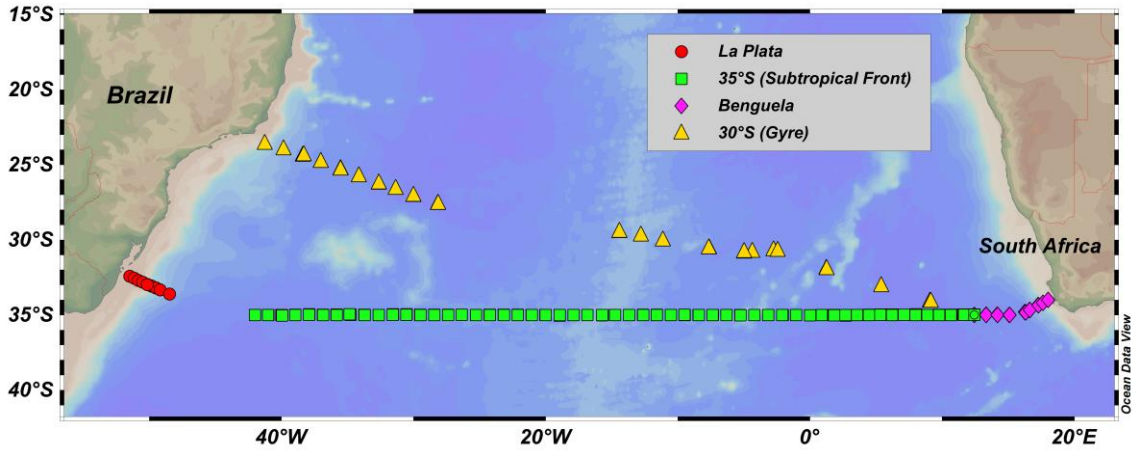

Figure 1. Sampling stations during the CO_2 South Atlantic Subtropical Project (October to December 2011), departing from Brazil to Africa in a survey across 35˚S of latitude adjacent to the Subtropical Front. The second leg of the cruise, departed from Cape Town, crossing the Benguela upwelling area and followed towards Brazil, crossing the Subtropical Gyre. Discontinuities of stations refers to bad weather and operational problems.

2.2. Oceanographic data and phytoplankton pigment analysis

In each oceanographic station, the vertical physical structure of the water masses was obtained from casts of a CTD SBE 911 profiler, equipped with temperature, salinity, pressure, dissolved oxygen, chlorophyll fluorescence and beam attenuation of

light sensors. The CTD was attached to a rosette system equipped with 12 Niskin bottles with 5L of capacity. Two separated casts were performed in each station: one to a maximum depth for chemical samples, followed by a cast limited to 300m for biological samples. Vertical transects of temperature were also measured with XBT Deep Blue profilers (surface to 760 m, provided by NOAA) in all stations and between stations. The gaps in Figure 1 represent logistical problems and unfavorable weather.

During the cruise, the oceanographic features were followed using ocean color satellite images to monitor alterations on sea surface temperature (SST) and estimated chlorophyll concentration. Composites of 8 days were used (http://oceancolor.gsfc.nasa.gov/cms/). In addition, the presence or absence of eddies was determined using high resolution weekly maps of Sea Level Anomaly (DT-MSLA), obtained for the period of the cruise. The altimeter products were produced by Ssalto/Duacs and distributed by Aviso (Archiving, Validation, and Interpretation of Satellite Oceanographic), with support from Cnes (http://www.aviso.altimetry.fr/duacs). Vortices and eddies were identified according to Chaigneau et al. (2009). These analyses were performed by Dr. C.A.E. Garcia's group at FURG, co-coordinator of the CO_2 South Atlantic Subtropical project.

Samples for chlorophyll-a concentration and photo-physiological parameters were chosen based on density and fluorescence profiles to represent when possible: i) the surface layer (4-8 meters), ii) the bottom of the mixed layer depth, iii) the depth of maximum fluorescence, iv) an intermediary between ii and iii; and v) bottom of the fluorescence peak. From a total of 92 samples, approximately 75 presented a remarkable DCM. When a DCM was not clearly observed, we have considered the highest fluorescence value (chlorophyll-a concentration), below the mixing layer, when higher than the surface values. High Performance Liquid Chromatography quantified pigment

profiles only for the surface and depth of maximum fluorescence. Sub-samples of 500 ml and 2L, for chlorophyll-a and HPLC pigments, respectively, were concentrated onto GF/F filters and immediately stored in liquid nitrogen until analysis in the laboratory.

Chlorophyll-a were extracted in 5mL 90% acetone + DMSO solution (6:4 – Shoaf and Lium 1976) for 24h in dark at -20°C, and quantified using a calibrated Turner AU-10 fluorimeter, through the non-acidification method (Welschmeyer 1994). A calibration factor obtained from a commercial chlorophyll-a standard (Sigma-Aldrich) was used to calculate the final chlorophyll-a concentration of fluorescence measurements.

The procedures for measuring chlorophylls, degradation products and accessory carotenoids measured by HPLC followed the method from Zapata et al. (2000), modified by Mendes et al. (2007). Pigments were identifiedfrom both absorbance spectra and retention times from the signals in thephotodiode array detector (SPD-M20A; 190 to 800 nm; 1 nm wavelengthaccuracy) or fluorescence detector (RF-10AXL; Ex. 430 nm/Em. 670 nm). Pigments were automatically quantified from peak integration provided by the LC-Solution software (Shimadzu), but all peak integrations were checked manually and corrected when necessary. The HPLC system was previously calibrated with pigment standards from DHI (Institute for Water andEnvironment, Denmark).

A total of 21 pigments were quantified, including chlorophylls, accessory photosynthetic pigments and accessory carotenoids (Table 1). The presence of some unambiguous marker pigments was used to infer the presence or changes in the proportion of specific phytoplankton groups, without assuming quantitative relationships. These were: Fucoxanthin as a marker for Diatoms, Hex-Fucoxanthin + Chl c_2 and c_3 for Haptophytes, Zeaxanthin for *Synechococcus* and DV-Chla for

Prochlorococcus (Wright and Jeffrey 2006; Jeffrey et al. 2011). Some pigments-based physiological indexes such as PSC and PPC (Barlow et al. 2002) were computed, as well as an index of degradation product of chlorophyll (Wright et al. 2010).

An index to derive the fraction of small size phytoplankton (f_pico) was calculated based on diagnostic pigments of small groups, according to Uitz et al. (2006) (Equation 1).

$$f\_pico = 1.01\ Chl\ b + 0.86\ Zea / \Sigma DP \qquad Eq\ (1)$$

where ΣDP = 1.41 Fuco + 1.41 Perid + 1.27 Hex-fuco + 0.35 But-fuco + 0.60 Allo + 1.01 Chl b + 0.86 Zea

A size parameter (or $S_{(f)}$, size factor) was calculated based on the phytoplankton community absorption spectra, which will refer to the combined effects of pigment packaging and concentration and composition of accessory pigments (Ciotti et al. 2002). The phytoplankton absorption data was obtained from a filter-pad technique, according to Tassan and Ferrari (1998), using a spectrophotometer Perkin Elmer, Lambda 35.

Table 1. Pigments quantified by the HPLC analysis and some pigments-based physiological and degradation indexes.

TChla	**Total chlorophyll-a**	Chlorophyll a (Chl a) + DV-Chlorophyll (DV-Chl)
ΣTC	**Total carotenoids**	Alloxanthin (Allo) + But-fucoxanthin (But-fuco) + βε-Carotene (βε-car) + ββ-Carotene (ββ-Car) + Diadinoxanthin (Diadino) + Fucoxanthin (Fuco) + Diatoxanthin (Diato) + Hex-fucoxanthin (Hex-fuco) + Lutein (Lut) + Peridin (Perid) + Violaxanthin (Viola) + Zeaxanthin (Zea) + Neoxanthin (Neo) + Prasinoxanthin (Pras)
ΣAP	**Accessory pigments**	**TC** + Chlorophyll *b* (Chl *b*)+ Chlorophyll c_1(Chl c_1)+ Chlorophyll c_2(Chl c_2)+ Chlorophyll c_3(Chl c_3)+ Mg DVP
PPC	**Photoprotective carotenoids**	Allo + βε-Car + ββ-Car + Diadino + Diato + Lut + Viola + Zea
PSC	**Photosynthetic carotenoids**	But-fuco + Fuco + Hex-fuco + Perid
-	**Degradation index**	Chlorophilide/Tchla (Chlide/Tchla)

2.3. Photo-physiological data

The subsamples used for determination of photo-physiological parameters were analyzed using a fluorescence induction and relaxation technique (Gorbunov and Falkowski, 2004), which yields the maximal photosynthetic efficiency (F_v/F_m) and the functional cross-section of light absorption (σ_{PSII}) of the phytoplankton community. Samples were dark-adapted for 30 to 60 minutes, at room temperature, in clean dark glass bottles and processed in flow-through mode with a bench-top FIRe instrument (Satlantic). The flow-through mode allows for better signal to noise results without damaging the cells with the multiple sequential flashes necessary for the procedure. The flow-through cuvette was rinsed with the dark acclimated samples for 2 minutes before the fluorescence profiles were registered for about 5 minutes. Note that in flow-through mode, the Fire instrument gain is automatically adjusted according mainly to the chlorophyll concentration. Because of that, blanks were processed as samples and all raw data were processed using a software package developed by MSc. Audrey Barnett (Fireworx 1.0.4 - https://sourceforge.net/p/fireworx/news/), developed for matlab. Blanks were 0.2µm filtrates of a nylon capsule filter (Polycap 75AS, Whatman) of each sample. Between stations, the cuvette was rinsed with a diluted solution of neutral soap and freshly produced mili-q water. The steps of Fireworx routine also included the normalization of data by the calibration of the blue led used (Figure 2). For logistic problems, the calibration files were prepared in the laboratory using known chlorophyll-a solutions several months after the cruise. Nonetheless, the instrument was monitored monthly before, during and after the cruise with a fluorescent dye and no significant response changes were observed in the past year. All parameters (i.e., F_o, F_m and σ_{PSII}) are means of all profiles adjusted during the 5 minutes of data collection that yielded 14 to 15 profiles in general. A quality control for the parameters was applied, for which

samples with coefficients of variation higher than 30% among the 5 minutes running were excluded.

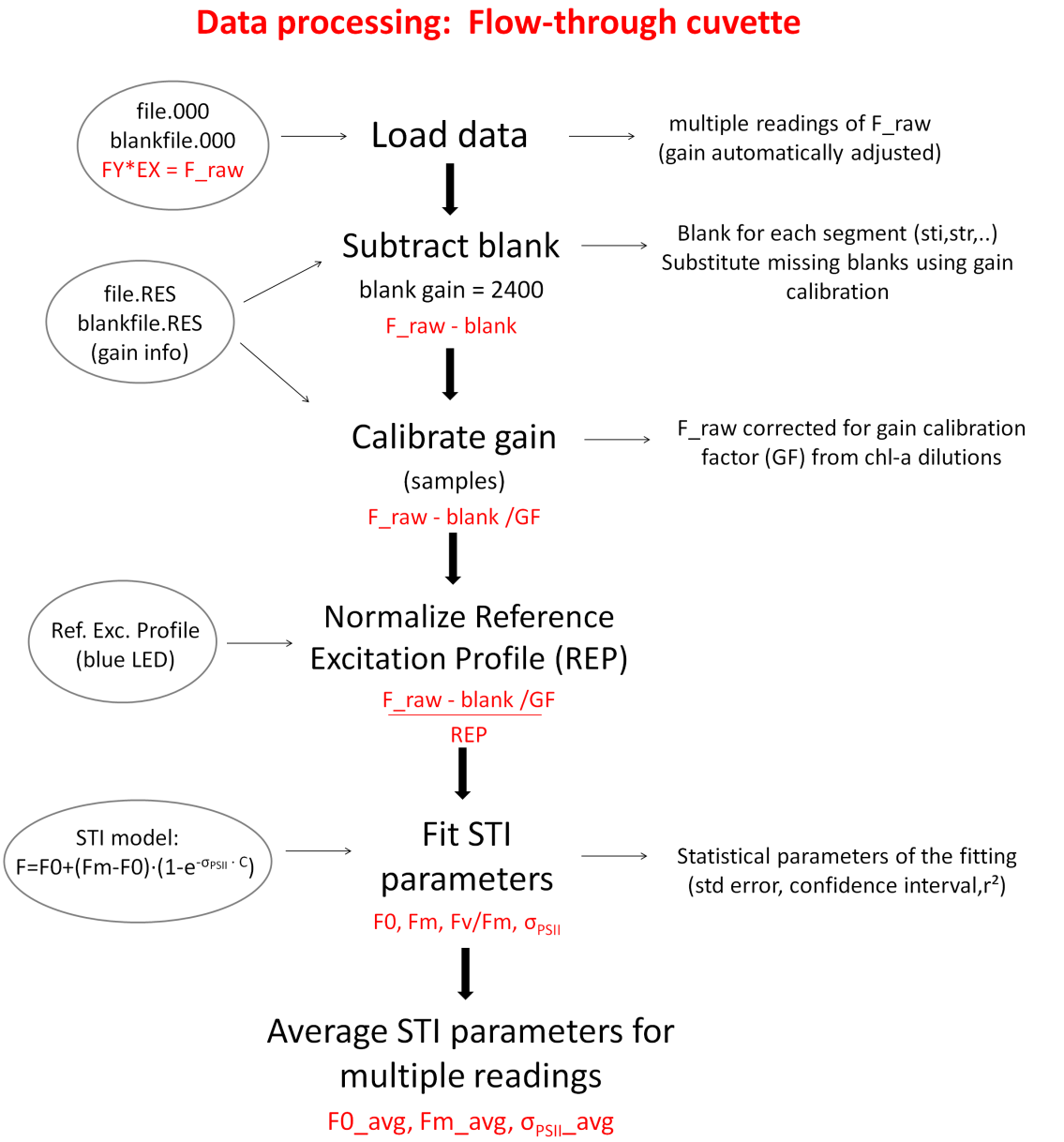

Figure 2. Flow diagram of the photophysiology data processing at fireworx (FIRe data processing software) to obtain F_v/F_m and σ_{PSII}

2.4. Data analysis

As mentioned before, the cruise sampled contrasting oceanographic regions (Figure 1), and the dataset were divided according: 1. The transect from coast to open ocean crossing the south continental shelf of Brazil under the influence of the La Plata

river plume; 2. The 35°S longitudinal section, influenced by mesoscale vertical instabilities across the STF; 3. The south Africa coastal waters, affected by the Benguela upwelling; and 4. The session across the subtropical oligotrophic gyre and the Brazil Current. For each region, near surface and the maximum fluorescence depth were treated separately. Note that general relationships between F_v/F_m and σ_{PSII} and chlorophyll-a were also constructed using fluorimetric data, providing a higher vertical resolution. The distribution of phytoplankton and the photo-physiological characteristics of the community were discussed in terms of the main physical drivers of the hydrographic structure for each of the four sectors, where relationships were tested through linear regression analysis and vertical profiles sections.

The relationships between the photochemical efficiency (F_v/F_m) and functional cross-section of light absorption (σ_{PSII}) were analyzed for each of the sectors, as well as for different layers (surface versus DCM). Although the relationships between both parameters found in the literature does not suggest a unique and strictly linear trajectory, as well as same taxonomic signatures (Moore et al. 2006, Fishwick et al. 2006; Suggett et al. 2009), we decided to present as such as a simple approach for comparison among sectors and depths, since our goal is not to derive a unique equation, but to identify consistent deviations.

A series of pairwise correlations were tested among the ratios of individual pigments and the total accessory pigments (Pigs/ΣAP) and the photo-physiological parameters, also for the different sectors. Additional parameters were expected to correlate to F_v/F_m and σ_{PSII}, such as $S_{(f)}$, f_pico, PSC, PPC, Chlide/TChla, and were also tested. Those analyses were performed at the statistic software R.

3. Results

3.1. Hydrography, pigments and photo-physiological parameters

The four sectors sampled showed expected contrasting oceanographic characteristics (Figure 3), and because of that, they are characterized by distinct sources for nutrient supply to the surface layers (not shown), resulting in distinct phytoplankton community structures, as will be presented below.

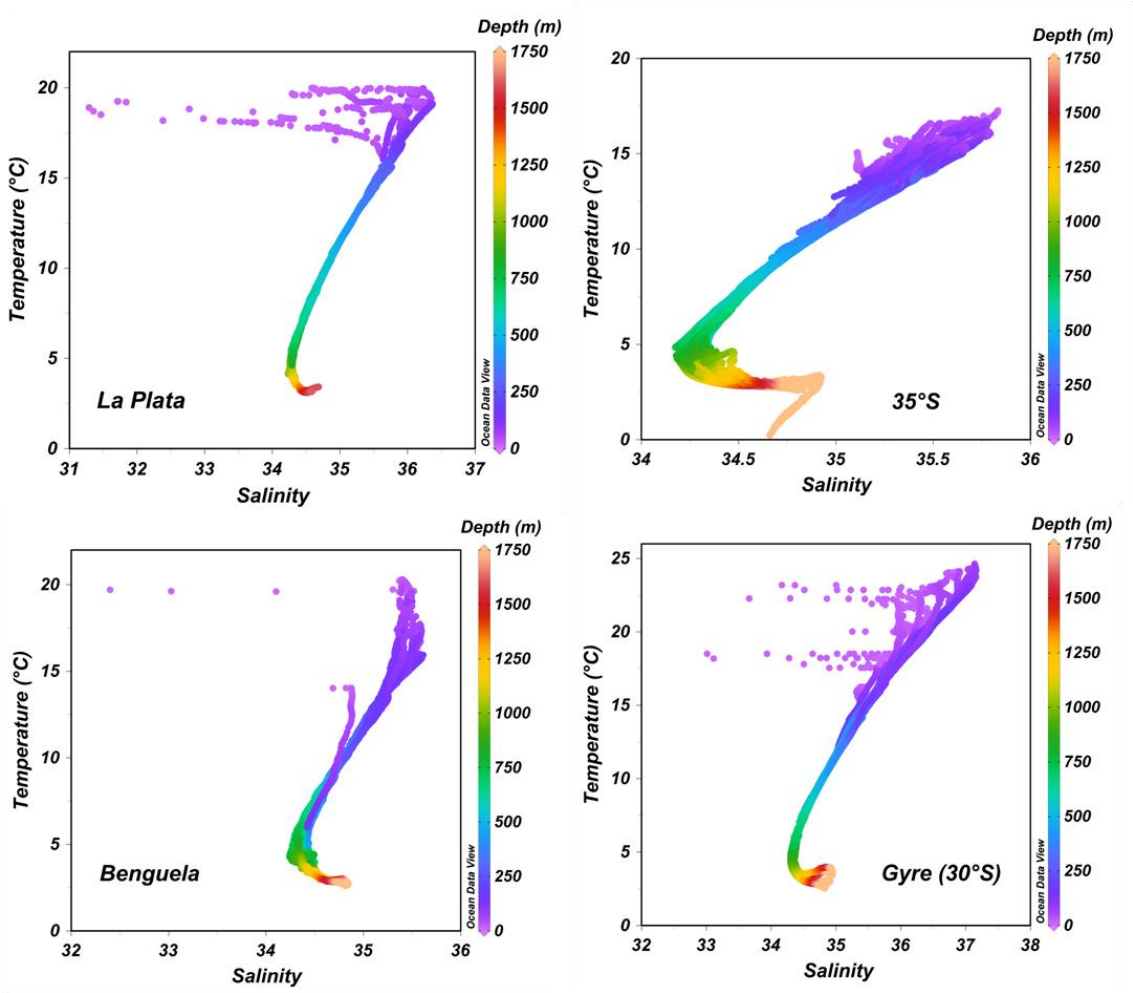

Figure 3. T-S diagrams for each of the analyzed sectors across the Southern Atlantic Ocean

The surface waters presented the largest range of variability in chlorophyll-a concentration in all sectors, with highest concentrations observed at the surface of Benguela sector (up to 5 mg m^{-3}) and the lowest at the Gyre (Figure 4). The highest F_v/F_m was also observed for the surface waters of the Benguela, varying from 0.29 to 0.56, and lowest at the 35°S sector, which varied from 0.11 to 0.38 at the surface and 0.16 to 0.38 at DCM, which shows a phytoplankton community, in general, represented

by low photochemical efficiency. In this sector, σ_{PSII} varied from 154 to 296 Å²/photon at the surface and 197 to 299 Å²/photon at DCM. F_v/F_m at the surface of the Gyre sector were not computed due to the low signal-to-noisy ratio of the dataset, however at DCM, despite the low chlorophyll-a concentrations, F_v/F_m was higher than at 35°S, ranging from 0.22 to 0.49. The mean values of F_v/F_m and σ_{PSII} at the Benguela sector were similar to the La Plata sector, except for the higher values of σ_{PSII} at the surface in the Benguela sector (Figure 4). F_v/F_m and σ_{PSII} were not significantly different between both layers, especially due to the low dynamic range of this parameters, except at the 35°S where F_v/F_m at the surface was higher than the DCM (t-test, $p<0.01$).

The main differences in the pigments ratios among the sectors are the higher DV-Chl/Tot Chla in the Gyre, along with a robust contribution of Chl b at DCM, as well as the large contribution of Zeaxanthin in the surface at this sector (Figure 5). The La Plata and Benguela sectors presented the largest contribution of Fucoxanthin (Fuco/ΣAP), while a significant increase in the Hex-Fucoxanthin ratios were observed at surface and DCM at the 35°S (Figure 5).

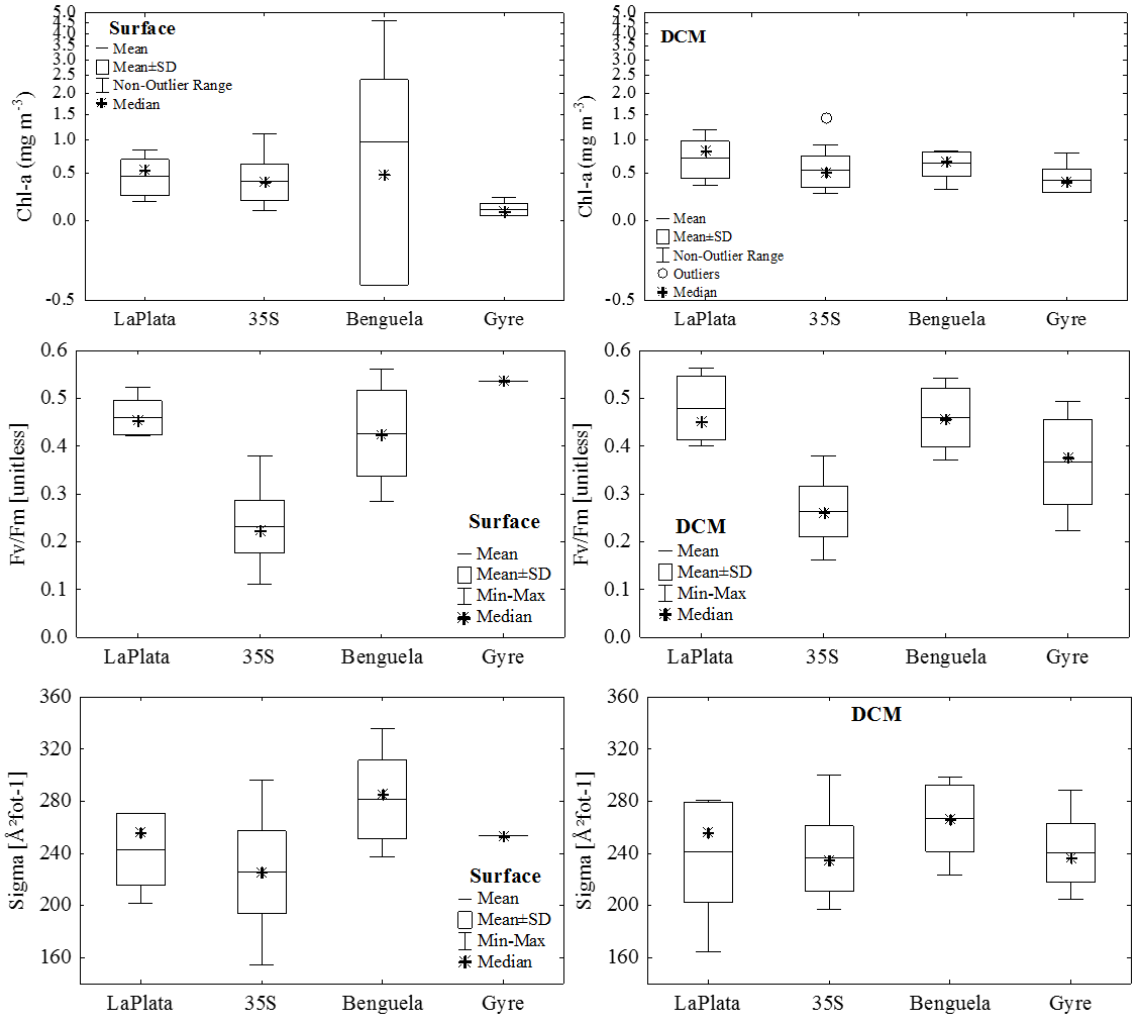

Figure 4. Basic descriptive statistics (Mean, Median and standard deviations) of Chlorophyll-a concentrations, $F_v/F_m$and σ_{PSII} for each sector and depth layer (surface and DCM). Chlorophyll-a concentrations are from fluorometry.

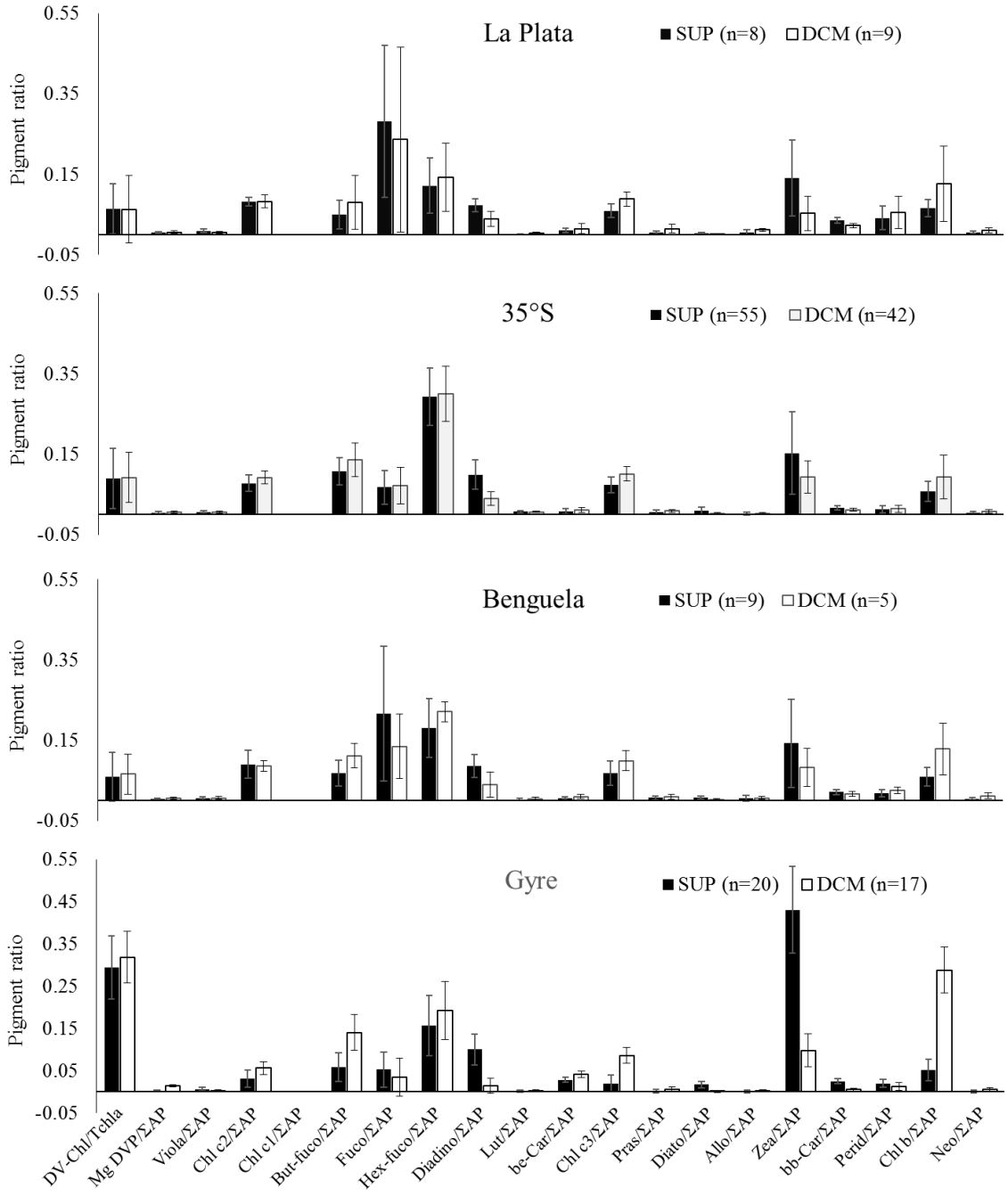

Figure 5. Pigment ratios from HPLC analysis for the fours sectors in the Subtropical South Atlantic Ocean. The acronyms in the x-axis are as in Table 1.

The relationships between photophysiological parameters and the oceanographic characteristics of each sector are described below:

Sector 1: La Plata plume waters

The observations from the La Plata sector clearly showed the influence of the Plata Plume Water (PPW) at the surface waters over the continental shelf, with salinity values

below 33 (Figure 6). Offshore, due to the encounter of Brazil and Malvinas Currents, observed water masses included the Subtropical Shelf Water (STSW) at the surface of the continental shelf break and the SACW over continental slope (Figure 3a).

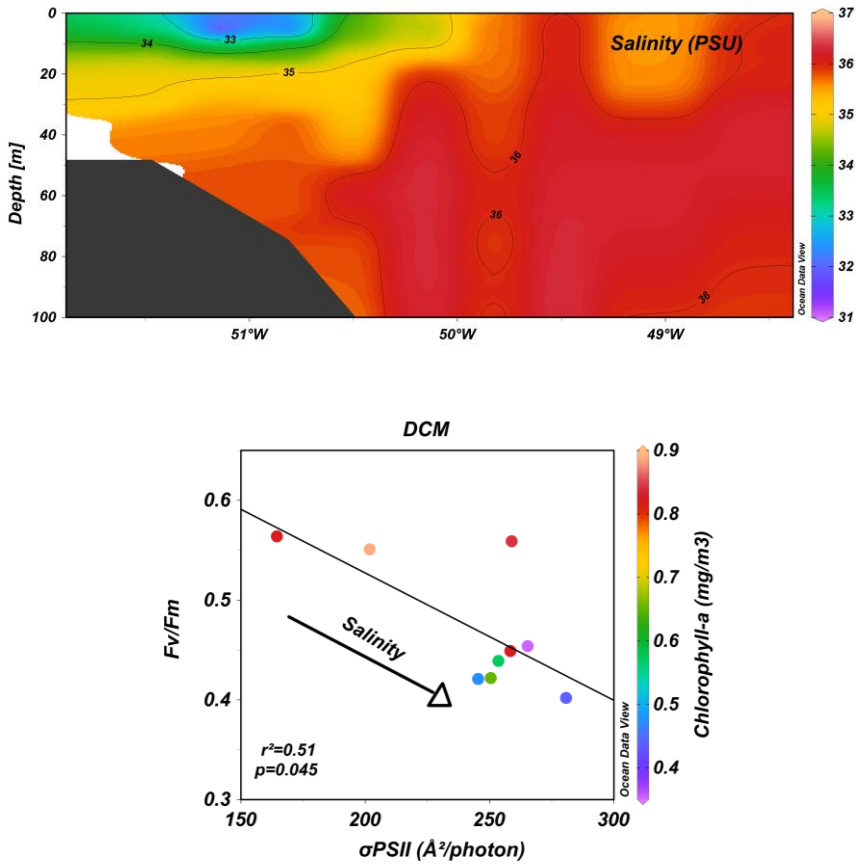

Figure 6. Salinity section at the La Plata influenced waters (above) and the relationship between F_v/F_m and σ_{PSII} at the DCM of the La Plata sector, indicating the trajectory of increase in salinity values (below)

Both F_v/F_m and σ_{PSII} were highly correlated with salinity at the DCM (r^2=0.67 and 0.66, respectively), with lower σ_{PSII} and higher F_v/F_m at low salinity waters, which were also related with higher Chl-a concentrations (Figure 6). The expected negative relationship between F_v/F_m and σ_{PSII} (see Chapter 3) was only observed at the DCM (r^2=0.51, n=9).

<u>Sector 2: 35ºS section across de STF</u>

Sharp vertical temperature gradients are observed across the entire section, due to the high spatial resolution between CTD casts, and a number of mesoescale features of the picnocline are clearly observed (Figure 7), likely related to the presence of cyclonic and anti-cyclonic eddies. Indeed, maps of Sea Surface Height (SSH) derived from altimetry (Figure 8) suggested the presence of an anti-cyclonic eddy at 5°E longitude, associated with a deepening of the picnocline (Figure 7). On the other hand, a shallowing of the picnocline between 10 and 20°W, suggesting an upwelling center associated with a mesoscale cyclonic eddy (Figure 8), promoted an increase in the chlorophyll-a concentration at the euphotic zone, and CTD fluorimeter casts suggest that the deep chlorophyll maximum remained above 60 meters responding to the feature.

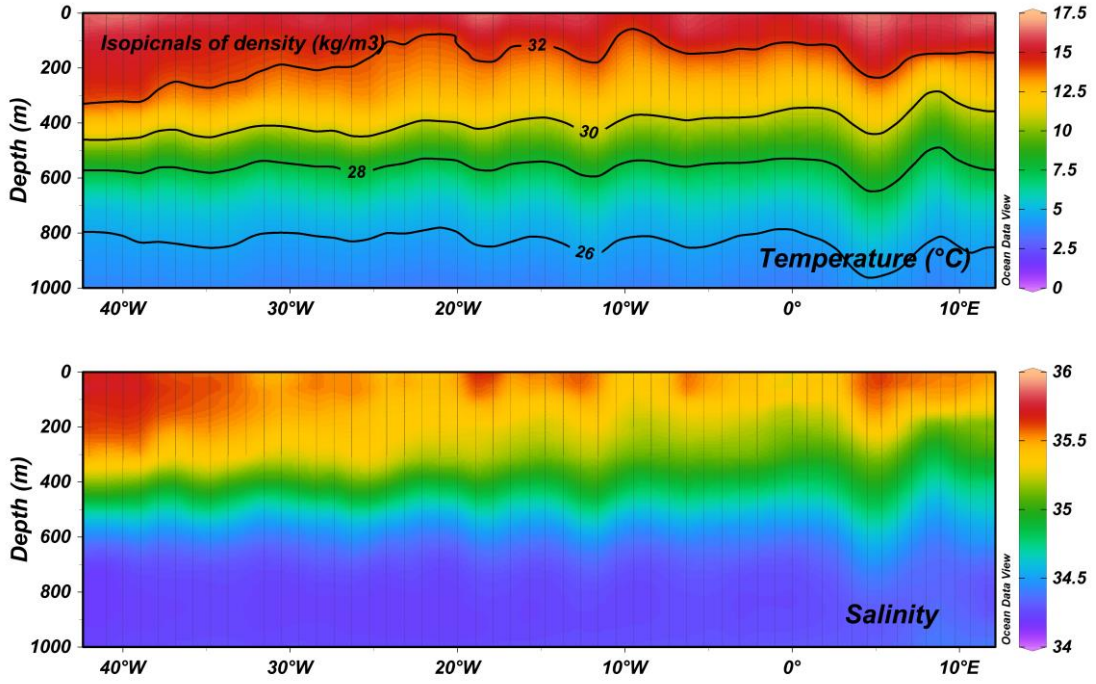

Figure 7. Temperature and salinity vertical sections across the 35°S sector at the South Atlantic Ocean

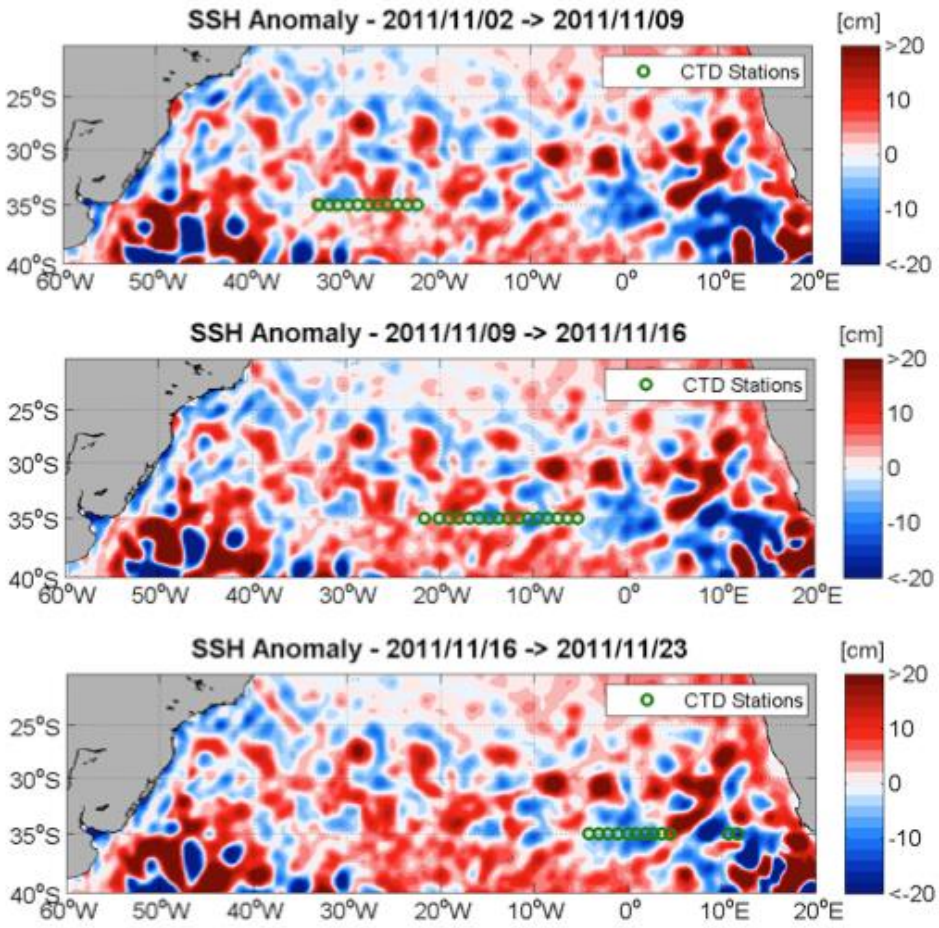

Figure 8. Sea Surface Height from altimetry weekly data from the South Atlantic Ocean obtained during the cruise (first leg from Brazil to Africa coast). The sampling stations are indicated in green. The red and blue cores indicate warm anticyclonic and cold cyclonic eddies, respectively.

The vertical distribution of chlorophyll-a throughout the first 50m is proportional to the vertical distribution of the functional absorption cross-section, especially between 10 and 20°W (Figure 9), where an increase in chlorophyll-a concentration was associated with higher σ_{PSII}. This patch of increased biomass was coincident with an increase in the relative proportion of diatoms, suggested by the diagnostic pigment Fucoxanthin, also corroborated by data obtained with the FlowCam (data not shown). However, higher photochemical efficiency would be expected, along with lower absorption cross-section. At DCM, the ratios of Fucoxanthin was also higher between 10 and 20°W.

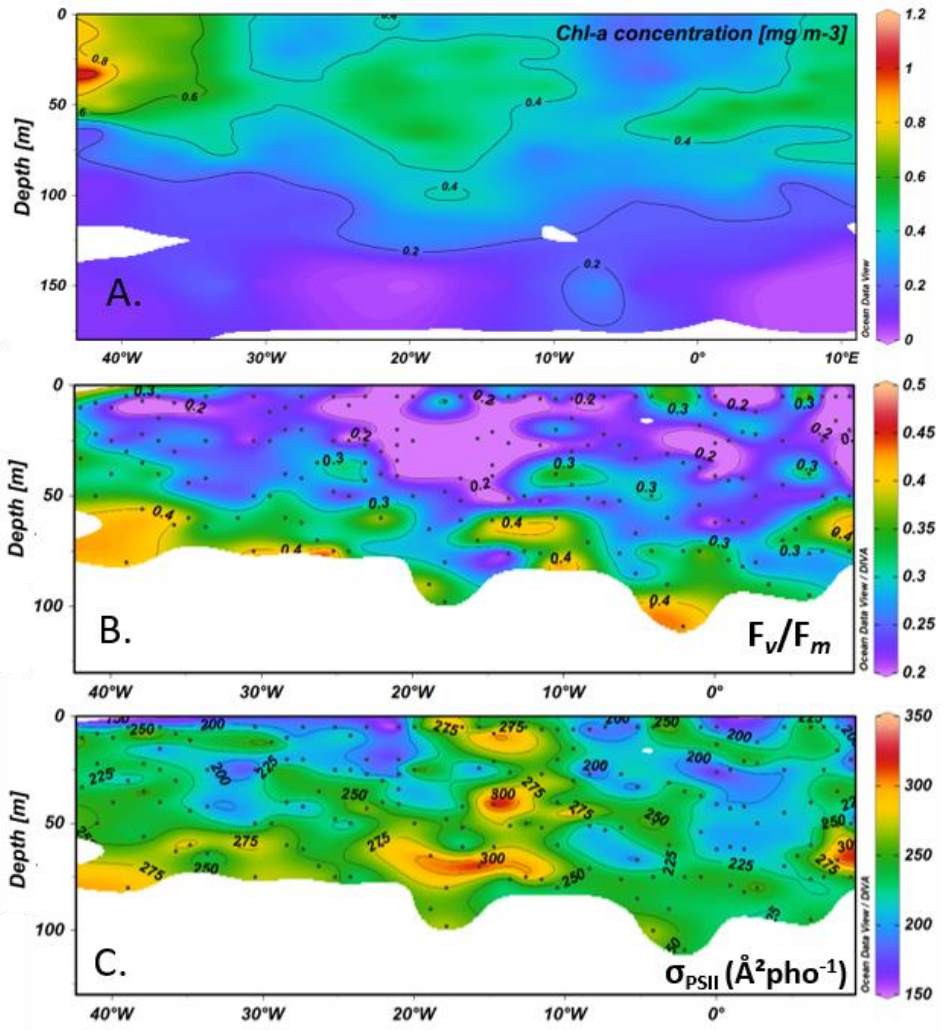

Figure 9. Vertical section of Chlorophyll-a, F_v/F_m and σ_{PSII} along the 35°S sector at the South Atlantic Ocean.

Sector 3: Benguela upwelling

The sector over the Benguela upwelling system shows low temperature waters reaching the surface over the continental shelf. Note however that the section of transects was oriented from Cape Town southwards to complete the 35˚S latitude line that had to be interrupted in the first leg of the cruise (Figure 10). Because of that, large gradients were observed in both temperature and salinity offshore, especially in the upper layers. In this sector, the highest chlorophyll-a concentrations were observed, reaching 8µgm^{-3}, associated to the coldest waters.

Positive relationships between F_v/F_m and temperature at the surface and between σ_{PSII} and temperature at the DCM were observed. Thus, although the number of samples is low to assign robust correlations, samples associated with the upwelled waters tended to present low F_v/F_m and low σ_{PSII}.

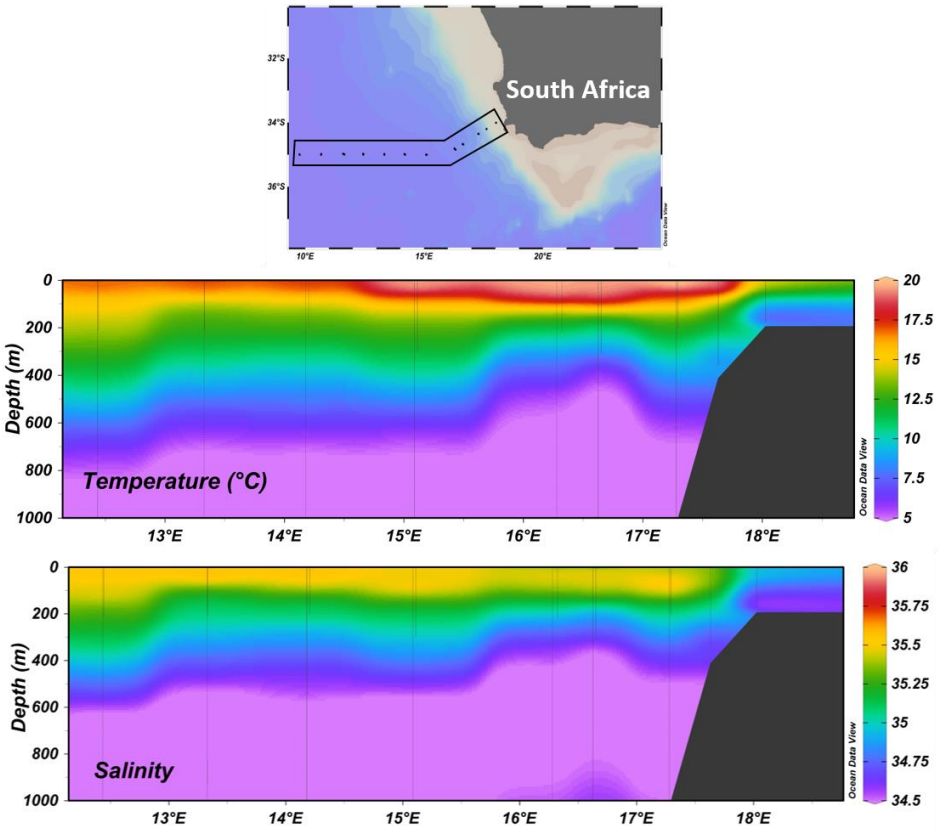

Figure 10. Temperature and Salinity sections across the Benguela sector sampled during the second leg of the cruise. The map shows the stations track to highlight the southward direction of this sampling.

Sector 4: Subtropical gyre at 30ºS and Brazil Current

The sector crossed the Subtropical Gyre towards the 30°S at the Brazilian coast, also intercepting the warm Brazil Current, between 30 and 40°W (Figure 11). Picnocline was deeper than in the 35°S sector, forcing the DCM deeper as well (about 100m). Warm core eddies can be clearly observed at the SSH data from altimetry (Figure 12), which were probably originated at the Agulhas Current, especially at 5°W and 10°W.

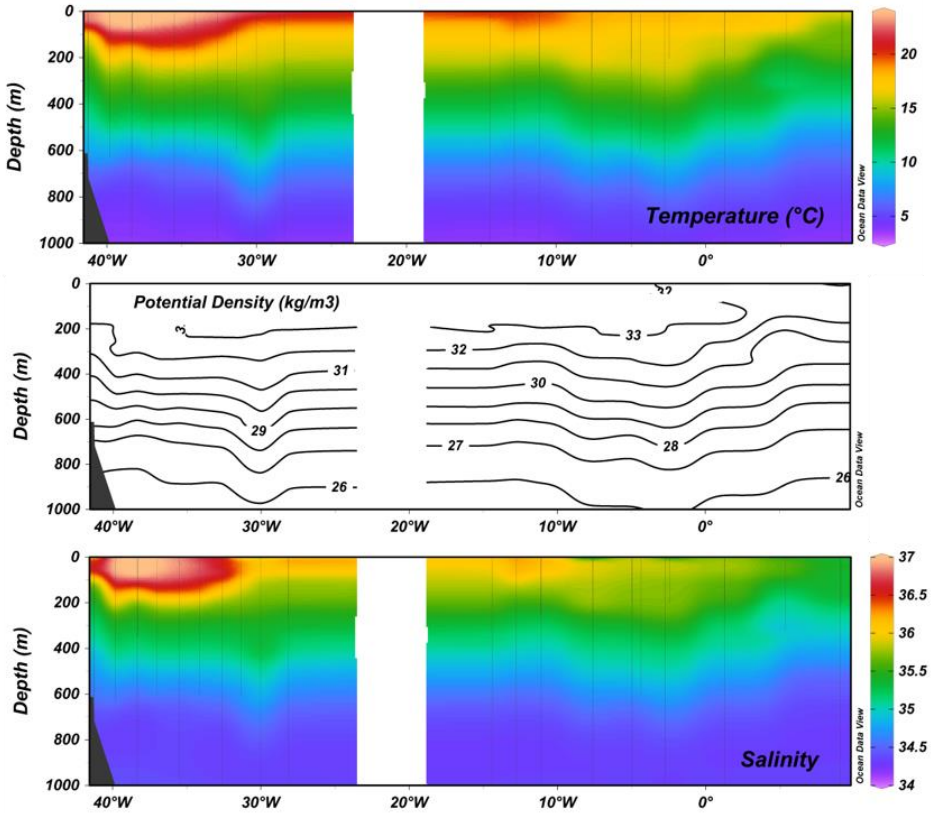

Figure 11. Temperature and Salinity vertical sections across the subtropical Gyre sector sampled during the second leg of the cruise.

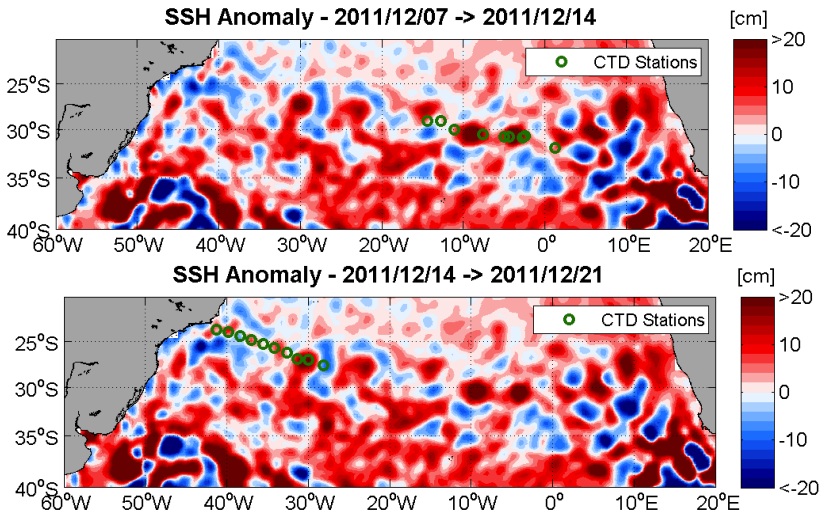

Figure 12. Sea Surface Height from altimetry weekly data from the South Atlantic Ocean obtained during the cruise (second leg from Africa to Brazil coast). The sampling stations are indicated in green. The red and blue cores indicate warm anticyclonic and cold cyclonic eddies, respectively.

The oligotrophic Gyre and Brazil Current waters were associated, as expected, with low chlorophyll-a concentration (<0.2 mg m^{-3}). The signal-to-noise ratio of the

photo-physiological derived data were extremely low at the surface with both F_v/F_m and σ_{PSII} values presented high coefficient of variation among fluorescence profiles of individual samples (Figure 13). This led to the exclusion of the majority of the surface samples by the quality control criteria applied (see methods). Low chlorophyll-a concentrations were also observed in other sectors; however, the community composition was likely responsible for the noisy photo-physiological data at the surface of the subtropical gyre.

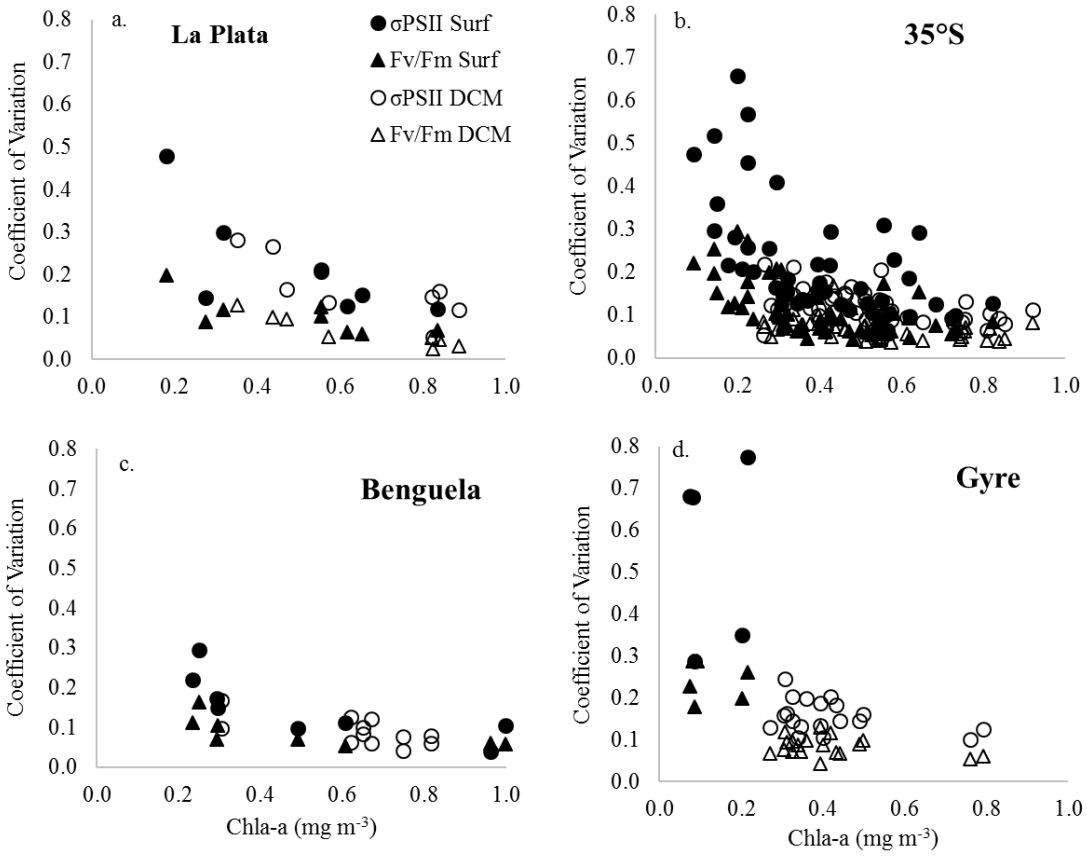

Figure 13. Relationship between the coefficient of variation among replicates of Fv/Fm and Sigma measurements and chlorophyll-a concentration separated by sector and depth layers (surface and DCM).

The highest F_v/F_mvalues were observed at the western side of the sector, while σPSII was consistent low across the DCM. Fv/Fm was positively related to the temperature and salinity (r^2=0.53 and 0.65, respectively), but the relationship (not shown) was linear above 18°C and salinity above 36, suggesting that the community

with better photosynthetic performance is influenced by the Brazil-Current waters at the western portion of this transect. This sector has also presented the highest proportions of DV-Chl at DCM, the diagnostic pigment of *Prochlorococcus* (Figure 5).

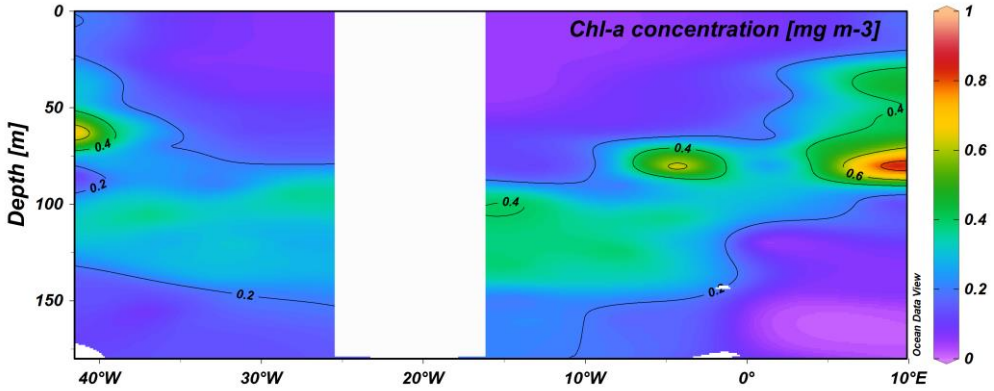

Figure 14. Vertical section of chlorophyll-a concentration across the Subtropical Gyre in the South Atlantic Ocean

In our dataset, the chlorophyll-a concentration computed from the two methods, fluorimetric (Chl-a [fluorometry]) and HPLC (Chl-a [HPLC]), were highly correlated (see methods), however 6% of the samples presented differences higher than 40% (Figure 15), and 6 samples presented differences higher than two-fold. These results were indicated in the text and their interpretation should be careful. Nonetheless, differences were found on the correlations analyses between pigments and photo-physiology parameters depending on the method (Tables 2 and 3).

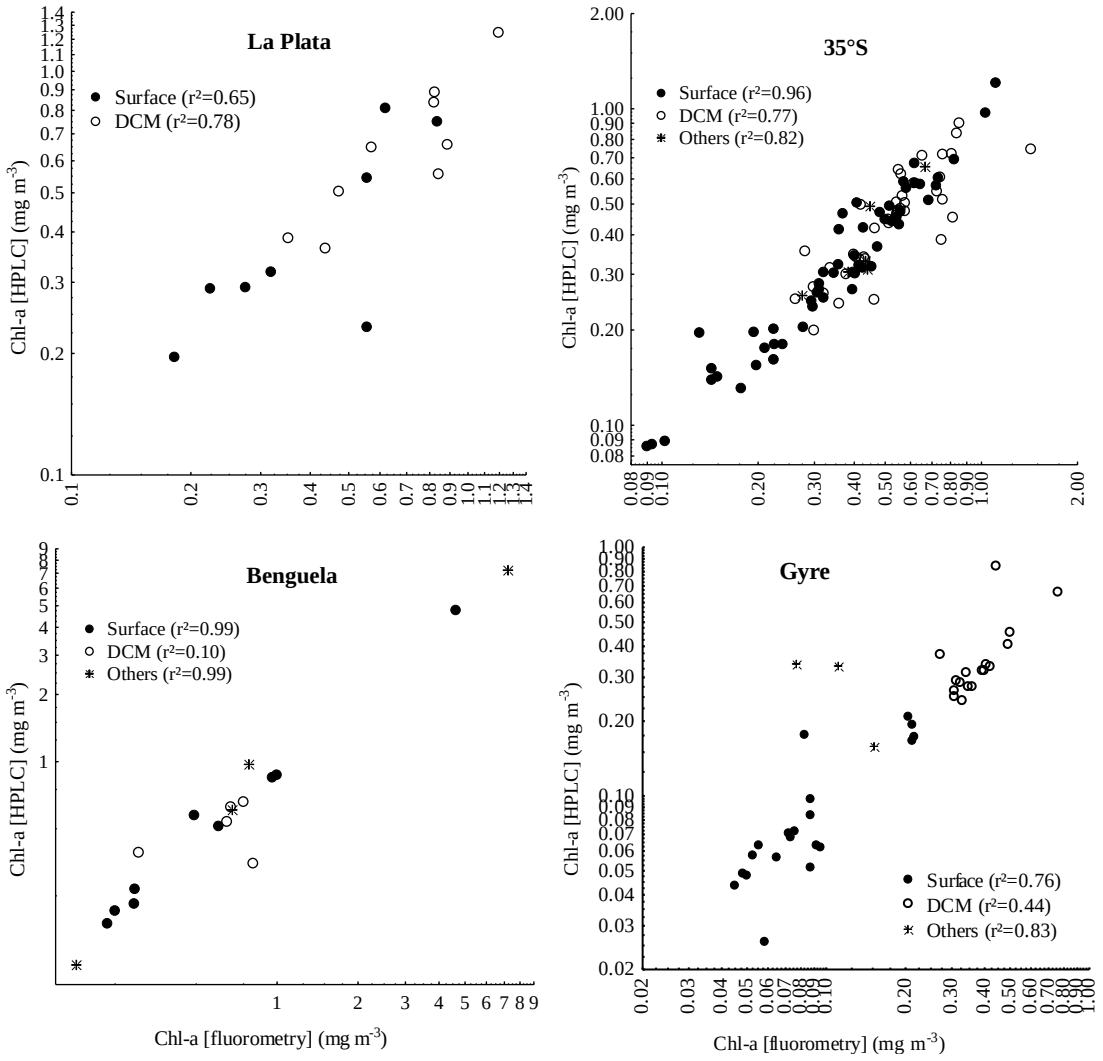

Figure 15. Comparison between the chlorophyll-a concentrations from two methods: HPLC and Fluorometry (Welschmeyer 1994) separated by sectors in the South Atlantic Ocean

3.2. F_v/F_m versus σ_{PSII} in large spatial scales

$F_v/F_m$and σ_{PSII} were not significantly correlated when the data from all sectors were polled together, however some trends were observed according to distinct depth layers, especially in the large transects, where high vertical resolution data were collected (35°S and Gyre) (Figure 16). Contrasting these two sectors, σ_{PSII} presented a narrower range of variability at the Gyre sector and a clear trend of correlation between F_v/F_m and σ_{PSII} in deeper waters. Indeed, at DCM, they were positively correlated in this sector (r^2=0.37, p<0.01), which is opposite to what it has been previously seen (Moore et al. 2005, Suggett et al. 2009). However, at DCM, the Chl-b proportion (also DV-Chl)

suggested the presence of *Prochlorococcus*. At surface waters of the oligotrophic gyre, higher proportion of Zeaxanthin compared to the 35°S sector, suggests the important contribution of *Synechococcus,* that summed to the low biomass, generated the noisy photo-physiological data. At 35°S, Zeaxanthin and DV-Chl were lower, followed by a significant increase in Hex-Fucoxanthin ratios, both at surface and DCM.

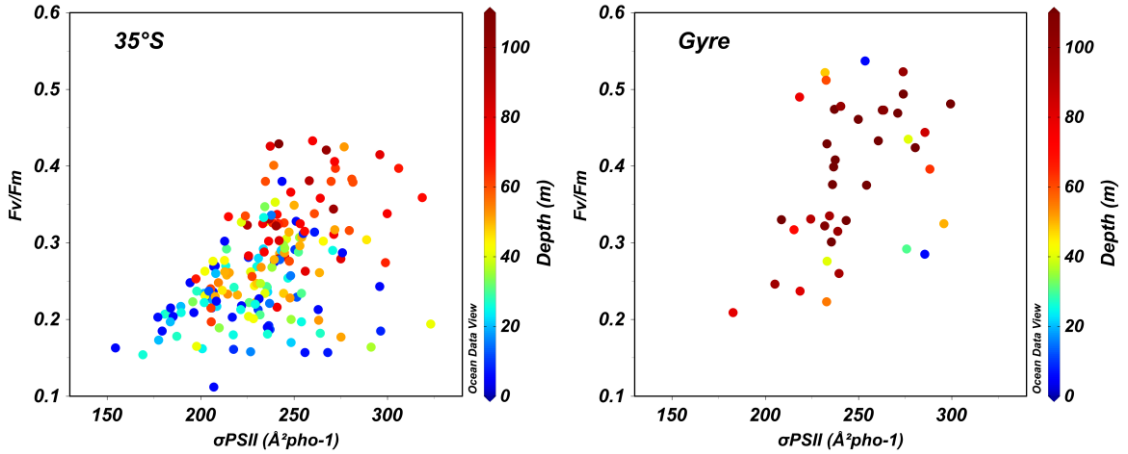

Figure 16. Relationship between σ_{PSII} and F_v/F_m for two sectors in the Subtropical South Atlantic Ocean where high vertical resolution data were obtained. The data presented here are samples from 4 to 5 depths in the water column (not only surface and DCM).

The averages of F_v/F_m and σ_{PSII} and their respective standard deviations give a summary of how these two parameters vary and relate to one another among sectors, also showing their dynamic ranges (Figure 17). The La Plata and Benguela sectors presented similar ranges F_v/F_m, but σ_{PSII} was higher for the Benguela sector in both surface and DCM. According with the pigment ratios (Figure 5), the La Plata sector showed important contribution of Fucoxanthin (i.e., marker of diatoms) near coast, while the stations near coast in the Benguela sector presented important contributions of the combination Fucoxanthin, Hex-Fucoxanthin and But-Fucoxanthin, that are marker pigments of diatoms and haptophytes.

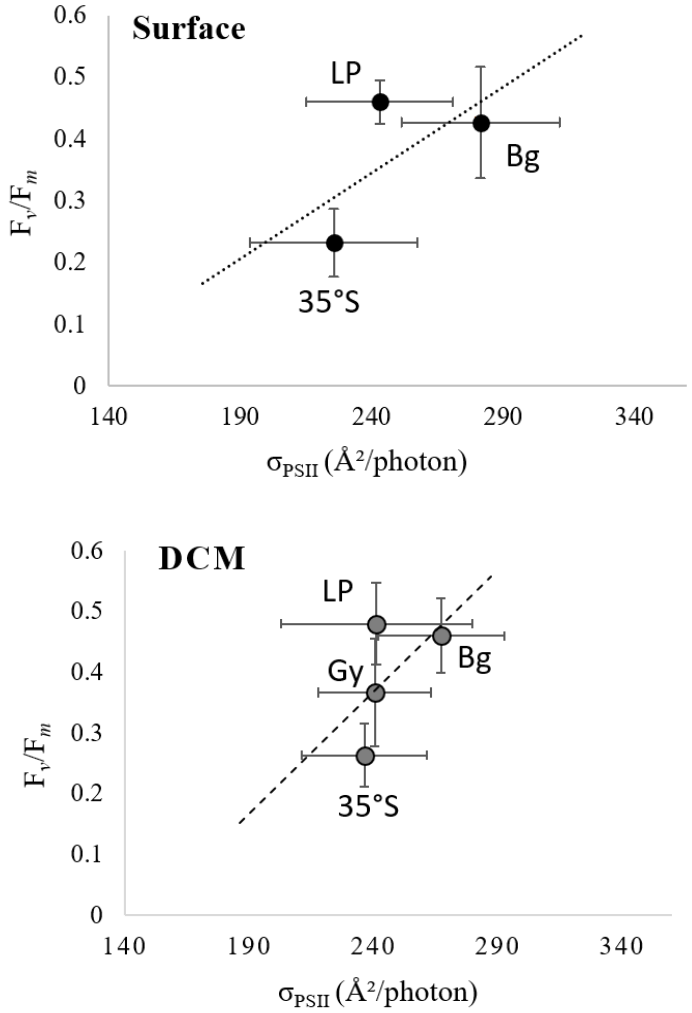

Figure 17. F_v/F_m versus σ_{PSII} measured for the four sectors of the Subtropical South Atlantic Ocean. Data represent the means (±Std deviation) of all samples, divided by surface and DCM layers.

3.3. Relationships between photo-physiological parameters and pigment ratios and between photo-physiological parameters and bulk bio-optical indices across different oceanographic features

Our approach was to investigate to what extent the accessory pigments can explain the variability observed in the photo-physiological parameters F_v/F_m and σ_{PSII} in large scale. The pigments ratios to the total of accessory pigments were correlated to the photo-physiology parameters, including the primary and the auxiliary set of pigments (e.g., Violaxanthin and Neoxanthin). In our dataset, the proportion of the diagnostic

pigments (Fucoxanthin, But-Fucoxanthin, Hex-Fucoxanthin, Peridin, Alloxanthin, Chl-b and Zeaxanthin) to the total of accessory pigments was about 70% (except for the Subtropical Gyre sector that was about 75%), so the other 30% of "non-diagnostic" pigments were considered in the analyses.

The pigments ratios that showed relationships with F_v/F_m and σ_{PSII} varied among the sectors, with important contribution of some photo-protective pigments, besides the exclusive diagnostic pigments. Individual photo-protective and photosynthetic pigments have shown important correlations to F_v/F_m and σ_{PSII}, but in some cases, the commonly used physiological indices, PSC and PPC, were not significantly correlated to photo-physiology. For example, at DCM of the 35°S sector, the proportions of Alloxanthin, Diatoxanthin and Diadinoxanthin were significantly related to F_v/F_m, however the pool of photo-protective carotenoids (PPC) was not significant.

In the La Plata sector, F_v/F_m was positively correlated to Chl *c3* at the surface and negatively correlated to Diadinoxanthin and, in less extent, to the proportion of Violaxanthin (Table 2). In this case, PPC was also significantly correlated to F_v/F_m at the surface (r^2=0.87). At DCM, F_v/F_m was correlated with the chlorophyll-a concentration. Although the higher values of F_v/F_m was related to higher phytoplankton biomass and lower σ_{PSII} at DCM, which suggested the presence of diatoms, the proportion of Fucoxanthin, a diagnostic pigment of this group, was not significantly related to F_v/F_m. σ_{PSII} was correlated to Fucoxanthin ratios at DCM, as well as the photo-protective carotenoids Alloxanthin and Lutein. At the surface, σ_{PSII} was negatively correlated to Chl *c2* and positively correlated to ββ-Carotene ratios (Table 3).

Table 2. Correlations between $F_v/F_m$and pigments ratios (Pigment/ΣA.P. and DV-Chl/TChl-a), Chl-a concentration (fluorometry and HPLC), PSC (photosynthetic carotenoids), PPC (photoprotective carotenoids), proportion of degradation products (Chlide/TChl-a), f_pico (Uitz

et al, 2006) and $S_{(f)}$ (Ciotti et al 2002). Only significant results ($p<0.05$) are shown. N is the number of samples considering concomitant pigments and photo-physiology data.

Fv/Fm	***Surface***			***DCM***		
	Pigments	**N, r**	**r^2, p**	**Pigments**	**N, r**	**r^2, p**
La Plata	Chlorophyll c3	05, .95	.90, .013	Chl-$a_{[fluorometry]}$	08, .79	.62, .020
	Diadinoxanthin	05, -.92	.85, .025	Chl-$a_{[HPLC]}$	n.s.	
	Violaxanthin*	05, -.97	.95, .005	Prasinoxanthin*	08, -.72	.52, .043
	PPC	05, -.93	.87, .020			
35°S	Violaxanthin	43, .43	.18, .005	Alloxanthin**	17, .65	.43, .005
	Diatoxanthin	43, -.41	.17, .007	Diadinoxanthin	40, -.53	.29, <.001
	βε-Carotene **	42, .40	.16, .008	Diatoxanthin	32, -.53	.28, .002
	Mg-DVP	43, .38	.14, .013	Chlorophyll c3	40, .38	.14, .015
	Diadinoxanthin	43, -.35	.12, .021	$S_{(f)}$	40, -.67	.46, <.001
				Chlide/TChl-a	40, -.37	.14, .018
Benguela	n.s.			Mg-DVP	05, -.93	.86, .023
				Fucoxanthin	05, .90	.81, .037
30°S (+Br current)	No photo-physiology data			Chlorophyll-b	17, .84	.70, <.001
				Chlorophyll c2	17, -.79	.62, <.001
				βε-Carotene	17, .78	.61, <.001
				Peridin	17, -.77	.60, <.001
				Lutein	13, -.74	.55, .005
				Hex-F	17, -.74	.55, <.001
				DV-Chl/TChla	17, .53	.28, .028
				f_pico	17, .76	.57, <.001
				PSC	17, -.64	.41, .005

* significant relationship when null pigment concentrations are included in the analysis (one sample in these both cases). Therefore, these relationships should be analyzed with caution. In general, null concentrations were excluded, since we assume linear correlations and that a gradient of variability in the pigment concentrations explain the photo-physiological parameters.

** the relationship is no longer significant if null concentrations are included in the analysis.

Table 3. Correlations between σ_{PSII} against pigments ratios (Pigment/ΣA.P. and DV-Chl/TChl-a), Chl-a concentration (fluorometry and HPLC), PSC (photosynthetic carotenoids), PPC (photoprotective carotenoids), proportion of degradation products (Chlide/TChl-a), f_pico (Uitz et al, 2006) and $S_{(f)}$ (Ciotti et al 2002). Only significant results ($p<0.05$) are shown. N is the number of samples considering concomitant pigments and photo-physiology data.

σ_{PSII}	***Surface***			***DCM***		
	Pigments	**N, r**	**r^2, p**	**Pigments**	**N, r**	**r^2, p**
La Plata	Chlorophyll c2	05, -.92	.86, .023	Lutein**	07, .82	.68, .023
	ββ-Carotene	05, .88	.78, .046	Alloxanthin	08, -.80	.64, .018
				Fucoxanthin	08, -.70	.50, .049
				PSC	08, -.80	.64, .017
35°S	Fucoxanthin	42, .48	.23, 0.001	Fucoxanthin	40, .59	.35, <0.001
	Hex-fuco	42, -.39	.16, 0.009	Chlorophyll c2	40, .44	.19, .005
	Lutein	42, -.32	.11, .036	Hex-fuco	40, .-41	.17, .009
	$S_{(f)}$	42, -.39	.16, .010	Lutein	40, -.40	.16, .011
				Chlorophyll c3	40, .35	.13, .025
				$S_{(f)}$	40, -.42	.17, .002
Benguela	n.s.			$S_{(f)}$	40, -.84	.71, .035

30°S (+Br current)	*no photo-physiology	Lutein Zeaxanthin	13, -.74 17, -.64	.56, .005 .42, .005

** the relationship is no longer significant if null concentrations are included in the analysis.

At 35°S, the dynamic range of F_v/F_m was low and it was not related to the biomass and diagnostic pigments. However, photo-protective pigments have shown an important role on F_v/F_m variability in both layers (Table 2). The packaging index $S_{(f)}$ was also correlated to the both photo-physiological parameters, and the best descriptor of F_v/F_m at DCM. In addition, F_v/F_m was negatively correlated to the proportion of degradation product of chlorophyll (Chlide/TChl-a). σ_{PSII}, on the other hand, was primarily explained by the variability of Fucoxanthin, a diagnostic pigment of diatoms, and in less extent by Hex-Fucoxanthin and Lutein (Table 3). At DCM, the proportion of Chl *c2* and *c3* were also correlated to σ_{PSII}. As Fucoxanthin and the accessory chlorophylls presented a positive impact on σ_{PSII}, and Hex-Fucoxanthin and Lutein show the opposite, the direct effect of the taxonomic groups on σ_{PSII} at this sector is not clear. In addition, the Fucoxanthin is a diagnostic pigment of diatoms, however is not exclusive, being present in several other groups. Much of the variability could be explained by the community size, however $S_{(f)}$ shows that higher σ_{PSII} would be related to larger cells, which is opposed to what is expected (Giannini and Ciotti 2016). The relationship between $F_v/F_m$and Chlide/TChla suggests the presence of senescent cells between 10 and 20°W at this sector, where an increase in biomass was observed. Vertical sections of Fucoxanthin ratios and the FlowCam data from the surface (not shown) suggested that this community would be dominated by large diatoms.

The photo-physiology data at the Benguela sector were influenced by the pigments composition only at DCM. F_v/F_m was negatively and positively correlated to the photosynthetic pigments Mg-DVP and Fucoxanthin, respectively, while σ_{PSII} was negatively correlated to $S_{(f)}$. The Mg-DVP is an accessory pigment present in most of

the phytoplankton groups, usually with small contribution, however important in the green algae of the group Prasinophyte.

In the subtropical oligotrophic gyre, complex relationships between photo-physiology and pigments proportion were observed at DCM. As mentioned before, this sector had a greater contribution of *Prochlorococcus* and the proportion of DV-Chla and Chl-b, as well as the fraction of picoplankton (Uitz et al. 2006) were significantly correlated to F_v/F_m, suggesting a positive contribution of this group to the photochemical efficiency of the community, especially in the western basin. An important contribution of βε-Carotene in F_v/F_m variability was observed. In addition, lower F_v/F_m values are driven by the presence of Chl *c2*, Hex-Fucoxanthin, Peridin and Lutein, which was expressed by the negative impact of PSC in F_v/F_m (Table 2). Therefore, a mixed phytoplankton community seemed to be related to the lower photochemical efficiency at the eastern basin of the gyre. σ_{PSII} was negatively correlated to the proportions of Zeaxanthin and Lutein (Table 3), suggesting this parameter is mainly controlled by the presence of *Synechococcus*.

4. Discussion

4.1. The role of pigments ratios in the phytoplankton community photo-physiology in large-scale process

The amount of information about photo-physiological parameters of natural phytoplankton derived from chlorophyll-a fluorescence at large spatial scale has increased in the last decade. A number of studies include observations derived from different oceanographic conditions: phytoplankton blooms (Moore et al. 2005; Suggett et al. 2006); mesoscale eddies (Bibby et al. 2008); Southern Ocean waters (Holeton et al. 2005; Suggett et al. 2009; Lin et al. 2016); tropical and subtropical Pacific and Atlantic waters (e.g. Behrenfeld et al. 2006; Moore et al. 2008; Browning et al. 2014,

Lin et al. 2016); shelf and coastal waters (Moore et al. 2006; Suggett et al. 2009). The variability found in these results encourages the search for patterns and for better interpretations of photo-physiology.

The studies above have discussed the influence of environmental variables and phytoplankton community structure in F_v/F_m and σ_{PSII}. These parameters, especially F_v/F_m, have historically described physiological stress driven by nutrient limitation (Cleveland and Perry 1987; Kolber et al. 1988; Geider et al. 1993, Behrenfeld 2006), however, other studies showed that natural communities are able to acclimate to nutrients-limitation conditions (Parkhill et al. 2001) making the response of photo-physiology more significantly related to phytoplankton taxonomy and dominant cell size (Moore et al. 2008, Suggett et al. 2009; Chapter 3 - now published as Giannini and Ciotti 2016), that at first order varies according with the dynamics of a given environment (Cullen et al. 2002). Although phytoplankton community structure is expected to drive the variability of both F_v/F_m and σ_{PSII}, and also the relationship between each other at least for eukaryotes, the data of the present work show no consistency across large-scale oceanographic regions.

The photo-physiology of phytoplankton in the South Atlantic Ocean is still poorly studied. Recently, Browing et al. (2014) in the mid-austral summer sampled a line of stations in 40°S latitude across the Subtropical Front, demonstrating that the variability of phytoplankton physiology was controlled by nutrients dynamics, which suggested limitation by iron in the eastern basin (south of the subtropical front), and by the balanced macronutrient-limited growth in the western basin (north of the convergence). The authors found unexpected relationships between F_v/F_m and the fractional contribution of some individual diagnostic pigments, such as Hex-Fucoxanthin and Zeaxanthin. The present study was conducted also in the mid-austral

summer along the 35°S and subtropical gyre, and the results showed robust relationships among photo-physiological parameters (F_v/F_m and σ_{PSII}) and a series of individual pigments ratios, assuming linearity (α=0.05). F_v/F_m vertical profile across the eastern basin of the transect at 35°S was similar to the distribution and magnitudes found by Browing et al. (2014).

The comparison between the three zonal sectors in the present study reveals a greater influence of individual photo-protective carotenoids in the variability of F_v/F_m at the 35°S latitude, while the relationship with the PPC index was not significant in this sector. The significant pigment ratios were mainly those involved in the epoxide cycle (Violaxanthin, Diatoxanthin, Diadinoxanthin) that varies enormously according to the previous light history of the algae (Lohr 2011). The physical processes along this sector promote vertical instabilities driven by eddies, which may bring nutrients to the euphotic zone but expose the phytoplankton community to higher light levels, explaining the importance of some photo-protective pigments in F_v/F_m. In the Subtropical Gyre, the main driver of F_v/F_mvariability were the photosynthetic pigments, some of them diagnostic of specific taxonomical groups. In this sector, different from the 35°S, the water column was stratified and the chlorophyll-a concentration was confined at the DCM, with very low biomass along the euphotic layer. Interestingly, the variability of the functional absorption cross-section at 35°W was mainly driven by a mixture of photosynthetic and photo-protective pigments (some of them diagnostic of specific groups), while at the DCM of the gyre, the significant pigments were not photosynthetic.

Differences between surface and deep chlorophyll maximum layers must be investigated with caution, since light and nutrients acclimation processes take place at the DCM, depending on the nitracline depth and euphotic depth (see Cullen et al. 2015

and references therein). The variability of chlorophyll-a concentration with depth do not always represent variability in biomass or carbon content, due to the photo-acclimation processes and differences in nutrients availability (Cullen 1982). Pigment ratios, however, can be helpful to understand the differences in photo-physiology at surface and at the DCM. Across the 35°S sector, where it is possible to contrast surface and DCM layers in large vertical and horizontal scale, the influence of photoprotective pigments on F_v/F_m was similar at the surface and DCM, except for the contribution of Chl *c3* ratios at DCM, however less significant, and the importance of Chlide/TChla and $S_{(f)}$. Chl *c2* and *c3* appeared as important pigments to explain σ_{PSII} variability, which can be related to specific groups, although we believe the presence of Chl *c*, in general, can be also related to degradation products, as well as the Chlide/TChla (Jeffrey et al. 1984), which will be discussed later.

The La Plata sector presented the expected relationship between taxonomy and cell size and the phytoplankton photo-physiology (Suggett et al. 2009): high chlorophyll-a concentrations and diagnostic pigments for diatoms, with higher photosynthetic efficiency and lower σ_{PSII}, were observed in low salinity waters; along the gradient of salinity, chlorophyll-a decreased, as did the photosynthetic efficiency, while σ_{PSII} increased. We expected to observe this same pattern in the Benguela sector, since costal upwelling would drive higher phytoplankton biomass and force community structure gradients from coast to open ocean as reported in previous studies (Fishwick et al. 2006, Lamont et al. 2014). However, the influence of the Benguela current upwelling appeared weak in our dataset (see Silio-Calzada et al. 2008).

4.2. The contribution of *Prochlorococcus* to photophysiology in the subtropical oligotrophic gyre

The distribution of photosynthetic pigments at the Subtropical Gyre sector was related to the contribution of *Prochlorococcus* at the DCM of this transect, which is likely responsible for higher photosynthetic performance at this layer, contrasting with the lower photochemical efficiency of the flagellates from the group haptophytes. Some of its photosynthetic properties may give *Prochlorococcus* a definite selective advantage for growth at depth in oligotrophic areas, particularly compared to *Synechococcus* (Partenski et al 1999). Here we have shown a better photosynthetic performance of this group at DCM compared to the small haptophytes cells, that were identified by the HPLC analysis. The presence of *Prochlorococcus* and Haptophytes were also observed by Araujo (2015), that sampled this longitudinal transect at the same period. The authors also confirmed the presence of *Synechococcus,* besides the *Prochlorococcus* at the surface.

Prochlorococcus is the dominant group in the tropical and subtropical oceans, being part of the most abundant marine picocyanobacteria groups in the worlds ocean, and are important contributors to the global primary production and carbon cycle (Partenski et al. 1999; Huang et al. 2012). Although currently reconized as a single type species (*Prochlorococcus marinus*; Chisholm et al. 1992; Guiry and Guiry 2016), to date, at least 11 *Prochlorococcus* lineages have been identified, among them clades adapted to high and low light (Huang et al. 2012). These authors suggested that low-light adapted genotypes could be more diverse than high-light adapted ones. Recent biochemical studies suggest that different *Prochlorococcus* strains may have different antenna systems specifically adapted to the light environment from which they have been isolated (Partenski et al. 1997). As far as we know there is no specific studies about the differences in the photochemical efficiency of PSII and the effective cross-section of light absorption for distinct ecotypes in natural environments, for both *Prochlorococcus*

and *Synechococcus*, and it is reasonable to suggest that different ecotypes or genotypes might have contrasting photosynthetic performances across large spatial scale in the global oceans, being a subject that deserves further studies.

The higher efficiency of *Prochlorococcus* has been discussed, and they were shown to have high values of F_v/F_m and low σ_{PSII}, following the relationships observed for eukaryotes (Suggett et al. 2009). Compared to other cyanobacteria groups, the *Prochlorococcus* have low amount of phycoerythrin acting as photosynthetic pigment (Steglich et al. 2003), as well as 3-times lower RCI:RCII (Partenski et al. 1997), which lead to the photo-physiology to behave similarly to the eukaryotes groups. Also, *Prochlorococcus* appears highly adapted for growth in a nutrient impoverished environment (see discussion in Moore et al. 2008). There is, however, scarce information on photophysiological properties of DV-Chls and *Prochlorococcus* phycoerythrin (Steglich et al. 2003). Thus, our dataset contributes for the interpretation of large-scale variability and characteristics of the photo-physiology of this group that is still undersampled.

4.3. Senescence diatoms after a mesoscale upwelling and their photophysiology

The importance of photo-protective pigments at 35°S were observed at both surface and DCM, but the ratio Chlide/TChl-a was inversely correlated to F_v/F_m at DCM. Indeed, vertical profiles have shown this index of degradation products have increased between 10 and 20°W, coincident with the higher biomass at the center of the eddy, elevated proportions of Fucoxanthin and lower F_v/F_m values. The same increase in Fucoxanthin at this portion of the sector was also observed by Browing et al. (2014) that sampled the same region two months later. The decrease in photosynthetic efficiency could then be related to the presence of senescent diatoms, suggested by the presence of chlorophyllide-a derived from chlorophyllase activity (Jeffrey 1974). That implies a

rapid process of inactivity in the photosynthetic apparatus after nutrients exhaustion, and samples presented high chlorophyll-a (pigment-containing cells) and high σ_{PSII}. The responses of both F_v/F_m and σ_{PSII} in this region to a physiological stress resembles what is usually observed in batch cultures after nutrients depletion at the stationary phase (Kolber et al. 1988; Parkhill et al. 2001; Suggett et al. 2009). Bibby et al. (2008) have also observed lower F_v/F_m and higher σ_{PSII} at the center of mesoscale eddies, although photo-physiological responses seem to be specific to the eddy type, location and its stage of development. The physiological response of F_v/F_m and σ_{PSII} in this small portion of the 35°S sector, probably due to the intensity of the bloom, seemed to happen in shorter time scale than compared to a taxonomic effect. A senescent community of diatoms in this region could explain the observed negative relationship between σ_{PSII} and the $S_{(f)}$ index, which is opposite to what is expected: large cells are expected to have lower σ_{PSII}, as well as lower $S_{(f)}$. Here, lower $S_{(f)}$ values (i.e. low absorption efficiency) was associated to higher σ_{PSII} and lower F_v/F_m. Although trends with cell size are clear (Ciotti et al. 2002), pigment packaging and concentration can also vary with the physiological state of the community, and might affect such expected relationship.

There are few studies showing direct effects of senescent communities on the photosynthetic efficiency as measured by the PSII fluorescence. Franklin et al. (2009) have shown that the PSII efficiency declines non-linearly with the increase in the proportion of heat-killed cells in a laboratory experiment. Veldhuis et al. (2001) also observed a decrease in photosynthetic activity of different laboratory-grown species with the decrease in cells viability just prior to full cell degradation and, according to these authors, the fact that non-viable cells still possess their photopigments allows clear identification in mixed communities, which could be used in field research. Our results corroborate such idea in the sense that senescent communities originated from

environmental stress, in this case nutrients exhaustion, are photosynthetically inactive but have pigment-containing cells, which can be observed by the chlorophyll-a profile at this section. Interestingly, the longitudinal profile at 40°S from Browing et al. (2014) shows relatively high density of total heterotrophic bacteria between 10 and 20°W sampled two months later than our sampling, which might suggest an intense consumption of the degradation products and dissolved excreted material.

In summary, the relationships discussed here aim to identify trends between pigment ratios and photo-physiology in order to assess the impacts of phytoplankton communities and photo-acclimation processes simultaneously on photosynthetic and absorption efficiencies at different large scale oceanographic regions. Although the chosen linear correlations resulted in low coefficients of determination, the existence of significant correlations are considered important results for the objectives of the study, that did not aim to construct predictive models. Such low predictive power can be related to non-linearity of relationships and the short dynamic ranges of photo-physiological data in some of the sectors studied here, e.g. in the oligotrophic gyre.

Some of the pigments that are considered as tertiary pigments in HPLC analysis and round-robin intercalibrations, such as the Violaxanthin, Prasinoxanthin and Lutein (Van Heukelen and Hooker 2011), presented their proportions significantly important and related to photo-physiological parameters in our study. Tertiary pigments are not among the most commonly measured pigments, however we show they might be important to help explaining some patterns in photo-physiology of natural phytoplankton communities exposed to contrasting environmental conditions.

As phytoplankton pigments composition provides a useful information on taxonomy, but also physiological state and, as shown here, photochemical and light absorption efficiencies, it can be a powerful tool to directly monitor potential primary

production in large-scale and improve future parameterizations. As the signature of dominant cell size is also clear in previous work and through some indexes presented here, the pigments composition from different cell size classes would significantly contribute to the assessment of primary production dynamics in the ocean, using a more direct and non-invasive method, such as the chlorophyll-a fluorescence technique.

CHAPTER 3

Parameterization of natural phytoplankton photo-physiology: Effects of cell size and nutrient concentration

1. Introduction

Measuring carbon primary production in the ocean is extremely challenging due to constraints that range from methodological issues, especially those associated with sample incubation (Bender et al. 1987; Grande et al. 1989; Marra 2002) and uncertainties in respiration and other metabolic rates (Bender et al. 1999; Williams et al. 2002), which can limit primary production measurements in large spatial and temporal scales. Consequently, non-invasive methods for measuring primary production in the oceans have been proposed and become increasingly popular among oceanographers, based on the flow of electrons through photosystem II (PSII) that can be measured by active fluorescence emitted from chlorophyll-*a* (Falkowski et al. 1986; Kolber and Falkowski 1993).

Active fluorometers are able to yield values of electron transfer rates (ETR) occurring during the photosynthetic process (Kolber and Falkowski 1993; Suggett et al. 2003; Oxborough et al. 2012) that can subsequently be converted into an estimate of carbon uptake (e.g. Lawrenz et al. 2013). Computation of ETR requires specific parameters obtained from fluorimetric measurements, including the PSII photochemical efficiency (Φ_{PSII}), under low and regulated actinic light, and the functional absorption cross-section of PSII (σ_{PSII}) (Kolber and Falkowski 1993). Active fluorescence yields from dark-acclimated samples, or under low light conditions, typically provide the maximal photochemical efficiency (Φ_{PSII}^{max} or F_v/F_m), while the effective photochemical efficiency (Φ_{PSII}' or F_q'/F_m') is measured under regulated actinic light.

Such fluorescence techniques have been widely used and improved in the last years (e.g. Oxborough et al. 2012), providing measurements of photochemical parameters at different temporal and spatial scales, and are thus a promising technique to better examine primary production in aquatic environments.

Photo-physiological parameters such as F_v/F_m and σ_{PSII} are used to evaluate the photosynthetic performance of different phytoplankton species and their growth conditions, but also reflect the environmental history and responses of selective pressure of evolution (Suggett et al. 2009a). It is therefore fundamental to understand the variability of such parameters in the ocean and how they relate to environmental conditions and the phytoplankton community distribution and, consequently, how they impact on primary production estimates of marine ecosystems. In natural communities, phytoplankton photosynthetic rates vary in response to physical forcing acting over a wide range of temporal and spatial scales. As ambient nutrient availability plays an essential role in F_v/F_m and σ_{PSII} variability, their relationships have been studied extensively (e.g. Behrenfeld et al. 2006; Bibby et al. 2008; Rattan et al. 2012). During nutrient limitation, phytoplankton cells typically exhibit an increased σ_{PSII} and concurrent decrease in F_v/F_m, arising from a loss of functional PSII reaction centers relative to the proportion of antenna complexes (Greene et al. 1992; Suggett et al. 2009a). However, laboratory experiments exposing cells to prolonged nutrient limitation, demonstrate that these impacts can be minimized via acclimation and maintenance of balanced growth (Parkhill et al. 2001); thus in natural conditions where nutrient limitation persists (e.g. Moore et al. 2013) physiological effects of nutrient-limitation are not as strong as taxonomic differences (Suggett et al. 2009a). Conversely, such trends may not be clear where cells may be episodically subjected to periods of

nutrient limitation, transient nutrient exposure and nutrient starvation, resulting in persistent unbalanced growth (Rattan et al. 2012).

Besides the impacts of environmental condition on both F_v/F_m and σ_{PSII}, several studies have demonstrated the influence of phytoplankton cell size and taxonomy on measurements of variable fluorescence, and hence on their photosynthetic rates (Suggett et al. 2004; Suggett et al. 2009b; Rattan et al. 2012; Moore et al. 2005). Specifically, whilst lower F_v/F_m and increased σ_{PSII} occurs via nutrient starvation, the same response also occurs via taxonomic changes under nutrient limitation: the small cells that are favored in low-nutrient environments exhibit lower F_v/F_m and higher σ_{PSII} values than larger cells (Fishwick et al. 2006; Suggett et al. 2009a). Variability of pigment concentration inside the cell appears to govern this trend (Suggett et al. 2004, 2009a; Moore et al. 2005; Blache et al. 2011). Therefore, influence of dominant cell size on the light absorption properties is a key factor (Ciotti et al. 2002, Uitz et al. 2008), such that community structure-driven changes in light harvesting likely plays a major role in influencing the maximum achievable ETR and carbon assimilation rates.

Despite the community structure influence on photo-physiology, choosing representative taxonomic-specific parameterizations of primary production models is an extremely difficult task, especially in coastal waters, where local hydrodynamics can lead to changes in the composition of phytoplankton communities on a time scale of hours to days. As an alternative to taxonomic-specific classification, natural communities can be classified into discrete groups according to dominant cell size (sensu Sieburth et al. 1978), still reflecting key environmental conditions, such as nutrient variability (Cullen 2002). Indeed, the relationship between cell size, photo-physiology and metabolism has been widely examined in the last few years (Suggett et al. 2009a; Lopez-Sandoval et al. 2014; Marañon et al. 2015). Therefore, understanding

the impacts of dominant cell size upon photo-physiology and ETR, and their subsequent conversion to estimates of carbon assimilation, is an essential step towards improving primary production models derived from active fluorometry.

The main goal of this study was to examine for the first time the relationship between the dominant size of natural phytoplankton communities and variability of photo-physiological parameters, i.e. F_v/F_m and σ_{PSII}, considering different ambient nutrients conditions. The study area included two sites of contrasting nutrient availability in a meso-oligotrophic coastal region in southeastern Brazil: a small and shallow bay and the adjacent deeper and advective channel (Figure 1) that were sampled on scales of days and months. As the bay exchanges water with the channel due to the tidal cycle, and nutrient concentration is consistently higher in the bay, the sampling design allowed discrimination of the effects of different levels of nutrient availability from cell size on the parameterization of fluorimetric photo-physiology.

2. Theoretical background

For a given phytoplankton cell, the relationship between fluorescence and photosynthesis rates can be developed as function of the relative efficiencies between these processes at PSII. Kolber and Falkowski (1993) proposed a model that associates the active PSII fluorescence emitted by samples containing live cells with the first step of electron transfer during the photosynthetic process. Measurements of electron transfer rates at PSII (ETR_{PSII}) allow the estimation of carbon uptake rates by phytoplankton (Pc) according to:

$$\mathrm{Pc} = \mathrm{ETR_{PSII}} \cdot \emptyset_e \cdot \mathrm{PQ}^{-1} \ , \qquad (1)$$

where $\emptyset_e$ is the ratio of electrons transferred per O_2 molecule produced during photosynthesis (mol O_2 (mol electron)$^{-1}$) and PQ (photosynthetic quotient) is the ratio between produced O_2 and fixed CO_2 (mol O_2 (mol C)$^{-1}$). ETR_{PSII} is a function of photo-

physiological parameters, i.e., the effective light absorption (σ_{PSII}) and the photochemical efficiency of PSII (Φ_{PSII}), and it is given by:

$$ETR_{PSII} = \sigma_{PSII} \cdot \Phi_{PSII} \cdot E \cdot \Phi_{RC} \quad , \qquad (2)$$

where Φ_{PSII} is dimensionless, σ_{PSII} is given in $m^2(RCII)^{-1}$ and E is the available irradiance (mol photons m^{-2} s^{-1}). Both σ_{PSII} and Φ_{PSII} can be directly measured from responses in active fluorescence (Kolber and Falkowski 1993; Kromkamp and Forster 2003). Φ_{RC} represents the quantum yield of electron transfer within the reaction center, which is constant and assumed to be unity (i.e. one electron is transferred per quanta absorbed and delivered to the reaction center). The fluorometer used in this study delivers excitation centered at 452nm, with a 30nm bandwidth, therefore the term σ_{PSII} is replaced by $\sigma_{PSII(452)}$ hereafter.

In order to compute ETR_{PSII} light-response curves, as equivalent to a photosynthesis-light curve (Jassby and Platt, 1976), Φ_{PSII} is measured across a gradient of light steps (Φ_{PSII}' or F_q'/F_m'), after a dark-step (Φ_{PSII}^{max} or F_v/F_m), which also provides $\sigma_{PSII(452)}$ for both conditions. However, measurements of $\sigma_{PSII(452)}$ can be extremely noisy under high actinic light conditions (see Oxborough et al. 2012), which indeed we observed in our dataset; and we therefore used an alternative ETR_{PSII} model that employs $\sigma_{PSII(452)}$ measured on dark-acclimated samples (Suggett et al. 2010). As such ETR_{PSII} at each light step of light-response curves were computed as follows:

$$ETR_{PSII} = \sigma_{PSII(452)} \cdot \frac{F_q'/F_m'}{F_v/F_m} \cdot E \qquad (3)$$

The maximal photochemical efficiency (F_v/F_m) was obtained after at least 20 minutes of dark-acclimation of the samples, in order to relax the energy-dependent non-photochemical quenching (i.e. the dissipation of absorbed excitation energy as heat), while the effective photochemical efficiency (F_q'/F_m') was measured from fluorescence transients obtained under actinic light and represents the product of non-photochemical

quenching and the efficiency of photochemical charge separation. ETR_{PSII} light curves were computed as averages of three replicates. Details of the protocol used in this work to obtain the fluorescence transients and the light curves parameters are found on Methods section.

Volumetric calculation of ETR_{PSII}, i.e., in mol electron m^{-3} h^{-1}, also requires knowledge of number of functional reaction centers per chlorophyll-a (n_{PSII}). Because direct measurements of n_{PSII} are notoriously difficult to perform in the field, many studies have assumed a fixed value (n_{PSII}=1/500; Kolber and Falkowski 1993), despite evidences that n_{PSII} varies across different phytoplankton taxa and growth conditions (Suggett et al. 2010; Oxborough et al. 2012). Finally, the conversion of volume-based ETR_{PSII} into carbon fixation estimates must also consider the "electron requirement for carbon fixation" (ϕe:c) (see Lawrenz et al. 2013) describing the efficiency with which electrons are invested into CO_2 fixation, which is also non-linear (Ralph et al. 2010).

3. Methods

3.1. Study region and sampling design

The study was conducted in the São Sebastião channel (SSC), a coastal region off São Paulo state in Brazil (Figure 1), where the regional hydrography is primarily controlled by remote winds, frontal systems and localized coastal upwelling events (Ciotti et al. 2014). The low year-round nutrient concentrations at SSC are modified by intrusions of the SACW (South Atlantic Central Water) during upwelling events off Ubatuba, located nearby the northern entrance of the SSC (Castro 2014), which would influence the primary production rates in this region via nutrient inputs (Saldanha-Corrêa and Gianesella 2008). Nevertheless, more recent studies show that the effects of the SACW in the channel are limited to the deep layers (Dottori et al. 2015) and that episodic nutrient enrichment occurs during the passage of frontal systems (Peres, 2013).

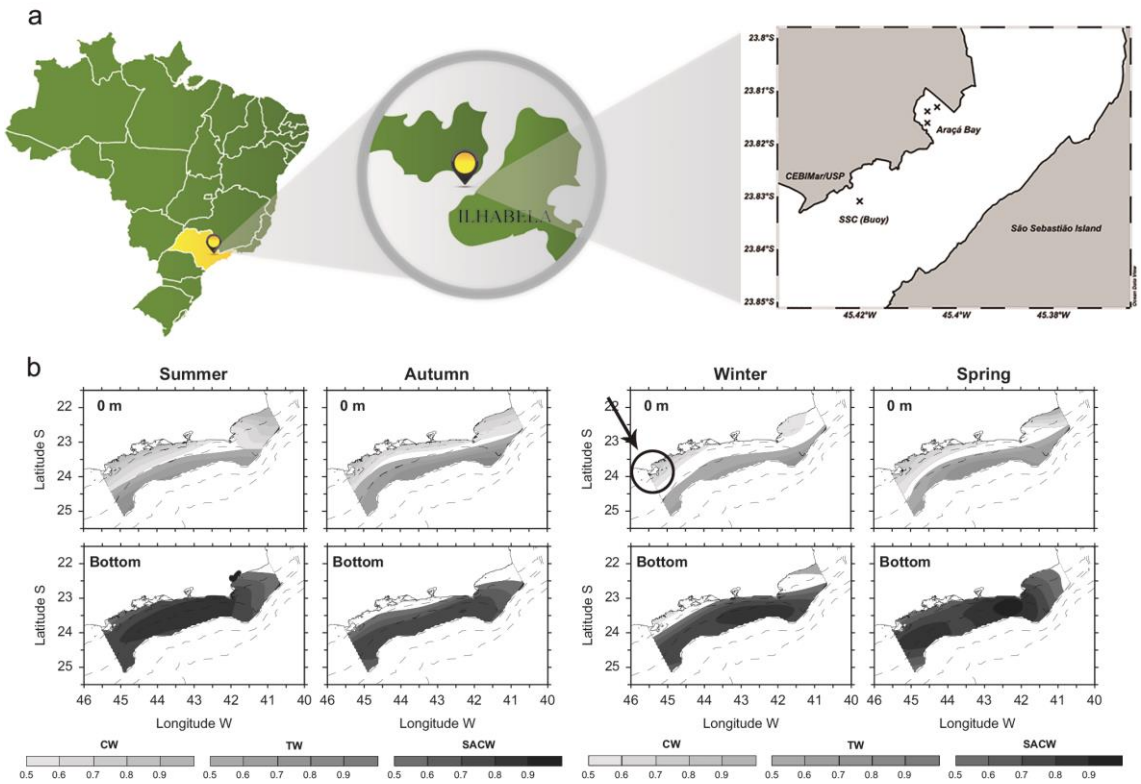

Figure 1. a. Study area located at the coastal region off São Paulo State in Brazil. The symbol 'x' indicates the two samplings areas: São Sebastião Channel (SSC) and Araçá Bay. b. Seasonality of water masses at the surface and bottom of São Sebastião coastal waters (Modified from Cerda & Castro, 2014). CW=Coastal Water; TW=Tropical Water; SACW=South Atlantic Central Water. The colourbars represent the water mass proportions (above 0.5) for each depth layer, derived from temperature and salinity indexes, according to Cerda & Castro (2014). The black arrow and the circle indicate the location of the São Sebastião Channel.

Previous studies carried out in the São Sebastião channel and adjacent continental shelf waters have shown generally low dissolved inorganic nutrient concentrations, due to the water masses that flow into the channel as well as for the relatively low continental runoff, which characterizes this region as meso-oligotrophic (Saldanha-Corrêa and Gianesella 2008). Nutrient analysis has revealed low nitrate concentrations, resulting in N:P ratios in general below 16:1, even for the deeper waters, where the influence of SACW upwelling occurs during spring months (Gianesella et al. 1999; Gaeta et al. 1999; Peres 2013, Saldanha-Corrêa 1993). Among those studies, the average nitrate, phosphate and silicate concentrations were below 10, 1 and 10 µmol/L,

respectively, where the highest values of nitrate (above 5µmol/L) were usually found at bottom waters of SSC during spring or summer (Gianesella et al. 1999; Peres 2013).

In the current work, three-days sampling surveys were carried out approximately every month from September 2013 to August 2014. The samples were collected at two different sites that were visited twice a day (morning and afternoon), to give approximately 12 samplings per survey. One site was located in the São Sebastião channel (SSC), near the CEBIMar/USP oceanographic buoy (14 m depth, http://www.simcosta.furg.br/portal/), while the other was inside Araçá Bay (AB; 1.5 m depth), which is located in the continental margin of the São Sebastião channel. A 5L-Van Dorn bottle was used to sample water from 1m depth, which was kept in dark, temperature-insulated bottles until laboratory processing. Three independent casts were performed and the samples were combined. The water collected from Araçá Bay was a pooled sample from three distinct points, as shown by Figure 1, in order to render a more representative sample of the bay. The analysis included quantification of chlorophyll-a concentration in distinct size fractions, determination of inorganic nutrient concentrations and phytoplankton photo-physiology measurements.

Significantly higher concentrations of dissolved inorganic nitrogen (DIN; nitrate, nitrite and ammonium), phosphate and silicate were found inside the Araçá Bay compared to the adjacent channel (t-test; $p<0.02$). Due to the low nutrient concentrations in the São Sebastião channel, we have assumed that events where N:P ratios (i.e. DIN:Phosphate ratios) were above the overall median are considered here as favorable nutrient conditions for the local phytoplankton community, which occurred for more than 70% of the cases inside the bay. Previously published studies do not allow for systematic analyses of nutrient conditions since they were episodic. The

median values chosen are, thus, based on a quality-controlled dataset available since June 2013.

3.2. Phytoplankton size dominance and the community size index

Fractionated phytoplankton biomass was estimated from four different size fractions of chlorophyll-a concentration, for which 250mL of water were pre-filtered through polycarbonate (5µm and 2µm pore sizes) or nylon (20µm pore size) membrane filters, and the respective filtrates were concentrated on GF/F filters (nominal pore size 0.7µm). In addition, a non-fractionated sample was directly concentrated in a GF/F filter to represent the total chlorophyll-a concentration. The microplankton fraction was obtained from the difference between the chlorophyll-a from total and the 20µm pre-filtered sample; the nanoplankton and ultraplankton correspond to the differences between the chlorophyll-a from the pre-filtered samples at 20 and 5µm and 5 and 2 µm filters, respectively; and finally, the picoplankton fraction resulted from the difference between the chlorophyll-a of the total and the pre-filtered sample through the 2µm membrane filter. For the 2µm pre-filtration, no vacuum was used, in order to avoid contamination of the samples by larger cells or detritus, and also to maintain the integrity of the sample, which is very fragile at this size fraction. Chlorophyll pigments were extracted in 5mL 90% acetone + DMSO solution (6:4 – Shoaf and Lium 1976), for at least 24h in dark and under -20°C, and the chlorophyll-a concentration was measured fluorimetrically with a calibrated Turner-Design fluorometer, through the non-acidification method (Welschmeyer1994). A calibration factor obtained from a commercial chlorophyll-a standard (Sigma-Aldrich) was used to calculate the final chlorophyll-a concentration from triplicates of fluorescence measurements.

Once the fractionated biomass was calculated, the dominant phytoplankton size was obtained from the different proportions among those size fractions, as shown in

Table 1. The dominant size categories include both dominance and co-dominance of size groups. The approach used here for the classification of community size dominance is a modification of that proposed by Ciotti et al. (2002), but including also co-dominance of size groups. Samples that did not contain either two size fractions above 30% or one size fraction above 40%, were classified as No Dominance (N.D.) and were excluded from later statistical analysis.

Table 1. Classification of the dominant community size of phytoplankton based on four size fractions of chlorophyll-a concentration: microplankton (Micro: >20 μm), nanoplankton (Nano: 5-20 μm), ultraplankton (Ultra: 2-5 μm) and picoplankton (Pico: <2 μm). The Mean Size Index ($\overline{SI(\mathrm{chl})}$) was calculated according to Equation 4 for each dominant size group.

Dominant Size Group	$\overline{SI(chl)}$**(±SD)**	**Size fractions**	**%Micro**	**%Nano**	**%Ultra**	**%Pico**
1	29.75(±1.46)	Microplankton	**> 40**	< 30	< 30	< 30
2	- *	Micro + Nanoplankton	**> 30**	**> 30**	< 30	< 30
3	20.74(±0.90)	Micro + Ultraplankton	**> 30**	< 30	**> 30**	< 30
4	-	Micro + Picoplankton	**> 30**	< 30	< 30	**> 30**
5	18.28	Nanoplankton	< 30	**> 40**	< 30	< 30
6	12.85(±0.25)	Nano + Ultraplankton	< 30	**> 30**	**> 30**	< 30
7	-	Nano + Picoplankton	< 30	**> 30**	< 30	**> 30**
8	11.81(±0.40)	Ultraplankton	< 30	< 30	**> 40**	< 30
9	9.23(±0.52)	Ultra +Picoplankton	< 30	< 30	**> 30**	**> 30**
10	-	Picoplankton	< 30	< 30	< 30	**> 40**
11	17(±0.62)	No dominance (N.D.)**	< 30	< 30	< 30	< 30

* The symbol "-" represents the absence of that dominant size group in our dataset.
** N.D. also includes samples that present only one size fraction above 30%.

In order to assign a representative size, in μm, for each group in Table 1, we estimated a size index ($SI(chl)$) for each sample based on the work proposed by Bricaud et al. (2004). Our approach used the percentages of the four chlorophyll fractions in the sample and a weighting function as a size index (Equation 4). It is important to note that the central sizes used for each fraction is an approximation, based on local dataset of phytoplankton sizes (unpublished data) and can be modified if

necessary. The index was then averaged for each size dominance group ($\overline{SI(chl)}$) of Table 1.

$$SI(chl) = (\%M \cdot 50 + \%N \cdot 15 + \%U \cdot 3 + \%P \cdot 1)/100 \qquad \text{Equation (4)}$$

The terms %M, %N, %U, %P in equation 4 are, respectively, the percentage of microplankton, nanoplankton, ultraplankton and picoplankton.

3.3. Physico-chemical data

Vertical profiles of water column temperature and salinity were obtained using two CTD systems (YSI Castaway CTD, YSI Inc. and AAQ-Rinko, JFE Adavantech Co., Ltda). Only the upper 1m data were used for the analysis, however, complete vertical profiles could be used to discuss and interpret the results. Sea level height was obtained in high resolution (30min) by an ADP (Aquadopp Profiler - Nortek -1MHz) deployed in a mooring system near the entrance of the Araçá bay (-23.817; -45.402).

The concentration of inorganic nutrients, such as nitrogenous compounds (nitrate, nitrite and ammonia), phosphate and silicate, were quantified spectrophotometrically (Hatch spectrophotometer, Model DR5000), according to Aminot and Chaussepied (1983). Most of the samples were analyzed fresh, but in some cases they were filtered and then frozen until analysis. The ambient N:P ratios were also calculated, as the ratio of DIN to phosphate. The nitrate and nitrite concentrations were summed, as nitrite concentrations were consistently low throughout the analyzed period.

3.4. Meteorological data

Surface radiation values (W/m^2) were obtained at 10-minute resolution from the CEBIMar/USP meteorological station (-23.823; -45.422). The radiation data provided by the sensor (spectral range from 400 to 1100nm) was approximated to the Photosynthetically Available Radiation (PAR: 400 to 700nm) multiplying the solar radiation by 45% (Kirk 1994). This conversion factor is in agreement with comparisons

made between the sensor and the PAR sensor at the CTD system used during the observations (factor of 41.9% - data not shown). PAR data was then converted from W/m^2 to µmol photons $m^{-2}s^{-1}$ using the factor of 4.57 proposed by Thimijan and Heins (1983). The surface PAR values were averaged for two hours preceding the samplings, that were finally averaged for each survey in order to have a mean irradiance intensity that our samples were subjected to. The meteorological station also provided wind speed (m/s) and direction (10-minute resolution) and daily precipitation rates (mm/day), which complements the overview of the environmental conditions preceding each field sampling.

3.5. Photo-physiology and electron transfer rate measurements

Photo-physiological data were obtained with a Fluorescence Induction and Relaxation System (FIRe) bench-top fluorometer (Satlantic LLP). Measurements were performed using the discrete sample mode, and the results are averages of independent measurements performed in triplicates. Fluorescence transients were measured after a saturating LED pulse and an iterative fitting routine was applied to the fluorescence induction curves as a function of the cumulative excitation light to derive F_0 (or F'), F_m (or F_m') and $\sigma_{PSII(452)}$as per Kolber et al. (1998). The data was processed using the Fireworx script for Matlab (Fireworx/2007, developed by A. Barnett and available at sourceforge.net/projects/fireworx and Matlab/2009). The parameters derived from the curve fitting allowed calculations of photosynthetic efficiencies in dark and light conditions (F_v/F_m and F_q'/F_m'). ETR_{PSII} light response curves were derived from intensities spanning 0–600 µmol photons $m^{-2}s^{-1}$ using 7 light steps. The actinic light source was turned on 25s before the start of the acquisitions at each light step to acclimate the cells to the light intensity, and dark intervals of 20s were used after each light step. The single turnover (STF) protocol was used with a flash length of 100µs

(blue LED) and 15 sequential repetitions, with a delay of 10s between acquisitions, to allow the recovery and re-opening of the closed reaction centers between repetitions, as the light curves are generated from static samples. The maximum rate of photosynthesis (ETR_{max}), light utilization efficiency (α_{ETR}) and light-saturation parameter E_k ($E_k = \alpha_{ETR}/ETR_{max}$) were calculated by fitting a hyperbolic tangent model (Jassby and Platt 1976) to the ETR_{PSII} light curves. The FIRe was calibrated with pure chlorophyll-a extract (Sigma-Aldrich) and monitored monthly.

3.6. Data analysis

Descriptive statistics shows the variability of temperature, salinity, irradiance, and inorganic nutrient concentrations in monthly averages. As mentioned previously, this is the first dataset describing nutrients with consistent temporal resolution for this region, especially inside the Araçá Bay. The variability of size-fractionated chlorophyll-a concentrations, the community size index (SI(chl)) and the community photo-physiological parameters (F_v/F_m, $\sigma_{PSII(452)}$, ETRmax and α) are also presented as monthly averages for both sampling sites. T-test analysis was used to compare means between both sampling sites for nutrients, chlorophyll-a concentration (total and four size fractions) and the photo-physiological parameters, using the software package Statistica v.12.

Multivariate exploratory analyses were performed using the PRIMER (v.6) in order to ordinate the samples according to the environmental variables through PCA (principal component analysis) and nMDS (multidimensional scale) plots. Then, the relationship between the environmental variability and the size classes of phytoplankton, using the micro, nano, ultra and picoplankton proportions, was tested using a RELATE analysis that compares the similarity matrix between both datasets in order to verify if the size classes distribution is related to the ordination of

environmental parameters variability. The same procedure (RELATE analysis) was performed to identify relationships between the environmental variables and the photo-physiological parameters of the phytoplankton community.

In addition to the ordination techniques to summarize the samples distribution according to environmental variables and photo-physiological parameters, the differences between the generated grouping samples were tested thorough a PERMANOVA analysis. The PERMANOVA was performed to test the hypothesis that there is no difference between the environmental variables distribution among the sampling surveys, both sites and different dominant size groups ($\overline{SI(chl)}$), also looking for the interaction among those three grouping factors. The resemblance matrices used for the multivariate analysis were based on Euclidian distance for the normalized environmental dataset, and Bray-Curtis similarity for the normalized data of community size fractions and photo-physiological variables.

Linear regression models were used to address the effects of phytoplankton dominant community size on the measured photo-physiological parameters (F_v/F_m and $\sigma_{PSII(452)}$), following the linearity suggested by the literature (Suggett et al. 2009a). Thus, the photo-physiological parameters were correlated to the mean size index ($\overline{SI(chl)}$) of the dominant size groups proposed by Table 1. The parameters of the ETR_{PSII} light curves, ETR_{max} and α_{ETR}, were also correlated to the mean size index.

To discriminate and explore the influence of nutrients upon the observed relationships between community size and photo-physiology, the dataset was split into two different levels of nutrients. The threshold used to discriminate nutritional conditions was the overall median of N:P values reported for the region, based on the dataset available since June 2013.Thus, positive and negative anomalies around the median represent high and low levels of nutrients, respectively. A number of distinct

thresholds were tested (e.g., silicate, DIN) however the best predictive responses were obtained when N:P was used. The linear regression between size and photo-physiological parameters were compared for both nutrients conditions using an ANCOVA test (SPSS software, V20). The effective photochemical efficiency (F_q'/F_m'), as a non-linear function of irradiance (Silsbe and Kromkamp2012) was fitted to an exponential model (Webb et al. 1974) and compared between the dominant size groups.

3.7. ETR_{PSII} primary production model parameterized by the dominant community size

According to the influence of phytoplankton community dominant size and nutrients availability on the phytoplankton photo-physiological variability ($\sigma_{PSII(452)}$, F_v/F_m and F_q'/F_m'), a parameterization of the Equation (3) was proposed in order to estimate ETR_{PSII} light curves for different community dominant size. The estimation of primary production values as carbon uptake (Pc: mgC mgChl-a^{-1} h^{-1}) from the ETR_{PSII} light curves required the use of a fixed value for n_{PSII} (=0.002; Kolber and Falkowski, 1993), as well as a fixed ratio of the electron requirement for carbon fixation (ϕe:C = 8). The latter is an approximate ratio found for natural communities dominated by cyanobacteria and small flagellates (Suggett et al. 2009b), which was chosen due to the dominance of small cells found in our study, based on the fractionated chlorophyll-a concentration.

4. Results

4.1. Oceanographic conditions and nutrients variability

The temperature of surface waters showed the expected seasonal pattern, varying from approximately 19 to 29°C, while the salinity ranged from 31 to 35 PSU, with no clear seasonality (Figure 2). Vertical profiles of temperature and salinity showed a more stratified water column during the summer surveys (data not shown). The variability of solar irradiance (average value of the two hours preceding each

sampling) ranged from very low values (around 60 µmol photon $m^{-2}s^{-1}$) in the morning samplings during winter to around 2000 µmol photon $m^{-2}s^{-1}$at noon during summer. It is important to note that even during winter months the irradiance can occasionally reach very high values in this subtropical region, such as in August 2014 (Figure 2), when the three-day average was 1000µmol photon m^{-2}.

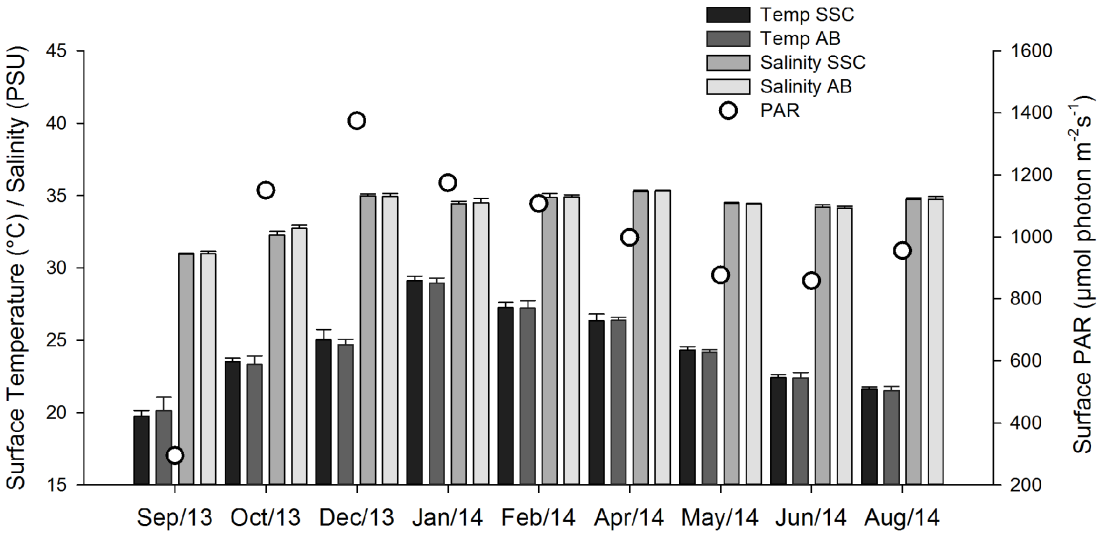

Figure 2. Temperature (°C) and Salinity (PSU) (bars) of the surface waters for each sampling site (SSC=São Sebastião channel; AB= Araçá Bay), and the incident PAR irradiance (µmol photon $m^{-2}s^{-1}$; open circles) for the study region. The temperature and salinity data are averages of the days during the sampling surveys and the whiskers are the standard deviations. The PAR data were averaged for two hours preceding the sampling, which were presented here as averages for each sampling.

The tidal cycle of São Sebastião coast is a semi-diurnal cycle with higher amplitudes in summer (Castro et al. 2008). During the present study, the highest tidal amplitude was observed in January 2014 (1.25±0.1m) while the lowest range was measured in May 2014 (0.78±0.06m), which was the only sampling carried out during a neap tide. All others samplings were performed during spring tides or during a transition phase.

From August 2013 to January 2014, north-easterly and westerly-south-westerly winds were predominant, in general with moderate speeds. High-speed wind gusts from

the west-southwest were registered for 20% of the data from September 2013. During the October 2013survey, strong winds from the east occurred on the second day of the sampling. The surveys from February 2014 toAugust 2014 showed predominant north-easterly winds (>50%), followed by south-westerly winds (approximately 20%). Strong south-westerly winds were recorded before the August 2014 sampling, due to the passage of a frontal system. Low precipitation was registered during all surveys (up to ~4 mm/day), except for February 2014, when the precipitation approached 65 mm/day.

The São Sebastião channel and the adjacent waters are characterized by low nitrogen availability, as described above (Methods). Our dataset also shows low nutrient concentrations (Figure 3), specially for the inorganic nitrogenates in the São Sebastião channel, and in general, molar N:P ratios were low for the entire dataset, varying from 0.23 to 9.5, with a median value of 2.23.Although still low, the N:P ratios for the Araçá Bay were significant higher (N:P=3.58 in the bay against 2.28 in the channel), as DIN and phosphate concentrations (t-test; $p<0.01$). Silicate concentrations did not differ between sites (t-test; $p>0.05$). An increase in the N:P ratios was observed in the September 2013 and February 2014 surveys at both sites, which coincided with the highest values of chlorophyll-a.

Nitrate plus nitrite concentrations varied from 0.16 to 2.02 µmol/L in the bay and 0.07 to 0.57 µmol/L in the channel, while the ammonium concentrations varied from 0.13 to 2.13µmol/L in the bay and 0.01 to 0.62 in the channel. In general, maximum DIN concentrations were recordedin September 2013 in the Araçá Bay, and the lowest concentrations were measured in December 2013 and January 2014 in the channel (Figure 3a and 3b). The phosphate concentrations ranged from 0.17 to 1.0 µmol/L in the bay and 0.09 to 0.71 µmol/L in the channel. In the Araçá Bay, thelowest phosphate values were recorded for January and February2014, however, the greatest

variability was observed in January, when the maximum values were also recorded (Figure 3c). A similar pattern was observed in the channel, except that the lowest phosphate concentration was observed in September2013. The silicate concentration ranged from 1.36 to 6.27 µmol/L in the bay and from 1.04 to 6.16 µmol/L in the channel (Figure 3d).

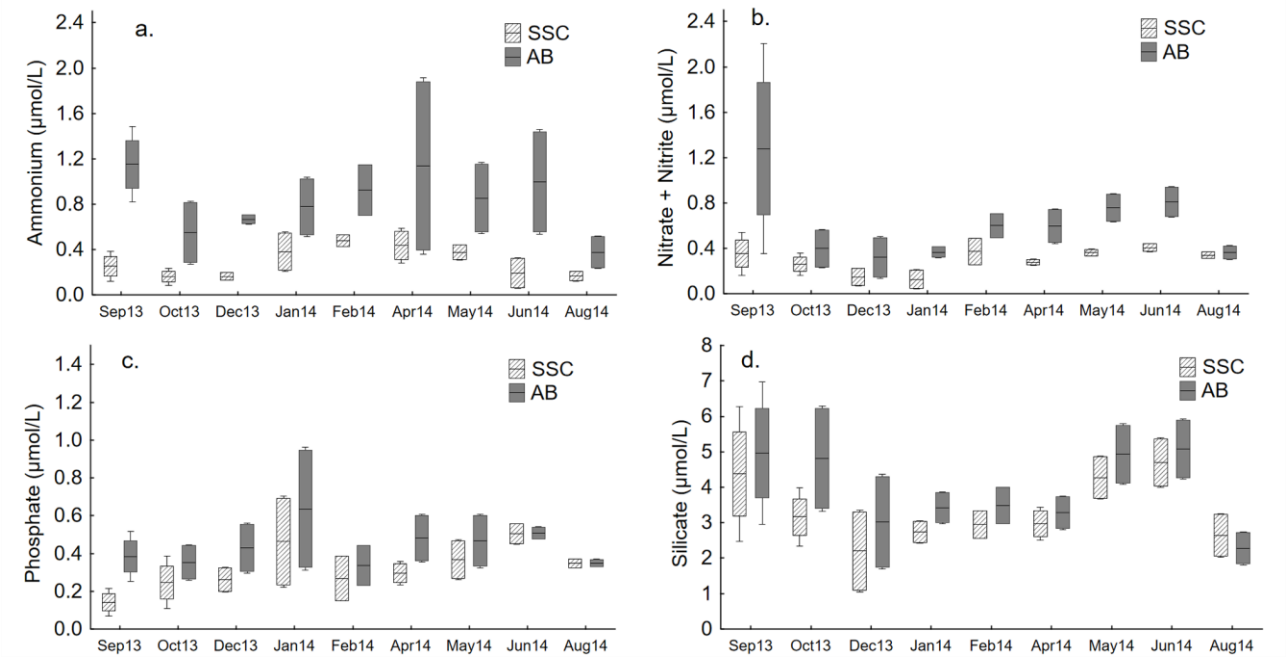

Figure 3. Variability of nutrient concentrations at the two study sites (SSC= São Sebastião channel; AB=Araçá Bay). a. Ammonium, b. Nitrate plus Nitrite, c. Phosphate and d. Silicate concentrations (µmol/L). Boxes represent the mean of the three sampling days within each survey and the standard deviations, and whiskers are the 95% confidence intervals. Note that the y-axis scales are different.

The multivariate PCA analysis shows the similarity among the samples according to environmental variables, where we could observe a clear clustering of different surveys varying across the temperature and salinity axis (Figure 4a). On the other hand, the sampling sites were clearly grouped according to variability in nutrients concentrations (not shown). The first two principal components explained comparable degrees of variability of the data, with PC1 = 36.7% and PC2 = 30%.

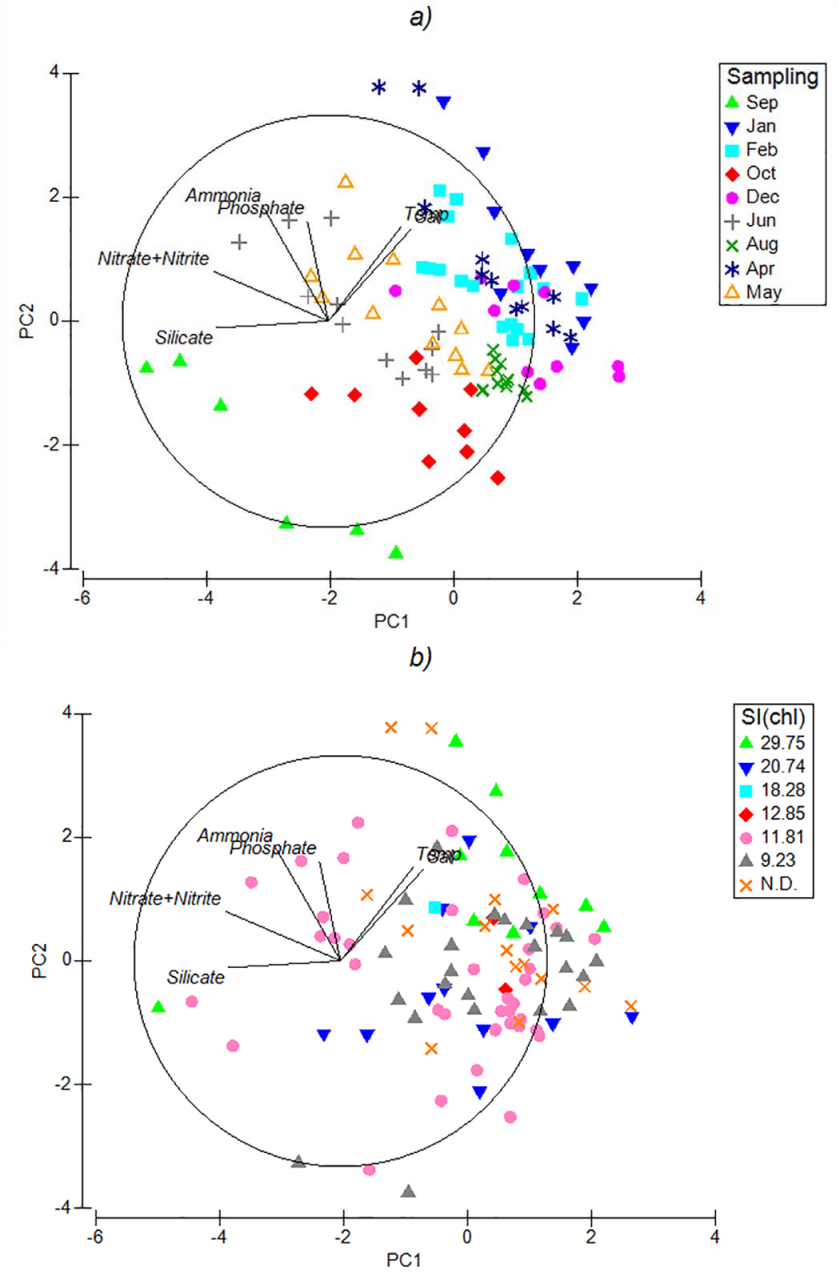

Figure 4. a. Principal Component Analysis (PCA) of the normalized data matrix of environmental variables coded with the samplings surveys (months). b. PCA of normalized environmental data, coded with the mean size index ($\overline{SI(chl)}$) of phytoplankton communities.

4.2. Distribution of the phytoplankton dominant community size

Total chlorophyll-a concentrations were significant higher in the Araçá Bay, as were the >5µm fraction, which includes the micro and nanoplankton($p<0.01$). Overall, the mean total chlorophyll-a in the bay was 2.49 mgm^{-3}, and the micro- and nanoplankton fractions were 0.67 and 0.32 mgm^{-3}, respectively. In SSC, the averages were 1.96, 0.37 and 0.18 mgm^{-3} for the total chlorophyll-a, microplankton and

nanoplankton, respectively. The chlorophyll-a from ultraplankton and picoplankton were not significantly different between the bay and the channel, with overall averages of 1.05 and 0.55 mgm^{-3} for ultra and picoplankton in the bay, respectively, and 0.88 and 0.53 mgm^{-3} in the channel. Figure 5 presents the variability in the proportion of the four size classes of phytoplankton over time.

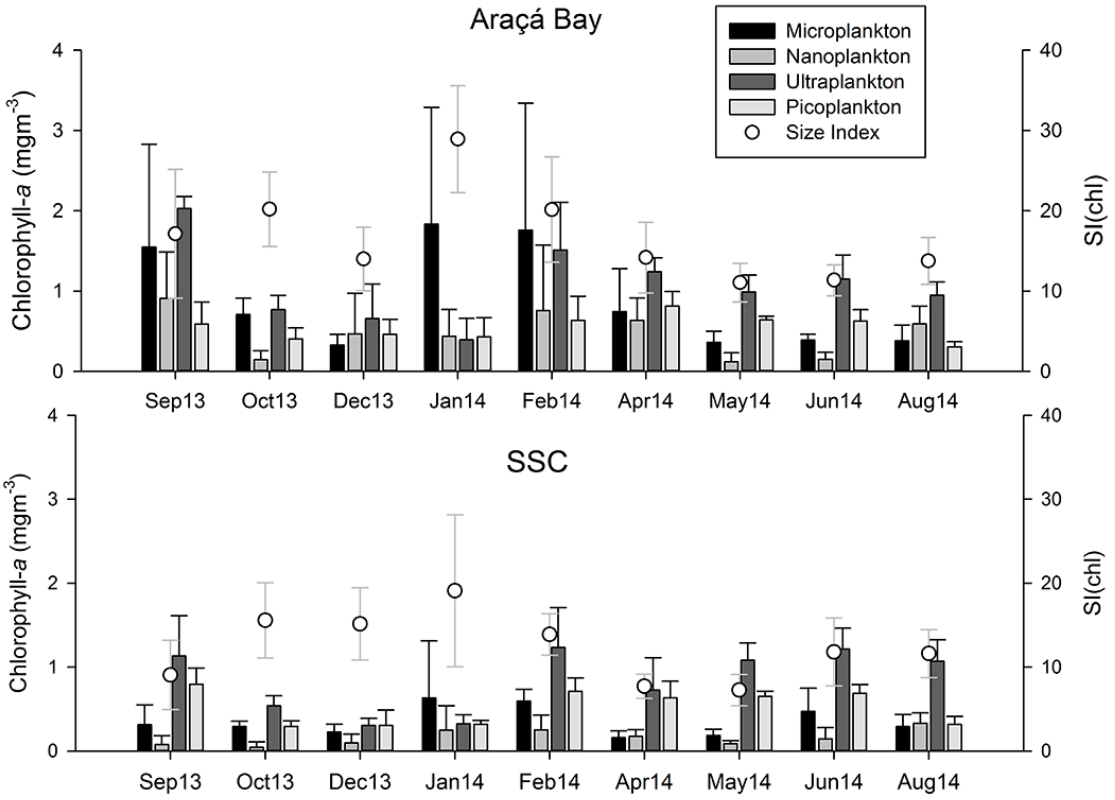

Figure 5. Variability of the phytoplankton size classes (mean±SD), based on fractions of chlorophyll-a concentration (mgm^{-3}) (y-left axis). The open circles are the size index (SI(chl)) calculated according to equation 4 for the dominant phytoplankton community for each sampling survey (mean±SD) (y-right axis).

According to the phytoplankton dominant size (Table 1), Group 8, with the largest proportion of ultraplankton (>40%), was the most abundant, occurring in 35.2% of the samples in the Araçá Bay and in 40% of the cases in the channel (Table 2). Samples dominated by the nanoplankton, as well as other dominance groups defined at Table 1, were nearly absent. Approximately 17% of the dataset did not show any dominance of size.

Table 2. Proportion of the dominant phytoplankton groups classified according to the criteria of size fractions dominance (Table 1) for the entire dataset and for each sampling sites. It is important to note that not all the groups discriminated in Table 1 were found in our dataset.

$\overline{SI(chl)}^{*}$	Size fraction	Total (%)	Araçá Bay (%)	São Sebastião Channel (%)
29.75	Microplankton	9.6	14.8	4.0
20.74	Micro + Ultraplankton	10.6	11.1	10.0
18.28	Nanoplankton	1.0	1.9	-
12.85	Nano + Ultraplankton	1.9	3.7	-
11.81	Ultraplankton	37.5	35.2	40.0
9.23	Ultra + Picoplankton	23.1	13.0	34.0
17.0	N.D.**	16.3	20.4	12.0

* $\overline{SI(chl)}$ or the mean size index was calculated from the current dataset for each category from Table 1.

** N.D. = no dominance

The PCA analysis of the environmental variables was also coded with the $\overline{\text{SI(chl)}}$ groups (Figure 4b) with absence of grouping samples, unless a slight trend of larger communities being related to temperature and salinity. The multivariate RELATE analysis corroborated these results, which showed the ordination patterns of environmental variables and phytoplanktonsize classes (micro, nano, ultra and picoplankton fractions) were not correlated (Rho=0.14 for 999 permutations). In addition, the results from PERMANOVAdid not present significant differences in theenvironmental parameters between $\overline{\text{SI(chl)}}$ groups (p=0.67), as opposed to the factors “survey” and “site” that were significant (p<0.01).

4.3. Variability in the phytoplankton community photo-physiology

Overall, averages of F_v/F_m and $\sigma_{PSII(452)}$ in the Araçá Bay were 0.41 and 288 $Å^2$/photon, respectively, while in the channel they were 0.39 and 304 $Å^2$/photon. For both parameters, no significant difference was observed between the sampling sites, with a clear co-variation throughout time (Figure 6a and 6b). However, the high coefficients of variation within the samplings (up to 19% for F_v/F_m and 15.3% for

$\sigma_{PSII(452)}$) highlight the large variability observed over short time scales, from hours to days, also clearly shown by the large errors bars (Figure 6).

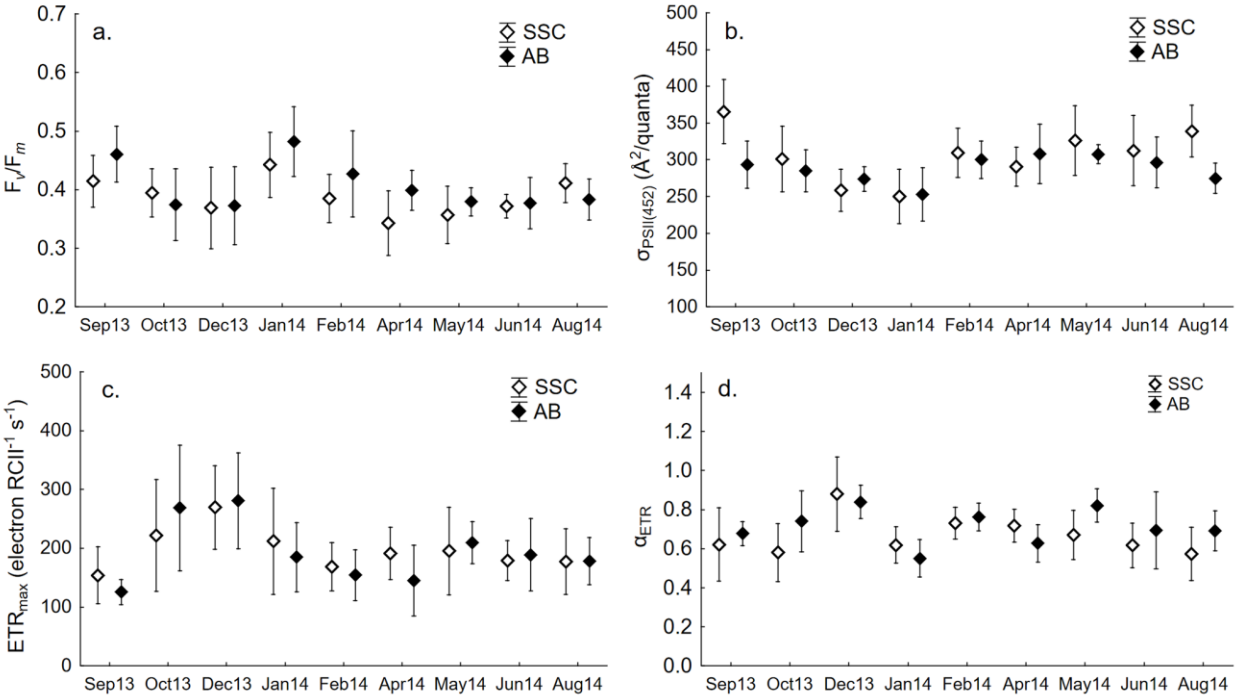

Figure 6. Variability of F_v/F_m (a), $\sigma_{PSII(452)}$(Å²/quanta) (b), ETRmax (electron $RCII^{-1}$ s^{-1}) (c) and α_{ETR} (d) across the sampling surveys (mean±SE) for both study sites (SSC=São Sebastião Channel, AB=Araçá Bay).

The ETR_{PSII} light curve parameters (ETR_{max} and α_{ETR}) did not differ between sites. In general, ETR_{max} tended to be higher during summer (Figure 6c), while α_{ETR} values were more consistent between seasons (Figure 6d). Mean ETR_{max} was 191.7 and 195.4 mol $e^{-}$$(molRCII)^{-1}s^{-1}$for the Araçá Bay and São Sebastião channel, respectively, while the mean α_{ETR} values were 0.72 and 0.68. We opted to present ETR_{max} and α_{ETR}, from which E_k can be inferred, however, the E_k data is not presented here since the spectral correction to account differences between natural and actinic light sources were not performed.

According to the RELATE analysis, the samples ordination of photo-physiological data ($F_v/F_m$and $\sigma_{PSII(452)}$) was not related to the environmental variables (Rho=0.04, for 999 permutations). Meanwhile, a nMDS (Non-metric Multidimensional Scaling) plot suggested a relationship between the variability of F_v/F_m and $\sigma_{PSII(452)}$ and

the distribution of the $\overline{SI(chl)}$ groups (Figure 7). $\sigma_{PSII(452)}$ was the primary factor to explain the clustering of the samples along the horizontal axis, being negatively correlated to most of the samples of the larger size groups. Secondly, there is a trend of larger cells being positively related to the F_v/F_m axis.

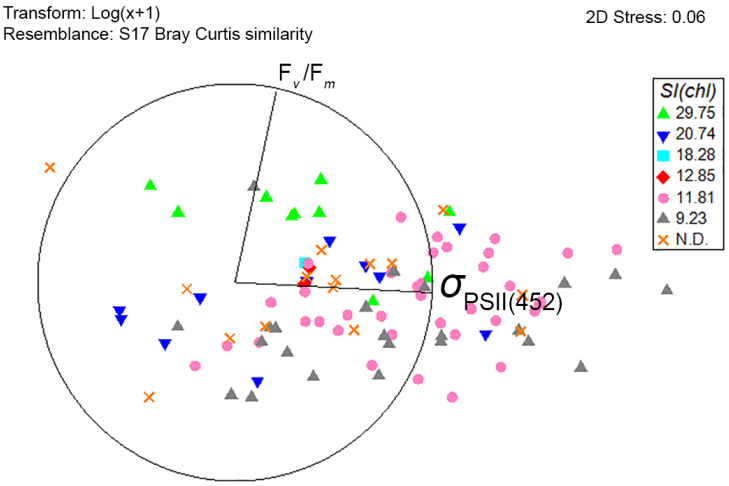

Figure 7. Non-metric Multidimensional Scaling (nMDS) ordination of the photo-physiological data, coded with the mean dominant size index $\overline{SI(chl)}$of phytoplankton communities.

4.4. Photo-physiology as a function of community size and nutrients availability

Significant linear relationships were found between the phytoplankton size index ($\overline{SI(chl)}$) and both photo-physiological parameters. F_v/F_m showed a significant positive relationship with the size index of the community (r^2=0.92; p=0.035), while $\sigma_{PSII(452)}$ presented a negative linear relationship (r^2=0.99; p=0.001) with the size (Figure 8). The relationships were significant only when N:P ratios were higher than the overall median values (Figure 8b,d). Otherwise, the correlation between $\overline{SI(chl)}$ and the physiological parameters were not significant, although the determination coefficients were 0.69 and 0.41 for F_v/F_m and $\sigma_{PSII(452)}$, respectively.

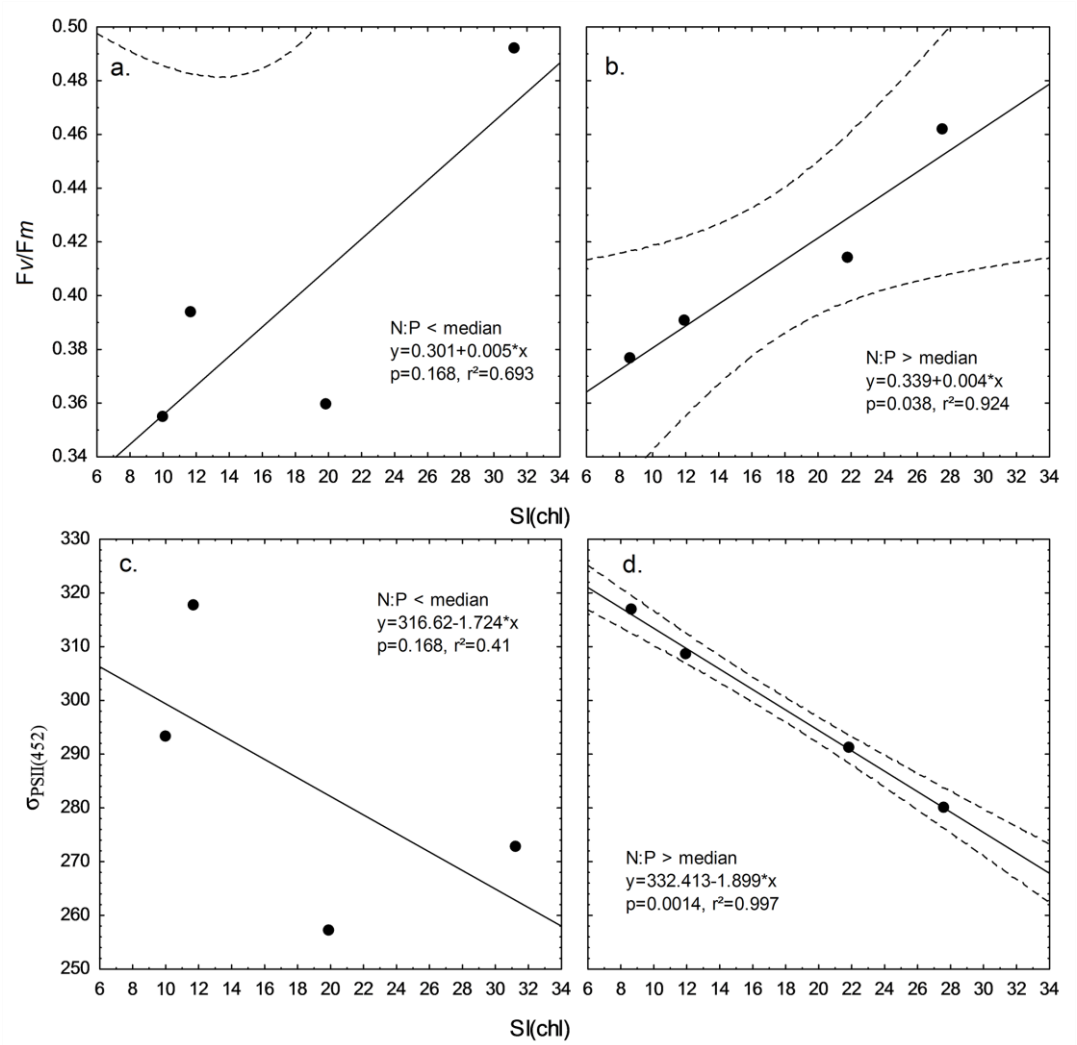

Figure 8. Linear regressions between the mean dominant size index ($\overline{SI(chl)}$) and F_v/F_m and $\sigma_{PSII(452)}$, under N:P ratio below the overall median (a, c) and under N:P ratio above the overall median (b, d). Dashed lines indicate 95% confidence interval of the linear regression analyses.

The ANCOVA analysis showed no significant differences between the slopes of the regression line derived from both sets of data, i.e., low and high N:P, with $p(\sigma_{PSII(452)})=0.91$ and $p(F_v/F_m)=0.55$. However, when N:P conditions are ignored, and all the data pooled in a single correlation, the regression is no longer significant. Thus, for the dataset analyzed here, the ambient nutrient conditions showed an important role in the expected relationship between cells size and F_v/F_m and $\sigma_{PSII(452)}$, suggesting that these relationships are valid only when the phytoplankton communities are exposed to N:P ratios above the overall median. The parameters ETR_{max}, α_{ETR} and E_k did not present significant relationships when directly correlated to $\overline{SI(chl)}$. It is important to

point out that the relationships and parameterization proposed here apply exclusively to communities where there is a dominance or co-dominance of specific size fractions, as described in Table 1.

For the samples where N:P is lower than the median, attempts to predict both F_v/F_m and $\sigma_{PSII(452)}$ using the available environmental variables were performed. Multiple regression analysis, using F_v/F_m and $\sigma_{PSII(452)}$ from individual samples (n=36) as dependent variable, and SI(chl) and the nutrients compounds as independent variables resulted in a model that included SI(chl), ammonium and phosphate as the predictive variables for F_v/F_m while $\sigma_{PSII(452)}$ was explained by SI(chl), ammonium and nitrate plus nitrite. However, the regression models explain only 28 and 30% ($p<0.01$) of the variability in F_v/F_m and $\sigma_{PSII(452)}$, respectively. Due to this low prediction power under low-nutrients conditions and as our central goal was to quantify the influence of community size in the ETR_{PSII} computation, our dataset allowed for parameterization of F_v/F_m and $\sigma_{PSII(452)}$ only when phytoplankton communities were exposed to higher nutrients levels, i.e. N:P ratios above the overall median.

The non-linear fitting of the decrease in F_q'/F_m' as function of irradiance provided exponential curves that were discriminated by two different models according to the size groups: one with dominance of microplankton and the co-dominance of micro and ultraplankton (groups 1 and 3 from Table 1) and the other one dominated by ultraplankton alone and the co-dominance of ultra and picoplankton (groups 8 and 9 from Table 1) (Figure 9). The error bars show that F_q'/F_m' values are significantly different between the two groups. The derived parameters provided two different models according to size. α and E_k for communities with relative smaller cells are 0.193 and 300.42, respectively, and 0.169 and 253.71 for the larger ones. E_k and α values presented here are the adjusted model coefficients and are not used as an absolute

measurement of photosynthesis efficiency or saturation light for the community. Nonetheless, the non-linear fitting of F_q'/F_m' can be used as an alternative method to derive α and Ek (Silsbe and Kromkamp, 2012).

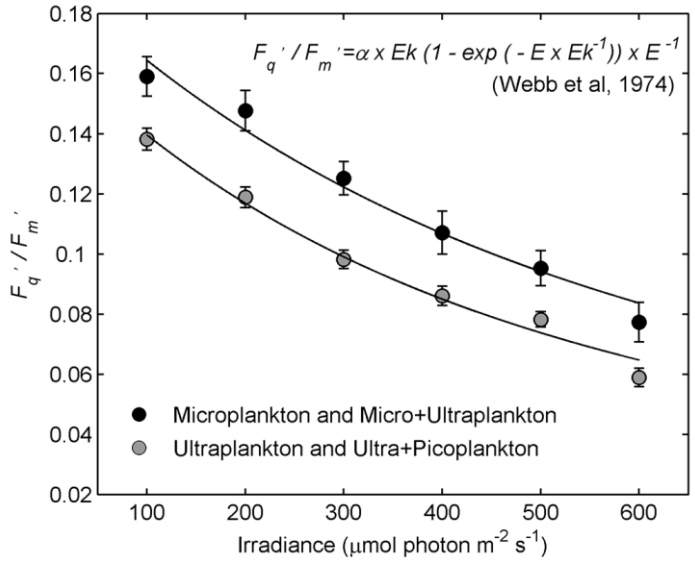

Figure 9. Non-linear curve fitting of effective photochemical efficiency (F_q'/F_m') as a function of irradiance for two phytoplankton size groups (the larger group includes communities dominated by microplankton and micro+ultraplankton and the smaller group is represented by the dominance of ultraplankton and ultra+picoplankton). The dots represent the averages and the whiskers are the standard errors.

We emphasize that the proposed parameterization only applies if there is a clear dominance of sizes in the community (refer to Table 1). For F_q'/F_m', we could discriminate two size groups, however it would be interesting to have a larger dataset of size dominance to better discriminate the role of the intermediate size groups on this parameter, as F_q'/F_m' tended to be higher for group 3 ($\overline{SI(chl)}$=20.7), when the curves were analyzed individually.

4.5. Photo-physiological model for primary production estimates

ETR_{PSII} light curves were modeled based on the photo-physiological parameterization for different phytoplankton community sizes that were exposed to N:P ratios above the median (Figure 10a). The communities co-dominated by ultraplankton and microplankton reached the highest values of ETR_{PSII} and Pc (Figure 10b), with

ETR_{max}= 218.2 mol $e^{-}(molRCII)^{-1}s^{-1}$and Pc_{max} = 2.59 $mgC(mgChl)^{-1}h^{-1}$. The lower values of ETR_{PSII} and Pc were observed for the microplankton-dominated community, where ETR_{max}=189.3 mol $e^{-}(molRCII)^{-1}s^{-1}$and Pc_{max} = 2.25$mgC(mgChl)^{-1}h^{-1}$. The Pc values provided by the model are reasonable and consistent with the primary production data available in the literature for this region (Gaeta et al. 1990; Saldanha-Corrêa and Gianesella 2008), which is important to encourage the use of the ETR-based primary production measurements for large temporal and spatial resolution data acquisition for the São Sebastião coastal waters and other high hydrodynamic regions.

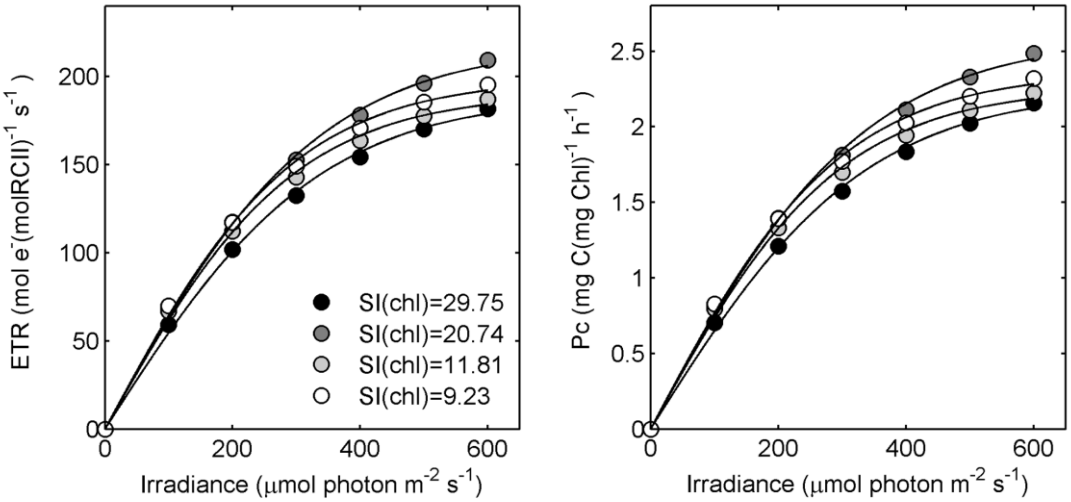

Figure 10. a. ETR_{PSII} light curves modeled from the parameterization according to the dominant size of the phytoplankton community. b. Carbon-based primary production estimates from ETR_{PSII} modeled according to the community size, using fixed values for n_{PSII}=0.002 (Falkowski and Kolber 1993) and ϕe:c=8 mol e^{-}/mol CO_2 (*sensu* Suggett et al. 2009b).

5. Discussion

In coastal waters, physical conditions change continuously over different spatial and temporal scales, dynamically affecting light and nutrient availability for primary producers (Cullen et al. 2002). A significant fraction of ocean primary production occurs in coastal regions (Longhurst 2007), and hence it is critical to develop tools for predicting changes in natural phytoplankton community structure and in turn its impact on net primary production. Our study proposes a new framework for modeling primary

production from photo-physiological parameters, based on their relationships to the size structure of the phytoplankton community. In addition, the results show for the first time how these relationships are altered by the ambient nutrients conditions on a temporal scale of days to months in a highly hydrodynamic region. The applicability of phytoplankton photo-physiology and ETR_{PSII} measurements to provide high-resolution primary production data was also presented.

5.1. Oceanographic and meteorological conditions and their relationships to the nutrients and phytoplankton variability

Physical processes in the oceans generally alter the availability of nutrients in the water column, which to a first order alters the dominant phytoplankton size structure and taxonomic composition (Cullen et al. 2002) and in turn manifests as altered photosynthetic and physiological rates (Finkel and Irwin 2000; Irwin et al. 2006) for a given time and place. In a very dynamic environment, such as that presented in our study (see also Castro et al. 2014; Cerda and Castro 2014), the relative importance of short-time scale physical processes, including tides and the intrusion of continental shelf water masses (Dottori et al. 2015), confound prediction of either nutrient concentrations or phytoplankton dominant sizes. During the monthly time scale of our present study, the two sites consistently exhibited distinct levels of nutrients whereas phytoplankton dominant size remained heterogeneous through time.

The high frequency meteorological data helped to explain episodic changes in nutrients availability, such as the stronger W-SW winds in September/13 followed by an increase in DIN concentration (see also Peres 2013). This nutrient accumulation was observed but we cannot discount that this may have arisen from a lower consumption of nutrients given that irradiance was also lower for this time point. These short time scale processes could not be related to changes in the phytoplankton community structure,

besides our sampling design did not generally allow for this pattern to be captured consistently. These questions are being addressed by long-term studies, with high temporal resolution, initiated in the region (www.simcosta.furg.br). In general, the meteorological data registered low precipitation year-round and wind fields followed the local seasonal regime (Castro 1990; Cerda and Castro 2014).

The Araçá Bay is extremely shallow (average 1.5m deep) and its volume of water is exchanged daily with SSC via the semi-diurnal tidal cycle, which reaches amplitudes of more than 1m during spring tides, as we observed. In the intertidal zone, most of the bay is covered by sand and mud, with a diverse and abundant benthic fauna (Amaral et al. 2010). The bay also receives two independent sources of continental outflows (a small river and a sewage outlet). Given that the SSC is highly advective, and there is a very significant increase in depth from the opening of the bay (i.e., from 1.5 to 5 m depth in few meters), we expect phytoplankton communities from the SSC waters to advect to the Araçá Bay with the tides where they are then exposed to lower hydrodynamics (longer residence times) and significantly higher nutrient levels. Indeed, about 75% of the samples with N:P ratios above the overall median were observed in Araçá Bay, suggesting the importance of this area as a nutrient (i.e. nitrogen) source for the local biota.

5.2. The photo-physiological model: effects of phytoplankton cell size and nutrients concentration

The absence of co-variation between the environmental data and the community size structure in our dataset enabled us to pool all samples based on the phytoplankton dominant size, however exposed to different ambient nutrients availability. The overall median values of N:P was used as a threshold. It is important to note that the chlorophyll concentration below and above the N:P threshold were 2.18 mgm^{-3} and 2.8

mgm^{-3}, respectively, highlighting that the low nutrient group is not affected by non-detectable or noisy fluorescence signal.

The photo-physiological parameters $F_v/F_m$and$\sigma_{PSII(452)}$ were linearly correlated, positively and negatively, respectively, to the community size dominance, expressed as the mean size index ($\overline{SI(chl)}$). Although our proposed classification according to dominant size has never been applied for photo-physiological studies in nature, previous studies have shown the relationships between cell size and photo-physiological parameters (Moore et al. 2005; Suggett et al. 2009a; Fishwick et al. 2006). However, in our study, the significant relationships derived here were dependent on a threshold of the ambient nutrients conditions, i.e. where ambient N:P ratios were higher than the respective overall mean; most likely, this threshold represents the effects of high nutrient dynamics over time, as our dataset comprises short-term processes at temporal scale of hours to months, and the phytoplankton communities are not established in a steady-state or balanced growth. Below this threshold the community is subjected to nutrient starvation. Thus, we did not find the inverse relationship between $\sigma_{PSII(452)}$ and F_v/F_mthat would be expected based on changes in taxonomy under a continuum of steady state conditions alone (data compiled by Suggett et al. 2009a).

Although our region has a consistently low nutrient concentration, the size dominance itself seemed to control about 90% of the variability in $F_v/F_m$and$\sigma_{PSII(452)}$ when N:P was above the overall median value. Possibly, the taxonomical distribution co-varies with changes in size dominance under this condition, once the history of nutrients impacts the establishment of phytoplankton communities and responses of chlorophyll-a fluorescence can be the product of taxonomic adaptive processes (Suggett et al, 2009a). Under nutrient starvation, none of the statistical approaches trying to predict the photo-physiological variability were successful.

Direct effects of nutrients limitation on F_v/F_m and $\sigma_{PSII(452)}$ have been largely discussed in the literature based on both natural communities and laboratorial experiments (Parkhill et al, 2001; Bibby et al, 2008; Suggett et al, 2009a; Rattan et al, 2012). Nutrient depletion decreases the efficiency of PSII photosynthesis, which is attributed to the increase in the synthesis of light harvesting pigments relative to the synthesis of reactions centers proteins, which are more demanding energetically, increasing $\sigma_{PSII(452)}$, and consequently decreasing F_v/F_m (Kolber et al. 1988; Falkowski et al. 1992). On the other hand, phytoplankton communities can acclimate to nutrient-limited conditions and achieve balanced nutrient-limited growth, e.g., to maintain their maximal F_v/F_m values (Parkhill et al. 2001). Additionally, nutrient-enrichment experiments in natural samples have demonstrated that nitrogen injections can promote an increase in the phytoplankton biomass without significant impacts on their physiological parameters, thus showing a reduced physiological response to nutrient additions compared with the importance of the community size structure and taxonomy (Moore et al, 2008).

In our study, the taxonomic variability does not seem to impact the relationships between photo-physiology and dominant size under N:P ratios above the median value, however it can play an important role in some cases, especially for the samples under lower N:P. Dominance of specific groups, such as cyanobacteria for example, can significantly alter the relationship between size and photo-physiology, due to the limited PSII absorption at the blue excitation waveband used in the FIRe fluorometer (e.g., Suggett et al. 2009a; see also Campbell et al. 1998). Similarly, we cannot discount possible artifacts to our low values of F_v/F_m via chlororespiration during dark-acclimation (Kromkamp and Foster 2003), which is an alternative electron pathway, where the electron carrier plastoquinone (PQ) is reduced through the respiratory activity

(Nixon 2000; Peltier and Cournac 2002). This process can increase under severe nutrient limitation (Behrenfeld and Kolber 1999, Mackey et al. 2008, Suggett et al. 2010). Oligotrophic waters are usually dominated by small cells, also the most abundant fraction in our dataset, which could explain low F_v/F_m values found at some cases.

5.3. Photo-physiology and primary production from active fluorometry

The relationships between dominant sizes and photo-physiology were used to model ETR_{PSII} light curves and an estimation of carbon fixation was presented. However, the use of chlorophyll-a fluorescence for primary production estimates should take into consideration a number of technical constraints associated with the measurements ETR_{PSII}, as outlined previously (Suggett et al. 2009b, Huot and Babin 2010). When comparing fluorescence techniques, it is important to consider the intensity and spectral quality of the actinic light and LED used for the fluorescence induction, as well as differences in the induction protocols, mainly the duration of fluorescence induction (single turnover or multiple turnover protocols). Usually, spectral corrections according to different light sources is required to reconcile light absorption coefficients across methods (MacIntyre and Cullen 2005) as well as across natural environments or incubations set ups in order to compare methods for primary production estimates (Suggett et al. 2010).

Whilst these various corrections were not possible in our study, we have used constant values for ϕe:C (electron requirement for carbon assimilation) from the literature to convert ETR_{PSII} light curves to Pc in terms of carbon (mgCarbon $mgChl^{-1}$ h^{-1}), producing values of Pc_{max} that were comparable to those previously published via C^{14}-uptake incubations technique for our region (Saldanha-Corrêa and Gianesela 2008); even so, we know that ϕe:C varies as a function of taxa (Suggett et al. 2009b) as well as with different oceanographic provinces and environmental conditions (Lawrenz et al.

2013). Indeed, further measures of ϕe:C are clearly warranted to verify the impacts of the dominant cells' size on this ratio and how this potentially varies across the highly dynamic nutrient-phytoplankton conditions. In the same manner, the number of PSII reaction centers per chlorophyll (n_{PSII}) proposed by Kolber and Falkowski (1993) have been measured on phytoplankton cultures and varied with both taxa and growth condition (Suggett et al. 2010). Recently, a novel approach proposed algorithms that derive n_{PSII} from fluorometry data (Oxborough et al. 2012). Unfortunately, our methodology did not allow for the measurement or estimation of this parameter, and a fixed value was assumed (Kolber and Falkowski 1993). Note that if there is a consistent relationship between the natural community size and n_{PSII}, the difference among the production curves as a function of Irradiance (Figure 10b) may not be as clear.

In summary, the current work is the first attempt to parameterize the photo-physiological parameters of natural phytoplankton communities derived from active chlorophyll-a fluorescence according to the community's dominant size-class and the ambient nutrient concentration. We proposed a framework for a fluorescence-derived primary production model (ETR_{PSII}-derived primary production) that can be further improved, through estimates of number of reactions centers and the ratio of electron requirement to carbon assimilation, and how they also vary with the phytoplankton community size structure. In addition, despite the applicability of the ETR_{PSII} model to understand physical controls on primary productivity in our region of interest, this model can be further validated with independent datasets. This work therefore represents a novel contribution to the growing efforts to apply active fluorescence-based techniques to understand variability of primary production in marine systems, more specifically at high hydrodynamic coastal waters.

CHAPTER 4

Direct comparisons of ^{14}C uptake and fluorescence-derived primary production rates, and the role of cell size, in phytoplankton cultures of *Thalassiosira* sp and *Tetraselmis* sp

1. Introduction

During the photosynthetic chain in autotroph phytoplankton, the energy provided by light absorption generates the transfer of electrons that is the machinery to provide energy for carbon fixation. The electrons can follow a linear flow or deviates to complex pathways, and this flow can be used to understand the physiological state of the cells and the efficiency with which light energy is invested into the final organic carbon assimilation. Much of this energy is utilized in physiological mechanisms as responses to photoacclimation, nutrients limitation, temperature and other processes the cells can be subjected to, especially in highly dynamic environments. Accordingly, the electron transfer rates (ETR) does not always linearly correspond to the rate of carbon fixation, due to alternative electron pathways (Prasil et al. 1996; Ralph et al. 2010) and the efficiency with which electrons are ultimately invested into fixed carbon still needs better comprehension (Lawrenz et al. 2015; Hancke et al. 2015).

ETR can be easily assayed through the emission of chlorophyll-a fluorescence from photosystem II (PSII) (Kolber and Falkowski 1993). One promising technique to assess ETR is the "Fast Repetition Rate fluorometry" (FRRf), which probes phytoplankton photo-physiology, specifically the emission of chlorophyll-a fluorescence to estimate photosynthetic electron transfer through PSII. However, a major weakness is that a conversion factor is required to compute the carbon uptake rates, termed the "electron requirement for carbon fixation" (K_C, mol electrons [mol

carbon]$^{-1}$; see Hancke et al. 2015), which has proven to be highly variable and difficult to predict. Furthermore, most of the works that computed K_C values have compared FRRf measurements in time scale of µs with carbon uptake incubations, in time scale of hours, and thus reconciling those measurements can be also a source of error. Few works have performed simultaneous incubations to obtain K_C in the same samples, which is a crucial methodological issue to be considered to advance towards good predictive models (Suggett et al. 2009b).

Environmental conditions have already been shown to significantly influence observed $K_C$variability (Lawrenz et al. 2015). The authors demonstrated relationships between K_C and parameters including temperature, nutrient concentration, and light attenuation, across a large global dataset, although the significant predictor variables of K_C distributions showed considerable spatial variability. As environmental and distinct nutritional conditions in the water will impose variations in the taxonomic structure of the phytoplankton in natural waters, assessing inter- and intraspecific plasticity in K_C is also necessary to fully resolve the mechanisms responsible for its variability (Suggett et al. 2009b; Lawrenz et al. 2015).

Distinct taxonomic groups of phytoplankton have shown large inherent variability in K_C for both laboratory-grown species (e.g. Fujiki et al. 2007; Suggett et al. 2009b) and natural communities (e.g. Boyd et al. 1997; Moore et al. 2003). Natural communities subjected to nutrient bioassays also show that $K_C$can be influenced by both taxonomic and physiological adjustments, in response to alleviation of nitrogen limitation (Hughes et al. 2015). Taxonomic classification is, however, not a trivial measurement, and thus is rarely performed for natural communities, so the cell size is, instead, considered a good proxy for community structure and reflects environmental conditions (Sieburth et al. 1978; Cullen et al. 2002).

Phytoplankton cell size plays an important role in several physiological traits. Small cells have higher light absorption, being less affected by self-shading and packaging effects than larger cells (Morel and Bricaud 1981; Ciotti et al. 2002; Finkel et al. 2004). However, larger phytoplankton are more efficient in utilizing absorbed light for photochemistry (Suggett et al. 2009a; Chapter 3, now published as Giannini and Ciotti 2016). Pigment packaging effects also dictate the plasticity of size-dependent photoacclimation under changing light (Finkel et al. 2004; Álvarez et al. 2016). Several metabolic rates are also shown to vary with phytoplankton size, in which intermediate groups of natural communities would have fastest metabolism due to a balance in light absorption efficiency, nutrient diffusion and assimilation and cellular surface-to-volume ratios (Lopez-Sandoval 2014). Effects of cell size were also demonstrated in the light harvesting and PSII repair in response to fluctuating light (Key et al. 2010), as well as in the nitrogen allocation to photosynthetic complex biosynthesis in diatoms (Wu et al. 2014), however in these cases taxonomic changes should be tested for consistency. All the size-scaling bio-optical and physiological performances already discussed in literature suggest that the cell size has also a significant and potentially predictable role on PSII light harvesting dynamics, ETRs and ultimately K_C, across a broad range of species.

Because of the effect of phytoplankton size upon photo-physiology and metabolic rates are complex, it is hard to ultimately understand the role of cell size in regulating the conversion of photosynthetic energy into fixed-carbon, however we believe that along with other rates, K_C also presents a size-scaling pattern. The hypothesis of this work is that phytoplankton cells size should have a predictable and important influence upon K_C. The central goal was then to examine whether cell size of two laboratory grown phytoplankton groups influences K_C, testing the consistency

across the taxa (genus *Thalassiosira* sp versus *Tetraselmis* sp) that have well-documented differences in photosynthetic physiology (Halsey et al. 2013) and are taxonomic groups commonly found in our region (coastal waters of southeastern Brazil). Photo-physiological and light harvesting properties, as well as ETR-derived parameters, were also compared among groups.

2. Methods

2.1. Cultures growth conditions and sampling design

Four non-axenic cultures of phytoplankton were grown in the laboratory, two strains of diatoms (Bacillariophyta) of the same genus: *Thalassiosira pseudonana* and *Thalassiosira weissflogii*; and two strains of green algae (Chlorophyta): *Tetraselmis* sp (strain CS-91) and *Tetraselmis* sp (strain CS-352). The *Tetraselmis sp* strains were obtained from the ANACC (Australian National Algal Culture Collection) and the diatoms were from the Climate Change Cluster department from UTS (University of Technology, Sydney). As the objective was to cover significantly different cell volumes, the choice of species was based on differences of at least one order of magnitude in cell volumes of these taxonomical groups commonly found in natural coastal waters of southeastern Brazil. The respective cell volumes were: 131.8, 1718.3, 300.9 and 1569.6μm^3 (see Table 1).

The cells were grown in triplicates, under 65µmol of fluorescent light with a blue filter, that were monitored with a LI-COR light meter on the shelf (light:dark cycle of 12:12 h), and kept at 20°C. Cells were grown in f/2 medium (Guillard and Ryther, 1962), prepared with autoclaved, 0.2µm filtered seawater collected from Sydney Harbour (Australia), and were maintained in semi-continuous batch mode through serial dilutions (Wood et al. 2005) to maintain cultures in exponential phase and under

balanced growth. The cultures were acclimated to the nutrient, temperature and irradiance regime for at least three transfers before commencement of sampling.

Growth rates were derived from daily measurements of *in vivo* fluorescence for all replicates during the experimental period (about 2 months). Samples for cell counts were collected every day during the entire experiment period, for at least one replicate, in order to have a ground-truth validation of the fluorescence-based growth. The growth rates (μ) were calculated through least-square linear regression of ln cell density over time, from which the growth rate is the slope of the regression fitting line (d^{-1}). The validation of growth rates through cell counting have shown high correlation with the *in vivo* fluorescence (r^2=0.90) for most of the growth curves, except for one replicate of *T. pseudonana* (r^2=0.60).

After acclimation and a series of dilutions during exponential growth, samples were collected for numerous biological and physiological analyses, such as the determination of chlorophyll-a and reaction center concentrations (Chl-a and RCII), photosynthetic unit size (PSU), cells size, biovolume and density, spectral light absorption (a^{chl}_{phy}), particulate organic carbon and nitrogen contents (POC and PON) and photo-physiological parameters based on Fast Repetition Rate fluorometry. Lastly, carbon assimilation rates through ^{14}C incubations were measured simultaneously to FRRf measurements (Electron Transfer Rates) to calculate the electron requirement for carbon fixation for the contrasting cell sizes.

2.2. Biological measurements

Chlorophyll-a and Reaction Center concentrations: Aliquots of the cultures were filtered (10 to 30mL) for chlorophyll-a determination through the non-acidification fluorimetric method (Welschmeyer, 1994) , for which the chlorophyll pigments were extracted in 5mL 90% acetone+DMSO solution (6:4 –Shoaf and Lium, 1976), for at

least 24h in dark and under -20°C. The calibration factor obtained with a chlorophyll-a standard was used to calculate the final chlorophyll-a concentration, and the values were averages of triplicates. The concentration of reaction centers (RCII) and thus the photosystem size unit (PSU; mol Chla/mol RCII) were derived from fluorescence parameters, discussed further in section 2.4.

POC/PON. Pre-combusted GF/F filters were used to retain the particulate material after filtration of aliquots of 15mL of the cultures. The filters were dried overnight at 60°C and kept in silica gel and in the dark until subsequent analysis with a CHN analyzer. The organic carbon (POC) and organic nitrogen (PON) in the filters were quantified and volume-based quotas were calculated in µg/mL.

Cell dimensions. Cell volume for all species was estimated from linear dimensions from images taken with a camera attached to a calibrated microscope (Nikon Automated Upright Fluorescence Microscope), using the Image-J image analysis software. We measured at least 60 cells by assigning different geometric shapes that were most similar to the real shape of each phytoplankton species (Sun and Liu, 2003). Cylinders were used for diatoms and ellipsoids for the green algae species.

2.3. Particulate light absorption and phytoplankton light-harvesting properties

Phytoplankton spectral light absorption from 400 to 750nm were measured for samples filtered onto 25mm GF/F filters, using an optic fiber UV/VIS spectrometer (Ocean Optics, Florida, USA), where sample blanks were measured separately. Particulate absorption was calculated using the QFT method (Roessler 1998) from the optical density of the material after correcting for residual scattering at 750 nm. The optical density (ODf) obtained from phytoplankton particles retained on the filter needs to be corrected for the filter amplification factor (β-factor), i.e. converted to optical density of particles in suspension (ODs) (Cleveland and Weidemann, 1993, Roessler

1998). We have used the quadratic function proposed by Finkel and Irwin (2001) for β-correct both diatoms and the values estimated by Arbones et al. (1996) for *Tetraselmis* sp. The particulate light absorption ($a_{ph}(\lambda)$; m^{-1}) at wavelengths between 400 and 700nm was calculated from ODs using the equation 1 (Tassan and Ferrari 1995).

$$a_{ph} = \frac{2.303\ ODs(\lambda)}{V/A} \quad (1)$$

Where ODs(λ) is the β-corrected optical density for all wavelengths, V is the filtered volume (m^3) and A is the clearance area of the filter (m^2). The chlorophyll-a specific absorption coefficient (a^{chl}_{ph}; $m^2(mgChl\text{-}a)^{-1}$) was obtained by normalizing the particulate absorption to the chlorophyll-a concentration.

The proportion of light harvested by the phytoplankton antenna complex directed to the photosystem II (PSII) was analyzed after a spectral correction performed to weight for the different light sources used for the measurements (Suggett et al. 2003; 2004). The effective cross-section of light absorption by the PSII was measured by fluorometry through excitation with a blue LED (peak wavelength of excitation at 450nm), and compared to the light absorbed by the chlorophyll-a after spectrally corrected for each species (Equation 2). The chlorophyll-a specific absorption was also weighted to the other lights sources used here, such as the actinic light of the FastAct chamber used for the carbon uptake estimates the growth light.

$$\bar{a}^{chl}{}_{phy} = \sum(a^{chl}(\lambda) \cdot E_{blueLED}(\lambda)) / \sum E_{blueLED}(\lambda) \quad (2)$$

2.4. Dark-acclimated photo-physiological state and the electron transfer rates

Photo-physiological parameters and the electron transfer rates (ETR) were measured through Fast Repetition Rate fluorometry (FRRf), using a FastOcean Fluorometer, attached to a FastAct chamber (both Chelsea Technologies, London, UK). Dark-acclimated measurements of F_v/F_m (maximal PSII photochemical efficiency) and σ_{PSII} (effective cross-section of absorption by PSII) were obtained by the FRR

fluorometer that was programmed to deliver saturating (ST: Single Turnover) flashes to PSII, induced by 100 flashlets at 2µs intervals from an excitation source of blue LEDs (peak excitation at 450nm, Fig. 2b).

ETR steady-state light curves were performed, with at least 20 acquisitions of 100 saturating flashlets under increments of actinic light, from 0 to 1400umol photon m²s¹. The actinic light steps provided ETR per cell unit volume calculated through two different equations: the Sigma-based algorithm (Kolber et al. 1988 – Equation 3a) and the Absorption-based algorithm (Oxborough et al. 2012 – Equation3b). Values of JVPSII (volume-based ETR) were also computed from both equations.

$$ETR^{vol}_{SIG} = \sigma_{PSII} \cdot F_q´/F_m´ \cdot (F_v/F_m)^{-1} \cdot E \cdot RCII^{vol} \quad (3a)$$

$$ETR^{vol}_{ABS} = a_{LHII} \cdot F_q´/F_m´ \cdot E \cdot cell^{vol} \quad (3b)$$

E is the irradiance (µmol photon m^{-2} s^{-1}), $F_q´/F_m´$ is the PSII photochemical efficiency measured under actinic light (dimensionless) and $RCII^{vol}$ is the concentration of functional PSII reaction centers per unit of cell volume, where RCII concentrations were calculated from fluorescence parameters as per Oxborough et al. (2012). Kn (the conversion factor used to scale fluorescence data to RCII) was cross-calibrated with the FastTrackaII fluorometer due to the fact the instrument was calibrated more recently than the FastOcean. The correction factor between the two fluorometers was x1.204. The same calibration factor was used to calculate a_{LHII} in Equation 3b, which is the absorption coefficient for PSII light harvesting (units of m^{-1}), calculated from dark FRRf data (Oxborough et al. 2012). $cell^{vol}$is the unit cell volume per volume of sample. Blank measurements of filtered samples were below 1% of the fluorescence signal and therefore were not subtracted from the bulk fluorescence signal. Physiological parameters derived from ETR light curves, such as ETR^{max} (maximum rate of electron

transport), Ek (light saturation parameter) and α_{ETR} (light utilization efficiency) were calculated by fitting a hyperbolic tangent model (Jassby and Platt 1976).

2.5. Carbon uptake rates and the electron requirement

Samples were collected from each culture (three biological replicates) for 15 min incubation, where the samples were spiked with radioactive ^{14}C (activity= 0.4µCi/ml). 3mL samples inoculated with ^{14}C were then measured in the FRRf under the actinic light (66 µmol $m^{-2}s^{-1}$ – growth light condition) for a 15min incubation where ETR was continuously measured, in order to compare the ETR against carbon assimilation for the same sample (to derive Kc with minimal methodological bias). After incubation, samples were transferred to a scintillation vial and ^{14}C activity was terminated by adding 150µl of 6M HCl. This drives-off any remaining ^{14}C into dissolved CO_2, which can then de-gases from the sample. After at least 24 hours, scintillation fluid was added to the samples which were then counted using a Scintillation Counter to measure disintegrations per minute (dpm) in the samples to calculate the $_{14}C$ production in 'mol Carbon m^{-3} day^{-1}' as per JGOFS protocols (Knapp et al. 1996). Dark samples were incubated in order to exclude any dark activity of carbon uptake, as well as blank samples were included in the analysis to account for the initial activity before the incubation (T0).

2.6. Data analysis

Most of the bioptical and light harvesting properties, i.e. proportion of light absorbed and directed to PSII, and photo-physiological parameters analyzed were expressed in unit cell volume base, and effects of the cell sizes were tested using a mixed-model nested-ANOVA, in which the taxonomic group was considered as a random factor (since we are not interested in the taxonomic effects of these two specific groups into photo-physiology), that was nested within the size factor (fixed). That

allowed for testing the consistence of the size effects when different taxonomic groups of phytoplankton are considered. The same approach was used for the photosynthetic parameters derived from ETR light curves, where two different algorithms were compared, and for the electron requirement for carbon fixation (K_C). Organic carbon content in the cells and the ratios to chlorophyll-a and organic nitrogen were statistically compared, as well as the production derived from inorganic carbon uptake (C^{14} uptake) and organic carbon increments (particulate organic carbon times growth rates). The coupling between the inorganic carbon uptake and conversion to organic compounds was also discussed.

3. Results

3.1. Physiological characterization at balanced growth

A series of biological and photo-physiological measurements were performed, ensuring the cultures were at mid-exponential phase and balanced growth. Table 1 presents the characterization of the species in terms of cell volume and abundance, chlorophyll-a concentration, photosynthetic unit size, and other parameters, as well as the results of the mixed-model nested-ANOVA. Dark-acclimated measurements of the effective cross-section of light absorption (σ_{PSII}) and the maximum photochemical efficiency of PSII (F_v/F_m) were lower and higher for the larger size cells, respectively, as expected (Suggett et al. 2009a). Such a response is mainly associated with the packaging effect of pigments that decreases the efficiency of light absorption per unit cell volume, due to self-shading effects (Morel and Bricaud 1981). Furthermore, the unit area of photosynthetic membrane space available per unit cell volume decreases as cell size decreases, and thus the small cells may have evolved higher σ_{PSII} in order to maintain high per-unit volume light-harvesting rates (Suggett et al. 2009a). Other parameters, such as the growth rate (μ), the concentration of chlorophyll-a and reaction

centers per unit cell volume (Chl-a^{vol} and RCII^{vol}) and the PSU (photosynthetic size unit) were different between taxonomical groups (group(size) effects – $p<0.01$), and the cell size was not the main driving factor (Table 1). Diatoms exhibited higher µ ($0.76d^{-1}$ for both groups), however a significant effect of size was observed for the *Tetraselmis* species, with higher µ for the small isolate ($0.57d^{-1}$ versus $0.24d^{-1}$). The same interaction was observed for the Chl-a^{vol}, however Chl-a^{vol} was significantly higher for the larger than smaller *Tetraselmis* isolate, suggesting an even stronger degree of packaging for this specie (Figure 1b). *Tetraselmis* species exhibited higher values of RCII^{vol} than from diatoms (Table 1), however RCII^{vol} tended to be higher for the smaller cells in both groups (Figure 1c).

Table 1. Growth rate, cell volume, dark-acclimated photo-physiological data (σ_{PSII} and F_v/F_m), cells density and cellular chlorophyll-a (Chl-a) and reaction centers (RCII) concentrations of the four species used in this study. Values are mean (± standard errors) of triplicates and the results of the nested-ANOVA are also presented. The columns "size" and "group(size)" indicate the sources of variations and the significant differences (**= $p<0.01$) according to the factors: cell size and taxonomic groups nested in sizes.

	***T. pseudonana* (small)**	***T. weissflogii* (large)**	***Tetraselmis sp* (small)**	***Tetraselmis sp* (large)**	**size**	**group(size)**
µ (d^{-1})	0.76 (±0.01)	0.76 (±0.02)	0.57 (±0.01)	0.24 (±0.01)	n.s.	**
Cell volume (μm^3)	131.8 (±9.13)	1718.3 (±28.2)	300.9 (±17.14)	1569.6 (±45.39)	-	-
σ_{PSII} (nm^2/RCII)	4.05 (±0.03)	3.58(±0.06)	2.90(±0.1)	1.82(±0.02)	**	n.s.
F_v/F_m (unitless)	0.54(±0.01)	0.60(±0.003)	0.55(±0.003)	0.60(±0.01)	**	n.s.
Chl-a (mg m^{-3})	522.3(±25)	389.92(±25.9)	398.46(±28.5)	194.8(±27.5)	n.s.	**
Cell Number (cell/ml)	$1.05e^6$($\pm0.16e^6$)	$9.8e^4$($\pm0.6e^4$)	$3.5e^5$($\pm0.34e^5$)	$1.74e^4$($\pm0.26e^4$)	n.s.	**
Chl-a per cell (pg $cell^{-1}$)	0.52(±0.06)	3.98(±0.22)	1.14(±0.03)	11.28(±0.50)	n.s.	**
RCII (nmol m^{-3})	587.38(±60.1)	390.4(±19.4)	876.8(±15.9)	182.6(±30.8)	n.s.	**
PSU (molChl $molRCII^{-1}$)	1007.5(±60.5)	1117.8(±47.3)	510.24(±45.6)	1210.5(±62.05)	n.s.	**
RCII^{vol} (nmolµm^{-3})	4.43(±0.65)	2.31(±0.001)	8.53(±1.02)	6.66(±0.2)	n.s.	**
Chl^{vol} (10^{-15}g µm^{-3})	4.01(±0.68)	2.32(±0.10)	3.82(±0.22)	7.22(±0.51)	n.s.	**

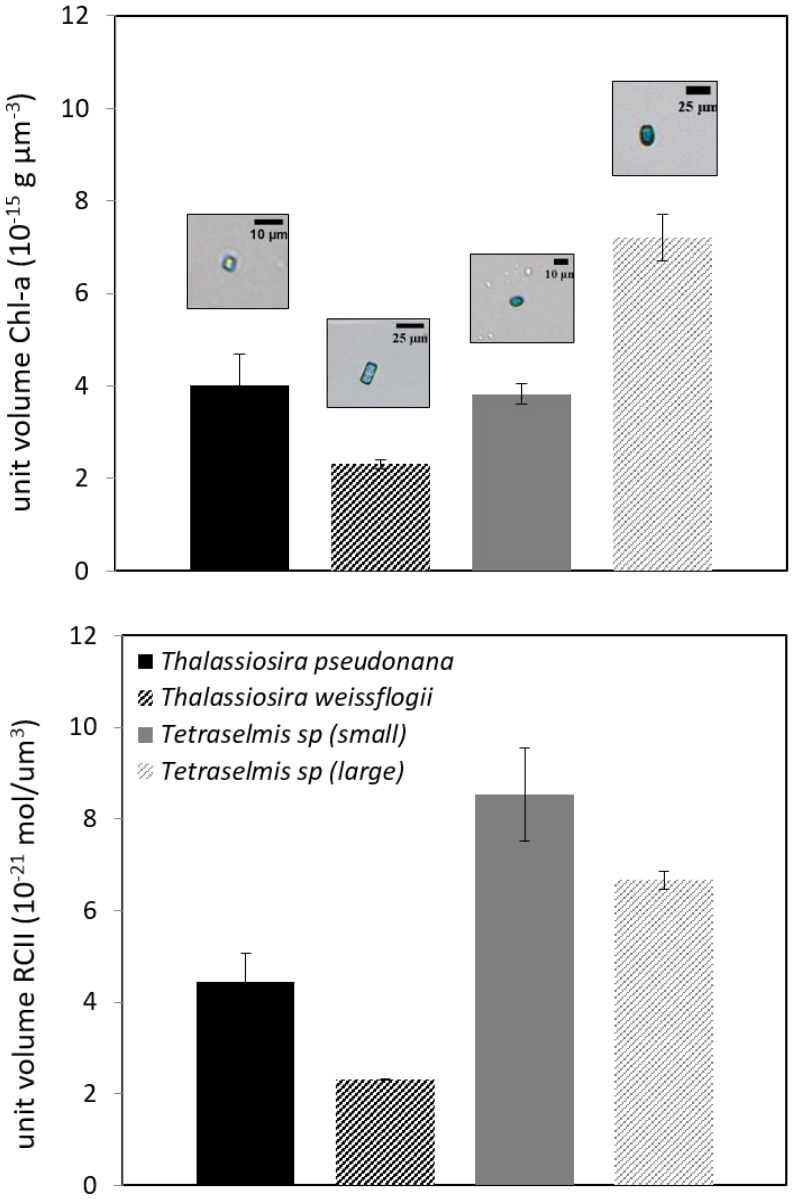

Figure 1. Unit cell volume concentrations of Chl-a (top) and RCII (bottom). Cell images were taken during the experiment with a calibrated Nikon microscopy.

3.2. Light harvesting properties

The chlorophyll-a specific light absorption by the phytoplankton cells were measured for the PAR wavelengths band (400-700nm), showing that the *Tetraselmis* species present a flattening in the absorption spectrum around the blue band (400 to 500nm), showing lower absorption at this portion compared to the diatoms (Figure 2a). The spectrally averaged specific absorption ($<a^{chl}_{phy}>$) are compared among the species in Table 2, that presents the light harvesting and absorption properties across the

isolates. The distinct spectral shapes of light absorption emphasize the importance of spectral corrections when the phytoplankton photo-physiological properties are measured under different light sources. Here, we have used three different light sources throughout our measurements and the appropriate spectral correction were applied in order to compare the light harvesting properties of the cells (see ratios in Table 2). The spectral shapes of each light source, with the respective normalized magnitudes, are compared in Figure 2b. The blue LED is the light source of the FastOcean (FRRf) used for the PSII photo-physiological measurements and the actinic light inside the FastAct chamber was used to perform the incubations for ETR versus Carbon uptake comparison. Lastly, the Figure 2b also shows the spectrum of the growth light where the cultures were acclimated before the experiments.

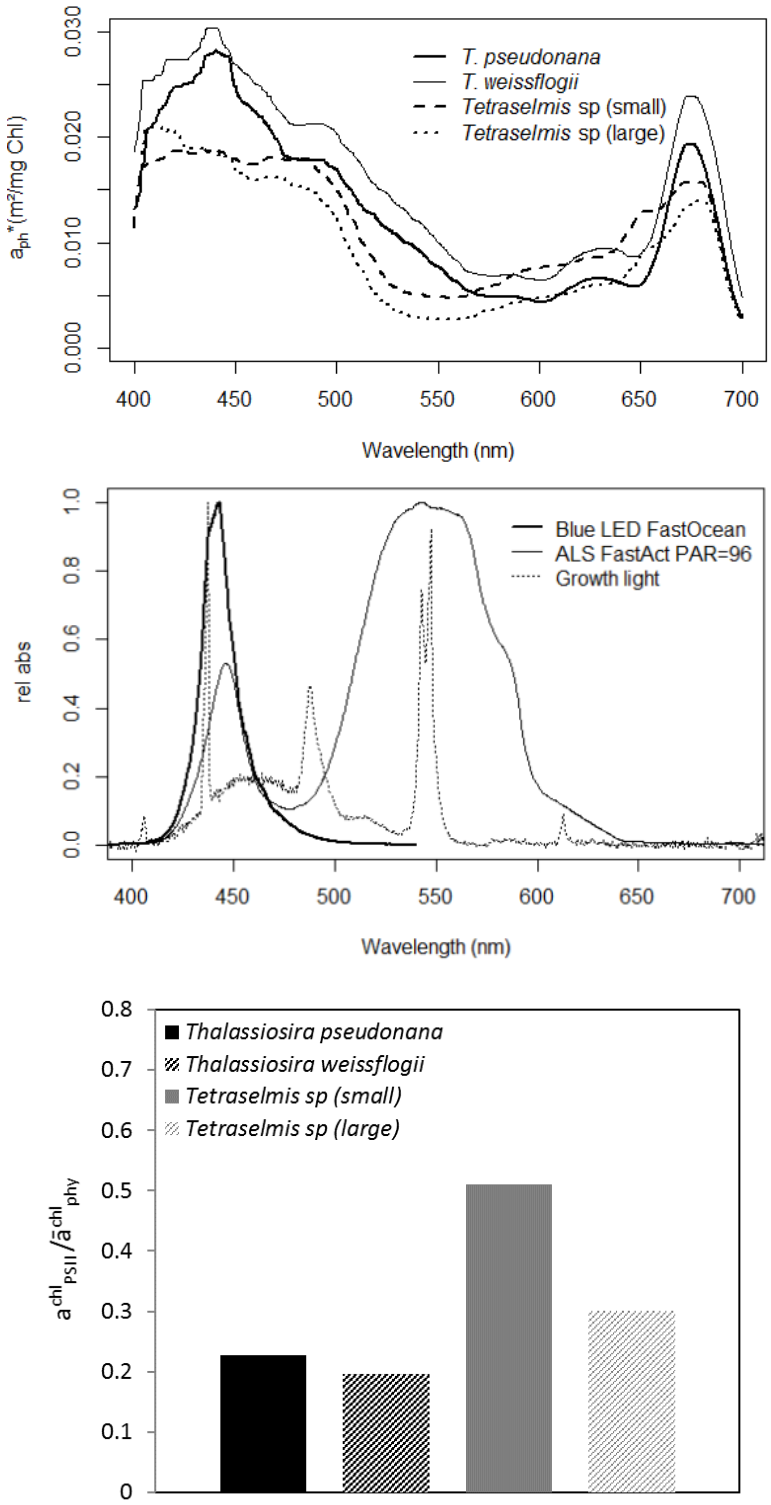

Figure 2. Spectral chlorophyll-a specific light absorption (upper panel); Normalized spectra of the different light sources used in this study: LED blue from FastOcean fluorometer, Actinic white light from the FastAct chamber used for the incubations and the spectrum of the growth light (middle panel) and the proportion of light absorbed and directed to the PSII weighted for the spectrum of the blue LED from FastOcean (lower panel)

The absorption weighted to the internal FRRf light source ($\bar{a}^{chl}_{phy}$ Frrf) was used to calculate the proportion of light that is absorbed by the PSII (a^{chl}_{PSII}) in relation to the total light absorbed by the cells (Figure 2c). As triplicates of a^{chl}_{phy} were not possible, the statistical analysis could not be performed, however it is clear that the small *Tetraselmis* has the largest proportion of absorbed light directed to the PSII compared to the other isolates. The size effect was then only clear for this group, while the difference seemed to be small for the diatoms. Such a trend was also observed for the PSII absorption per unit volume for the small Tetraselmis (a^{vol}_{PSII}), although the difference amongst species was not statistically significant (Table 2). In general, the *Tetraselmis* presented higher proportion of light directed to the PSII, that corroborates to the higher RCII concentration per unit volume for this group (Figure 1c).

Table 2. Light harvesting and absorption coefficients measured for each species as well as the spectral weighting factor among different light sources. a^{chl}_{PSII} (m^2 $mgChl^{-1}$) = ($\sigma_{(478)}$· 602300 / FvFm) · (n_{PSII} ·893510); a^{vol}_{PSII} ($10^{-15} m^2$ μm^{-3}) = ($\sigma_{(478)}$ · 602300 / FvFm) · (molRCII/cell vol); $<a^{chl}_{phy}>$ (m^2 $mgChl^{-1}$) is the spectrally averaged optical absorption between 400 and 700nm; $\bar{a}^{chl}_{phy}$ Frrf, $\bar{a}^{chl}_{phy}$ FastAct and $\bar{a}^{chl}_{phy}$ Growth (m^2 $mgChl^{-1}$) are the spectrally weighted optical absorption to compensate for the Frrf LED, FastAct chamber and Growth light spectra, respectively. Last two columns are the nested-ANOVA results (**= p<0.01).

	T. pseudonana	***T. weissflogii***	***Tetraselmis sp* (small)**	***Tetraselmis sp* (large)**	**size**	**group(size)**
a^{chl}_{PSII} (m^2 $mgChl^{-1}$)	5.85^{-3} ($\pm 2.7^{-4}$)	3.66^{-3} ($\pm 1.26^{-4}$)	6.23^{-3} ($\pm 1.92^{-4}$)	3.59^{-3} ($\pm 1.94^{-4}$)	n.s.	**
a^{vol}_{PSII} ($x10^{-15} m^2$ μm^{-3})	19.06 (±0.61)	10.95 (±2.02)	56.79 (±4.63)	19.68 (±4.36)	n.s.	n.s.
$<a^{chl}_{phy}>$ (m^2 $mgChl^{-1}$)	1.31^{-2}	1.08^{-2}	7.85^{-3}	6.64^{-3}	-	-
$\bar{a}^{chl}_{phy}$ Frrf(m^2 $mgChl^{-1}$)	2.58^{-2}	1.86^{-2}	1.22^{-2}	1.19^{-2}	-	-
$\bar{a}^{chl}_{phy}$ FastAct (m^2 $mgChl^{-1}$)	1.12^{-2}	9.18^{-3}	5.73^{-3}	4.33^{-3}	-	-
$\bar{a}^{chl}_{phy}$ Growth (m^2 $mgChl^{-1}$)	1.72^{-2}	1.33^{-2}	8.99^{-3}	7.82^{-3}	-	-
Growth light / Frrf LED	0.67	0.72	0.74	0.66	-	-
FastAct / Growth light	0.65	0.69	0.64	0.55	-	-
FastAct / Frrf LED	0.43	0.49	0.47	0.36	-	-

3.3. Electron transfer rates (ETR)

ETR light curves were calculated and show that the green algae sustain higher ETR than the diatoms per unit cell volume (Figure 3), which minimizes the role of the cell size in this case. Overall, maximum ETR per unit cell volume (ETR^{vol}_{max}) was significantly higher for the green algae (Table 3), as well as the saturation light intensity (Ek), which is consistent with different quenching dynamics and dissipation of excess light energy for this taxonomic groups (e.g. Wagner et al. 2006), regardless of cell size. The significant interactive effect indicates that the taxonomic group was more important than cells size to determine the photo-physiological differences in terms of the ETR parameters, such as $ETR^{vol\ max}$, Ek and $\alpha_{ETR}{}^{vol}$. Similar results were observed for the physiological parameters derived from JVPSII regarding the effects of cell size and taxonomical groups, except that the significance of the interaction group(size) for ETR^{max} was lower than the ETR^{volmax} (Table 3). The cells size did not present a significant and consistent role in the variability of the ETR parameters.

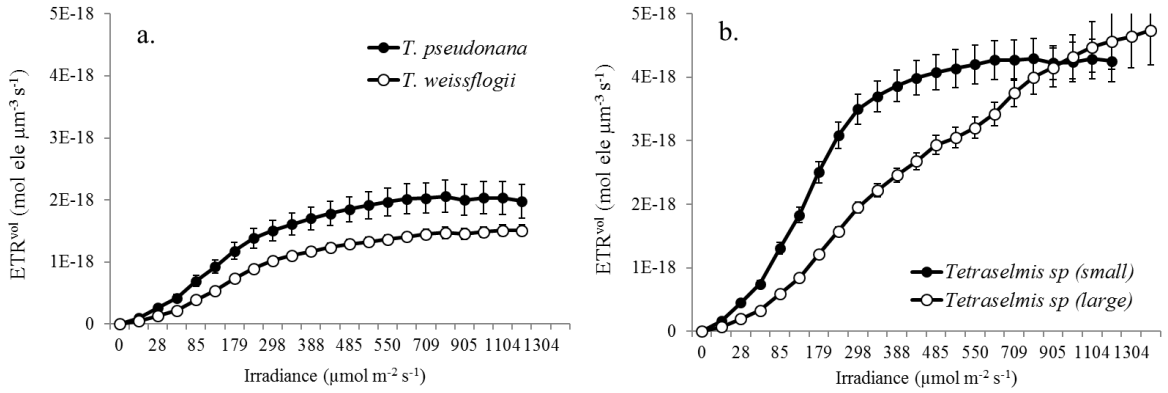

Figure 3. Electron Transfer Rates light saturation curves per unit cell volume (ETR^{vol}: mol electron $\mu m^{-3}\ s^{-1}$) for the diatoms (a) and for the green algae (b).

Table 3. Photo-physiological parameters derived from the unit cell volume ETR (ETR^{vol}) and from volume-based ETR (JVPSII) light saturation curves computed through the Sigma and Absorption-based algorithms. The parameters were obtained from the fitting model from Jassby and Platt (1976). Last two columns are the nested-ANOVA results (** = p<0.01 and * = p<0.05).

		T. pseudonana	***T. weissflogii***	***Tetraselmis sp*- small**	***Tetraselmis sp* - large**	**size**	**group(size)**
ETR^{vol} SIG	**Ek**	279.77(±39)	347.26(±10.9)	264.12(±6.14)	701.54(±73.8)	n.s.	**
	$ETR^{vol\ max}$	$2.03e^{-18}(\pm2.2e^{-19})$	$1.44e^{-18}(\pm5.5e^{-20})$	$4.3e^{-18}(\pm3.1e^{-19})$	$4.9e^{-18}(\pm6.02e^{-19})$	n.s.	**
	α_{ETR}^{vol}	$7.4e^{-21}(\pm1e^{-21})$	$4.1e^{-21}(\pm4.8e^{-23})$	$1.62e^{-20}(1.03e^{-21})$	$7.0e^{-21}(\pm2.3e^{-22})$	n.s.	**
ETR^{vol} ABS	**Ek**	279.77(±39)	347.26(±10.9)	264.12(±6.14)	701.54(±73.8)	n.s.	**
	$ETR^{vol\ max}$	$1.68e^{-18}(\pm2.2e^{-19})$	$1.24e^{-18}(\pm7.7e^{-20})$	$3.57e^{-18}(\pm2.6e^{-19})$	$4.1e^{-18}(\pm5.01e^{-19})$	n.s.	**
	α_{ETR}^{vol}	$6.12e^{-21}(\pm8.4e^{-22})$	$3.56e^{-21}(\pm1.2e^{-22})$	$1.35e^{-20}(8.56e^{-22})$	$5.81e^{-21}(\pm1.88e^{-22})$	n.s.	**
JVPII Sig	**Ek**	279.77(±39)	347.26(±10.9)	264.12(±6.14)	701.54(±73.8)	n.s.	**
	ETR^{max}	23.46(±2.98)	21.47(±2.5)	18.06(±1.27)	11.8(±2.72)	n.s.	*
	α_{ETR}	0.08(±0.01)	0.06(±0.005)	0.07(±0.006)	0.016(±0.003)	n.s.	**
JVPII ABS	**Ek**	279.77(±39)	347.26(±10.9)	264.12(±6.14)	701.54(±73.8)	n.s.	**
	ETR^{max}	19.48(2.48)	17.83(±2.09)	15.0(±1.06)	9.8(±2.26)	n.s.	*
	α_{ETR}	0.07(±0.007)	0.05(±0.005)	0.057(±0.005)	0.014(±0.002)	n.s.	**

Table 3 compares the photo-physiological parameters derived from ETR light curves calculated via different equations: from Sigma (ETR^{vol}_{SIG}) and Absorption (ETR^{vol}_{ABS}) algorithms (Oxborough et al. 2012). The new approach proposed by Oxborough et al. (2012) to calculate a volume-based ETR (or JVPSII) through an absorption-based algorithm (Eq 3b) has an advantage over the Sigma-based algorithm (Eq. 3a) because, once the instrument is calibrated with a direct measurement of RCII concentration, JVPSII can be calculated simply from dark acclimated data and the photochemical efficiency under actinic light. Here, we have used the same calibration factor to estimate RCII for both algorithms, so the differences here are based on using a_{LHII} or σ_{PSII}. The Sigma-based algorithm assumes zero connectivity between RCs (open RCs estimated from qP), while the absorption algorithm does not require the assumption of RCs connectivity type. The differences observed for ETR^{vol} were small, however the absorption-based algorithm tended to compute lower $ETR^{vol\ max}$ and α_{ETR}^{vol} than the Sigma-based algorithm for all the species. However, it is important here that this difference was consistent across the species.

3.4. Electron requirement for carbon assimilation (K_C)

The differences in the Kc are presented in Figure 4, where cell size did not show consistent differences overall. Besides the differences among species, K_C values were in general close or below the theoretical expected value for Kc in optimal growth (4 to 6 mol e^-(molC)$^{-1}$; Genty et al. (1989); Suggett et al. 2009b). The large diatom shows the lowest K_C, followed by the small *Tetraselmis*, although both presented K_C values below 4. The mean $K_C$for the small diatom was 4.5, which is close to values found in the literature for both cultures (Hancke et al. 2008) and for natural communities dominated by diatoms, however the K_C measured for *Thalassiosira weissflogii* was lower in our study compared to previous reported values (Suggett et al. 2009b). The explanation for the low K_C values will be discussed later, which is likely related to systematic methodological issues regarding both carbon fixation and ETR estimates (Lawrenz et al, 2015). The large *Tetraselmis* presented the highest electron requirement (K_C=6.04), which suggests this species to be the least efficient in converting light energy into fixed carbon.

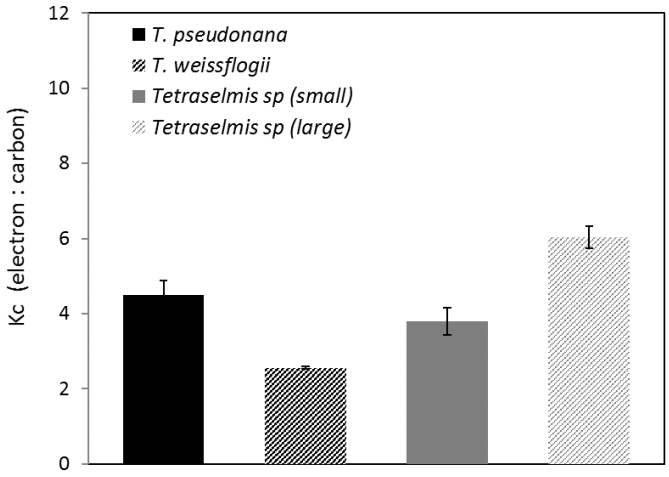

Figure 4. Electron requirement for carbon assimilation (K_C) obtained from simultaneous measurement of ETR and gross carbon uptake (^{14}C uptake). The nested-ANOVA have shown significant interactive effect of group(size) for $p<0.01$

3.5. Elemental cellular composition and carbon productivity

The productivity was estimated from ^{14}C uptake measurements and from POC and growth rates from each species. The triplicates' averages and standard errors of the daily productivity are shown in Table 4, which varied from about 1 to 9 µgC mL^{-1} d^{-1}. In average, the same gradient was observed across the isolates for both measurements (^{14}C uptake and POC), where the large *Tetraselmis* isolate was the less productive and the small diatom (*T. pseudonana*) the most productive. The comparison between both measurements per cell unit is presented in the Figure 5 for all the samples, which allows to have an overview on how inorganic carbon assimilation is used to build organic cellular elements against other processes that consume the assimilated carbon.

Table 4. Gross primary productivity based on ^{14}C uptake and net productivity based on cellular organic carbon increments (POC data) and elemental cellular composition (proportion of organic carbon to chlorophyll-a (C : Chla-a) and organic nitrogen (C : N)).

	T. pseudonana	***T. weissflogii***	***Tetraselmis sp* - small**	***Tetraselmis sp* - large**	**size**	**group(size)**
P^{14}_C (µgC mL^{-1} d^{-1})*	8.61(±0.06)	7.94(±0.61)	5.31(±0.95)	0.9(±0.03)	n.s.	**
P_{POC} (µgC mL^{-1} d^{-1})	7.25(±1.21)	7.05(±0.77)	6.36(±0.23)	1.59(±0.30)	n.s.	**
C : Chl-a	18.3(±2.7)	23.6(±0.58)	28.1(±0.87)	33.5(±0.92)	n.s.	**
C : N	4.75(±0.29)	4.68(±0.04)	6.01(±0.06)	4.62(±0.17)	n.s.	**

*spectrally corrected to account for the difference between the incubation actinic light and the growth light

** ($p<0.01$)

The relationship between P^{14}_C and P_{POC} for the small diatom shows that all the carbon assimilated is used to build the organic structure of the cells (fall into the 1:1 line), while the large diatom presented the replicates varying across the 1:1 line. Although one of the replicates of *T. weissflogii* presented P^{14}_C higher than P_{POC}, suggesting other processes might be reducing the assimilated carbon inside the cells in this sample, in general, both diatom groups have shown the inorganic carbon assimilation to organic carbon ratios per cell around the central 1:1 line. For the

Tetraselmis isolates, this relationship tended to be below the 1:1 line, especially for the large isolate.

Table 4 also shows the C : Chl-a and C : N ratios, with significant differences across taxonomical groups. The carbon to chlorophyll-a ratio tended to be higher for larger cells, but the interactive effect of taxonomical groups and size shows that the cell sizes are not the main controlling factor. The same interaction was observed for C : N ratios, however the smaller cells tended to have slightly higher C:N. In general, the C : N suggests carbon limitation in the cultures, although the balanced-growth were not apparently affected.

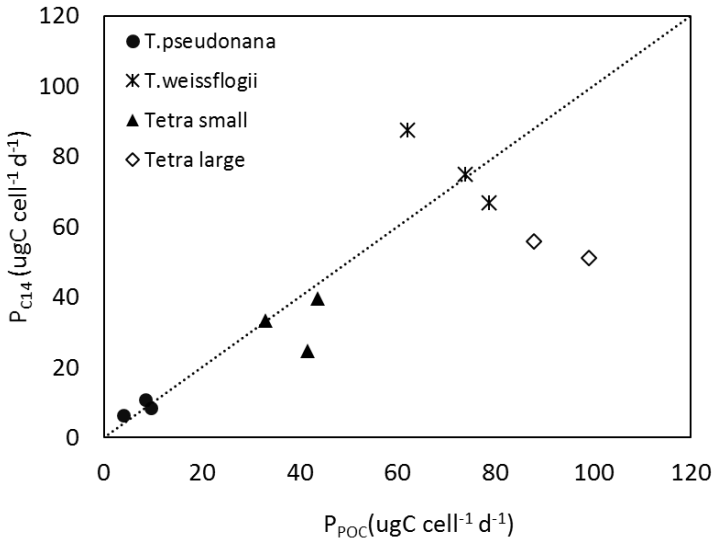

Figure 5. Daily gross primary productivity estimated through ^{14}C uptake against the net organic carbon productivity (POC x growth rate).

4. Discussion

In general, the effects of cell size in the light harvesting properties analyzed here, as well as in the ETR-derived photosynthetic parameters and electron requirement for carbon fixation were taxa-dependent. As expected, the only parameters significantly related to cell size, regardless of taxa, were the maximal photochemical efficiency and the cross-section of PSII light absorption. However, all the complex interactions among

the utilization of light energy and the final carbon assimilation prevented the electron requirement to have a consistent effect of cell size. The same approach would be encouraged using other phytoplankton groups, but it is important to note the groups used here are common groups found in natural communities (diatoms and chlorophytes), which were chosen randomly, however inspired by the natural community composition usually associated with subtropical coastal waters. The main focus of this study was the direct conversion of absolute rates of electron transfer into carbon fixation rates and the investigation of the role of cell size in regulating this ratio. K_C values are extremely variable, especially when including field work studies (Suggett et al. 2009a; Lawrenz et al. 2015; Hancke et al. 2015; Hoppe et al. 2015). Lawrenz et al. (2015) have shown a global average of 10.9 mol e^- (mol CO_2)$^{-1}$, although that were well discriminated when different oceanographic regimes and biogeographic regions were clustered. Suggett et al. 2009 have reviewed previous values of Kc across natural and cultures conditions, where communities dominated by diatoms presented Kc between 4 and 12 mol e^- (mol CO_2)$^{-1}$, while they found cultures-based values for diatoms (*Thalassiosira weissflogii*) around 6 mol e^- (mol CO_2)$^{-1}$. Those studies have shown that in many cases, the use of an assumed value between 4 and 6 mole-(molC)-1 to ETR-derived production will yield biased estimation of primary production (Lawrenz et al. 2015).

In our study, K_C values were close or below the theoretical values for most of the species, except for the large *Tetraselmis*. Low electron requirement values (< 4 mol e^-(mol CO_2)$^{-1}$) have been previously shown (Boyd et al. 1997; Corno et al. 2006; Hoppe et al. 2015), however it is important to carefully consider the distinct measurements protocols applied among studies, especially regarding the incubation time (our protocol allowed for gross primary production estimates) and light sources, that requires

appropriate spectral corrections. Low Kc values are difficult to reconcile and it is likely originated from methodological issues, as well discussed by Lawrenz et al. (2015). Here, we have two potential sources of uncertainties in K_C estimates: i) variability and possible underestimation of RCII concentration and ii) non-systematic errors in the carbon fixation measurements.

The RCII concentration were obtainedfrom an algorithm incorporated in the data processing in the FastPro (FRRf software). The algorithm is based on the dark-acclimated fluorescence parameters and a constant that was obtained from calibration against an O_2 flash-yield system (Oxborough et al. 2012). However, the calibration was performed for the FastTrackII fluorometer and thus we cross-calibrated the FastOcean we used against the FastTrackII to derive another calibration factor (=1.204). It is possible that the FastOcean underestimates RCII even after this correction, and a direct calibration against the O_2 flash-yield system would be necessary. Similar K_C values (from 2.7 to 6 $mole^{-}(molC^{-1})$) were reported by Hoppe et al. (2015), in which they have also used a FastOcean fluorometer to investigate the interactive effects of ocean acidification and distinct light regimes in Antarctic diatoms. Unlike our approach, the authors have compared ETR to net primary production (NPP), that is lower than the gross primary production (GPP), once part of the inorganic carbon assimilated have been released by respiration after a certain period of incubation (Ryther 1956). The incubation time is a crucial information to be considered to differentiate NPP from GPP and compare K_C among studies. The short incubation time used here (15min) approximates the measurement to the GPP.

Another issue that probably interfered with our K_C estimates is the uncertainty in the estimation of C uptake. The ^{14}C assimilation method for quantifying the inorganic carbon fixation by the phytoplankton cells (Steemann-Nielsen 1952) utilizes the initial

inorganic carbon measured in the sample, the precise amount of ^{14}C-labeled carbon added before incubation and the amount of ^{14}C incorporated in particulate organic matter. After a known incubation-time, one can calculate the rate of inorganic C fixation. However, it is based on the assumption that the uptake of added ^{14}C-labeled inorganic carbon is proportional to the uptake of unlabeled ^{12}C carbon during the incubation in a closed container. Possibly, there could be a shortage of DIC (dissolved inorganic carbon) within the cultures medium that would result in ^{14}C inorganic carbon being drawn down in a higher rate than expected, and this fast assimilation may limit the inorganic carbon to be fully replaced by the atmosphere equilibration. That would overestimate the carbon uptake during the time of the incubation, especially in such a short-time incubation. This hypothesis is corroborated by the C : N ratios data, that suggests low cellular quota of carbon, probably reflecting a DIC limitation. Although that is observed for all species, the balanced growth does not seem to be affected.

Few works have performed simultaneous incubations to reconcile the electron transfer rates and the carbon uptake (^{14}C uptake) in the same sample. In recent years, most of the work have compared instantaneous FRRf measurements (time scale of μs) and carbon uptake incubations (the shortest being around 1h). Thus, the timescale of the measurements for those comparison has been an important methodological issue (Suggett et al 2009b). The simultaneous incubation has the advantage of using the same light source for both ETR and ^{14}C measurements (the actinic light in the FastAct chamber – spectrum at Fig2b), so there is no need to weight the PAR irradiance of the incubation lights as is usually done. Weighting the σ_{PSII} measurement for the actinic light source would however lower Kc values up to 49%. We have presented Kc without the spectral correction of σ_{PSII}, once the incubations were performed in the same incubation light for ETR and ^{14}C fixation (E_{PAR}=66 μmol photon $m^{-2}s^{-1}$), with the aim to

compare the cell size effect on Kc. Table 2 shows that the weighting function factors among the species were similar, which would keep the same statistical results. As we have considerations about a possibly systematic underestimation of ETR and overestimation of ^{14}C uptake, we keep the non-weighting values (LED *versus* actinic light) to avoid including extra noisy, although we are aware of its importance (Boyd et al. 1997; Macintyre and Cullen (2005); Suggett et al. 2003; Suggett et al. 2004).

Although systematic errors can be associated to ETR estimates and DIC limitation as discussed above, we believe still other sources of uncertainties in the ^{14}C uptake of the large *Tetraselmis* occurs. The proportion of carbon assimilation and the net carbon production estimated from POC data (Fig. 4) have shown low values of C-uptake for this species in relation to the net production. It is reasonable that a non-systematic error in the ^{14}C uptake takes place, and underestimates of gross photosynthesis may occur due to isotope disequilibrium between the intracellular and extracellular CO_2 pools (MacIntyre and Cullen 2005; Suggett et al. 2009b), and distinct assimilation of isotope carbon among species, that could possibly underestimate the carbon uptake in the large *Tetraselmis*.

The slower growth rate of the large *Tetraselmis* compared to the others species used here might influence the short-term ^{14}C uptake rates and energy allocation, as it has been observed to occur in diatoms under nutrient limitation, but could be present in other taxa (Halsey et al. 2010). In addition, the light-harvesting properties of this species suggest special features that could be driving this complex interpretation. The cells are extremely pigment packed and the effective light absorption is low, however they reach higher electron transfer rates than the diatoms and the non-photochemical quenching dynamics seem to be more efficient (higher NPQ values – not shown), also presenting high Ek (=701.5 umol photon m^{-2} s^{-1}).

In addition, it is possible that contamination by small autotrophic or bacteria consuming inorganic carbon during incubation have occurred, especially because one of our replicates was excluded due to contamination, although we could not detect it in the replicated we performed the experiment. Uptake of labeled ^{14}C by heterotrophic bacteria and aerobic anoxygenic photosynthetic microorganisms may also contribute to uncertainties and the influence of these organisms on the measured ^{14}C activity is yet to be determined (Corno et al. 2006). Underestimating ^{14}C uptake for the large *Tetraselmis* could also explain the highest Kc found for this group (around 6), that even with a systematic underestimation of ETR, could still be responsible for the higher K_C than the other species.

Regardless of complexities in estimating absolute ETRs, Carbon uptake, and hence Kc, the hypothesis that the cell size has a significant effect on the electron transfer efficiency and the electron requirement for carbon fixation was not confirmed, and the taxonomic group significantly influenced the size response. It is possible that the size difference was not large enough to show contrasting responses, although we have tried to use different orders of magnitude in cell volumes. Our data suggest that such parameters more strongly depend on differences in the strategies of distinct taxonomic groups to grow and maintain their biomass (Halsey et al. 2013; 2014). Although similar photosynthetic efficiencies, differences in the lifestyle strategies to allocate photosynthetically-derived products have been observed for these two specific taxonomical groups (diatoms and green algae) under a range of nitrate-limited growth rates (Halsey et al. 2013). The differences are then related to lifetimes of newly fixed carbon during different phases of the cell cycle. This distinct allocation of end products of carbon could influence the carbon uptake in short time incubations, with the electron requirement reflecting such effects rather than differences in cell size, given the same

nutrients and light conditions. More important is to consider these differences for natural environments, although this kind of study still need to be done in laboratory.

The effects of taxa-specific strategies towards allocation of photosynthetic energy and carbon increments according to growth rates can be intimately related to the role of the phytoplankton communities to deal with natural transient nutrients conditions and the maintenance of the primary production at nutrient-limited regions, where the enrichment may occur in different time-scales. The phytoplankton taxa used here (diatoms and green algae) are common organisms found in coastal subtropical waters, however, the use of laboratory-grown cultures, although necessary, is enormously biased when we try to explain photo-physiology strategies and energy utilization in natural environments, especially when organisms with very complex optical and physiological characteristics, such as the large *Tetraselmis* used here, are used to investigate patterns that seem to be clear in nature. Thus, we emphasize the need for a careful interpretation of phytoplankton culture data.

In summary, whilst cell size strongly influences the efficiency of light absorption and photochemistry, species-specific responses in photosynthetic energy allocation dominated the differences observed in how absorbed light is utilized to carbon assimilation, i.e., in the electron requirement for carbon assimilation. As such, interactive effects of cell size and taxonomy in the growth strategy to maintain biomass and production is critical to better understand the dynamics of primary production rates derived from photo-physiology in natural and highly productive sites.

GENERAL CONCLUSIONS

The study presented an advanced overview of the fluorescence technique, proposing novel approaches that contribute to the improvement of primary production measurements from photo-physiology, especially in highly dynamic environments. The central hypothesis was that the variability in key phytoplankton characteristics, driven by contrasting communities that in turn are responses of environmental forcing, can be used to improve the parameterization of primary production models based on photo-physiology.

The first main question relates to the impacts of the community structure and their physiological responses on the fluorescence-derived photo-physiological parameters. In a spatial scale, the pigments composition strongly influenced the photo-physiology of natural communities throughout vertical mesoscale processes, once it represents the combined effects of phytoplankton biomass, taxonomy and acclimation processes, however highlighting for the contribution of photoacclimation-related pigments compared to the taxonomy diagnostic ones. In a temporal scale, the effects of the dominant size of the community could be quantified when nutrients were injected in a dynamic coastal environment. In this case, more than 90% of the variance in photo-physiology was explained by the community size when N:P ratios were above median values.

Although the knowledge on how dominant size fractions of phytoplankton vary in time and space are extremely useful tool to understand the overall dynamics of the pelagic environment, the bio-optical proxies of phytoplankton dominant cell size in the literature could not explain the variability of bulk efficiencies of photochemistry or light absorption, even in a given oceanographic region. In contrast, for a costal site, it was

possible to construct a primary production photo-physiological model in which the parameters depended upon the dominant size classes of natural phytoplankton communities, physically fractionated, and the ambient nutrient concentration. This suggests that either the bio-optical proxies used are not good descriptors of phytoplankton photochemistry or that the covariance among size, taxonomy and acclimation processes in the costal site sufficed for the parameterization based on size alone to be successful.

Secondly, the work approached the uncertainties in reconciling ETR and Carbon uptake measurements. We have also compared primary production values using ETR:Carbon conversion rates (K_C) from the literature with rates measured in two taxonomic groups, commonly found in our study region, under laboratorial controlled conditions, given the complexity of such measurements. Using rates from the literature, the calculated primary production values were similar to previous values for this region (using C^{14}), reinforcing the viability of this technique for obtaining primary production data in larger temporal and spatial scale. From cultures data, we have shown K_C rates for the two groups tested, which can improve such estimates for this and other coastal areas.

Finally, the study have analyzed the impacts of phytoplankton community structure, more especifically of cells size and taxonomy, on K_C and other physiological rates, under controlled growth conditions (same temperature, nutrients and light). For a balanced growth, differences between taxonomic groups were more significant than differences according to the respective cells size. Although the use of laboratory grown cells is essential to derive constants and rates that are extremely difficult to obtain in natural samples, such as the direct electron requirement for carbon assimilation, the results should be carefully utilized when compared to natural communities. We have

shown the importance of interactive effects of cell size and taxonomy in the energy allocation to assimilate the organic carbon and maintain the biomass, which is also crucial to better understand the dynamics of primary production rates derived from photo-physiology in natural environments.

REFERENCES

Álvarez, E., X. A. G. Morán, A. Lopez-Urrutia, E. Nogueira. 2016. Size-dependent photoacclimation of the phytoplankton community in temperate shelf waters (southern Bay of Biscay). Mar. Ecol. Prog. Ser. 543: 73-87.

Amaral, A. C. Z., A. E. Migotto, A. Turra, Y. Schaeffer-Novelli. 2010.Araçá: biodiversidade, impactos e ameaças. Biota Neotrop. 10(1): 219-264.

Aminot, A., and M. Chaussepied.1983. Manuel des analyses chimiques en milien marin. Brest: Centre National Pour L'exploitation Des Oceans (CNEXO).

Araujo, M. 2015. Estrutra das comunidades de fitoplâncton no Atlântico sul subtropical: variação espacial e relação com parâmetros ambientias. Master Thesis - Oceanography (Universidade Federal do Rio Grande, IO-FURG).

Arbones, B., F. G. Figueiras, M. Zapata. 1996. Determination of phytoplankton absorption coefficient in natural seawater samples: evidence of a unique equation to correct the pathlength amplification on glass-fiber filters. Mar. Eco.l Prog. Ser. 137: 293-304.

Barlow, R. G., J. Aiken, P. M. Holligan, D. G. Cummings, S. Maritorena, S. Hooker. 2002. Phytoplankton pigment and absorption characteristics along meridional transects in the Atlantic Ocean. Deep-Sea Res I 47: 637–660.

Behrenfeld, M.J and Z. S. Kolber. 1999. Widespread iron limitation of phytoplankton in the South Pacific Ocean. Science. 283: 840–843. doi:10.1126/science.283.5403.840

Behrenfeld, M. J., K. Worthington, R. M., Sherrell, F.P., Chavez, P. Strutton, M. McPhaden, D.M., Shea. 2006. Controls on tropical Pacific Ocean productivity revealed through nutrient stress diagnostics, Nature, 442: 1025–1028.

Bender, M., K. Grande, K. Johnson, J. Marra, P. J. L. Williams, J. Sieburth, M. Pilson, C. Langdon, G. Hitchcock, J. Orchardo, C. Hunt, P. Donaghay, and K. Heinemann. 1987. A comparison of four methods for determining planktonic community production. Limnol. Oceanog. 32:1085-1098.

Bender, M., J. Orchardo, M. Dickson, R. Barber, and S. Lindley. 1999. In vitro O_2 fluxes compared with ^{14}C production and other rate terms during the JGOFS Equatorial Pacific experiment. Deep-Sea Res. I. 46: 637-654.

Bibby, T. S., M. Y. Gorbunov, K.W. Wyman, P. G. Falkowski. 2008. Photosynthetic community responses to upwelling in mesoscale eddies in the subtropical North Atlantic and Pacific Oceans. Deep Sea Res. Part II: Top. Stud. Oceanogr. 55:1310-1320.

Boyd, P. W., J. Aiken, and Z. S. Kolber. 1997. Comparison of radiocarbon and fluorescence based (pump and probe) measurements of phytoplankton photosynthetic characteristics in the Northeast Atlantic Ocean. Mar. Ecol. Prog. Ser. 149: 215–226.

Bricaud, A., H. Claustre, J. Ras, K. Oubelkheir. 2004. Natural variability of phytoplanktonic absorption in oceanic waters: Influence of the size structure of algal populations. J. Geophys. Res. 109(C11010), doi:10.1029/2004JC002419.

Browning, T. J., H. A. Bouman, C. M. Moore, C. Schlosser, G. A. Tarran, E. M. S. Woodward, and G. M. Henderson. 2014. Nutrient regimes control phytoplankton ecophysiology in the South Atlantic. Biogeosciences 11: 463–479.

Campbell, D., V. Hurry, A. Clarke, P. Gustafsson, G. OQuist. 1998. Chlorophyll Fluorescence Analysis of Cyanobacterial Photosynthesis and Acclimation. Microbiology and molecular biology reviews. 62(3):667-683. 1092-2172/98/$04.0010

Castro, B.M.1990. Wind driven currents in the channel of São Sebastião: winter, 1979. Braz. J. Oceanogr.38(2):111–132.

Castro, B., L. B. Miranda, L. S. Silva, et al. 2008. *Processos Físicos: Hidrografia, Circulação e Transporte.* In: A.M.S. Pires-Vanin. (Org.). Oceanografia de um Ecossistema Subtropical: Plataforma de São Sebastião, SP. São Paulo: Editora da Universidade de São Paulo, p. 59-121.

Castro, B. M. 2014. Summer/winter stratification variability in the central part of the South Brazil Bight. Cont. Shelf Res. 89:15-23, doi:10.1016/j.csr.2013.12.002i.

Cerda, C., B. M. Castro. 2014. Hydrographic climatology of South Brazil Bight shelf waters between São Sebastião (24°S) and Cabo Sao Tome (22°S). Cont. Shelf Res. 89:5-14. doi:10.1016/j.csr.2013.11.003i.

Chaigneau, A., G. Eldin, and B. Dewitte. 2009. Eddy activity in the four major upwelling systems from satellite altimetry (1992-2007). Prog. Oceanogr. 83: 117–123.

Chisholm, S. W., S. L. Frankel, R. Goericke, R. J. Olson, B. Palenik, J. B. Waterbury, L. West-Johnsrud and E. R. Zettler. 1992. *Prochlorococcus marinus* nov. gen. nov. sp.: an oxyphototrophic marine prokaryote containing divinyl chlorophyll a and b. Archives of Microbiology 157: 297-300.

Ciotti, A. M., J. J. Cullen, and M. R. Lewis. 1999. A semi-analytical model of the influence of phytoplankton community structure on the relationship between light attenuation and ocean color. J. Geophys Res.: Oceans. 104: 1559-1578.

Ciotti, A. M., M. R. Lewis, and J. J. Cullen. 2002. Assessment of the relationships between dominant cell size in natural phytoplankton communities and the spectral shape of the absorption coefficient. Limnol. Oceanogr. 47:404–417.

Ciotti, A. M., M. Mahiques, O. Moller. 2014. The meridional gradients of the S-SE Brazilian continental shelf: Introduction to the special volume, Cont. Shelf. Res. 89:1-4, doi:10.1016/j.csr.2014.08.008.

Claustre, H. 1994. The trophic status of various oceanic provinces as revealed by phytoplankton pigment signatures, Limnol. Oceanogr. 39(5): 1206–1210.

Cleveland, J. S., and M. J. Perry. 1987. Quantum yield, relative specific absorption and fluorescence in nitrogen-limited Chaetoceros gracilis. Marine Biology 94: 489–497.

Cleveland, J. S., M. J.Perry, D. A. Kiefer, M. C. Talbot. 1989. Maximal quantum yield of photosynthesis in the northwestern Sargasso Sea. Journal of Marine Research, 47, 869-886.

Cleveland, J. S. and Weidemann, A. D. 1993. Quantifying absorption by aquatic particles: A multiple scattering correction for glass-fiber filters. Limnol. Oceanogr. 38(6): 1321-1327.

Corno, G., R. M. Letelier, M. R. Abbott. 2006. Assessing primary production variability in the North Pacific subtropical gyre: a comparison of Fast Repetition Rate Fluorometry and 14C measurements. J. Phycol. 42: 51-60.

Cullen J. J. 1982. The deep chlorophyll maximum: comparing vertical profiles of chlorophyll a. Can. J. Fish. Aquat. Sci. 39:791–803.

Cullen, J. J., P. J. S. Franks, D. M. Karl, and A. Longhurst. 2002. *Physical Influences on Marine Ecosystem Dynamics*. In: A.R. Robinson, J.J. McCarthy, and B.J. Rothschild [eds.], The Sea. p. 297–336.

Cullen, J. J. 2015. Subsurface Chlorophyll Maximum Layers: Enduring Enigma or Mystery Solved? Ann. Rev. Mar. Sci. 7: 207–239.

Eppley, R. W. 1980. Primary productivity in the sea. Nature. 286: 109–110.

Falkowski, P. G., Y. Fujita, A. Ley, and D. Mauzerall.1986. Evidence for cyclic electron flow around photosystem II in Chlorella pyrenoidosa. Plant. Physiol. 81:310-312.

Falkowski, P. G., R. M. Greene, R. J. Geider. 1992. Physiological limitations on phytoplankton productivity in the ocean. Oceanography. 5(2): 84-91.

Falkowski, P. G. 1994. The role of phytoplankton photosynthesis in global biogeochemical cycles. Photosynth. Res. 39: 235–258.

Falkowski, P. G. and J. A. Raven. 2007. Aquatic Photosynthesis. 2Ed. Princeton Ed. 488p.

Field, C. B., M. J. Behrenfeld, J. T. Randerson, P. Falkowski. 1998. Primary Production of the Biosphere: Integrating Terrestrial and Oceanic Components. Science 281: 237-240.

Finkel, Z. V. and A. J. Irwin. 2000. Modeling Size-dependent Photosynthesis: Light Absorption and the Allometric Rule. J. Theor. Biol. 204:361-369.

Finkel, Z. V. and A. J. Irwin. 2001. Light absorption by phytoplankton and the filter amplification correction: cell size and species effects. J. Exp. Mar. Biol. Ecol. 259: 51-61.

Finkel, Z. V., A. J. Irwin, O. Schofield. 2004. Resource limitation alters the 3/4 size scaling of metabolic rates in phytoplankton. Mar. Ecol. Prog. Ser., 273: 269–279.

Fishwick, J. R., J. Aiken, R. Barlow, H. Sessions, S. Bernard and J. Ras. 2006. Functional relationships and bio-optical properties derived from phytoplankton pigments, optical and photosynthetic parameters: a case study of the Benguela ecosystem. J. Mar. Biol. Assoc. UK.86(6):1267-1280.

Fitzwater, S. E., G. A. Knauer, and J. H. Martin. 1982. Metal contamination and its effect on primary production measurements. Limnol. Oceanogr. 27: 544–551.

Franklin D. J., C. J. Choi, C. Hughes, G. Malin, J.A., Berges. 2009. Effect of dead phytoplankton cells on the apparent efficiency of photosystem II. Mar. Ecol. Prog. Ser. 382: 35–40.

Fujiki, T., T. Suzue, H. Kimoto, T. Saino. 2007. Photosynthetic electron transport in Dunaliella tertiolecta (Chlorophyceae) measured by fast repetition rate fluorometry: relation to carbon assimilation. J. Plankton Res. 29(2): 199-208.

Gaeta, S. A.; D. S. Abe; S. M. Susini, R. M. Lopes; P. M. Metzler. 1990. Produtividade primária, plâncton e covariáveis ambientais no Canal de São Sebastião durante o outono. Rev. Brasil. Biol. 50(4): 963-974.

Gargett, A. E. &Marra, J. 2002. Effects of upper ocean physical processes - turbulence, advection, and air-sea interaction - on oceanic primary production. In: The Sea, Vol.12, ed. A. R. Robinson, J. J. McCarthy, and B. J. Rothschild, John Wiley & Sons, NY, 19-49.

Geider, R. J., R. M. Greene, Z. Kolber, H. L. MacIntyre, P. G. Falkowski. 1993. Fluorescence assessment of the maximum quantum efficiency of photosynthesis in the western North Atlantic. Deep-Sea Res. I, 40(6): 1205-1224.

Genty, B., J. M. Briantais, N. R. Baker. 1989. The relationship between the quantum yield of photosynthetic electron transport and quenching of chlorophyll fluorescence. Biochim. Biophys. Acta (BBA) - General Subjects. 990:87-92.

Gianesella, S. M. F, M. B. B. Kutner, S. M. Saldanha-Correa, M. Pompeu. 1999. Assessment of plankton community and environmental conditions in São Sebastião Channel prior to the construction of a produced water outfall. Rev. Bras. Oceanogr. 47(1):29-46.

Giannini, M. F. C. and A. M. Ciotti. 2016. Parameterization of natural phytoplankton photo-physiology: Effects of cell size and nutrient concentration. Limnol. Oceanogr. doi: 10.1002/lno.10317

Goericke, R. and J. P. Montoya. 1998. Estimating the contribution of microalgal taxa to chlorophyll a in the field-variations of pigment ratios under nutrient- and light-limited growth. Mar. Ecol. Prog. Ser. 169: 97-112.

Gorbunov, M. Y., and P. G. Falkowski. 2005. Fluorescence induction and relaxation (FIRE) technique and instrumentation for monitoring photosynthetic processes and primary production in aquatic ecosystems. International Society of Photosynthesis, 1029–1031.

Govindjee. 1995. Sixty-three years since Kautsky: chlorophyll a fluorescence. Australian Journal of Plant Physiology 22: 131-160.

Govindjee. 2004. *Chlorophyll a Fluorescence: A Bit of Basics and History*. In G. Papageorgiou and Govindjee (Eds) Chlorophyll a Fluorescence: A Signature of Photosynthesis. pp. 2-42 Springer, Dordrecht, The Netherlands.

Grande, K. D., P. J. L. Williams, J. Marra, D. A. Purdie, K. Heinemann, R. W. Eppley, and M. L. Bender. 1989. Primary production in the North Pacific gyre: a comparison of rates determined by the 14C, O2 concentration and 18O methods. Deep-Sea Res. 36: 1621–1634.

Greene, R. M., R. Geider, Z. Kolber, P.G. Falkowski. 1992; Iron-induced Changes in Light Harvesting and Photochemical Energy Conversion Processes in Eukaryotic Marine Algae. Plant. Physiol. 100:565-575. 0032-0889/92/100/0565/11/$01.00/0

Guillard, R. R. L., and J. H., Ryther. 1962. Studies of marine planktonic diatoms. I. Cyclotella nana Hustedt and Detonula confervacea (Cleve) Grun. Can. J. Microbiol. 8: 229–239.

Guiry, M. D. and G. M. Guiry. 2016. AlgaeBase. World-wide electronic publication, National University of Ireland, Galway. http://www.algaebase.org; searched on 22 September 2016.

Halsey, K. H, A. J. Milligan, M. J. Behrenfeld. 2010. Physiological optimization underlies growth rate-independent chlorophyll-specific gross and net primary production. Photosynth Res. 103:125–137.

Halsey, K. H., R. T., O'Malley, J. R., Graff, A. J., Milligan, M. J., Behrenfeld. 2013. A common partitioning strategy for photosynthetic products in evolutionarily distinct phytoplankton species. New Phytologist, 198: 1030–1038.

Halsey, K. H., J. R., Milligan, M. J., Behrenfeld. 2014. Contrasting Strategies of Photosynthetic Energy Utilization Drive Lifestyle Strategies in Ecologically Important Picoeukaryotes. Metabolites, 4: 260-280.

Hancke K., T. B. Hancke, L. M. Olsen, G. Johnsen, R. N. Glud. 2008. Temperature effects on microalgal photosynthesis-light responses measured by O2 production, pulse-amplitude-modulated fluorescence, and 14C assimilation. J. Phycol. 44: 501–514.

Hancke K., T. Dalsgaard, M. K. Sejr, S. Markager, R. N. Glud. 2015. Phytoplankton Productivity in an Arctic Fjord (West Greenland): Estimating Electron Requirements for Carbon Fixation and Oxygen Production. PLoS ONE 10(7): e0133275. doi:10.1371/journal.pone.0133275

Henriksen, P., B. Riemann, H., Kaas, H. M. Sorensen and H. L. Sorensen. 2002. Effects of nutrient-limitation and irradiance on marine phytoplankton pigments. J. Plankton Res., 24(9): 835-858.

Heukelen, L. V. and S. B. Hooker. 2011. The importance of a quality assurance plan for method validation and minimizing uncertainties in the HPLC analysis of phytoplankton pigments. In: Roy S. et al. Phytoplankton pigments:

characterization, chemotaxonomy, and applications in oceanography. p.845. Cambridge Uni Press, New York.

Holeton, C. L., F. Nédélec, R. Sanders, L. Brown, C. M. Moore, D. P. Stevens, K. J. Heywood, P. J. Statham, and C. H. Lucas. 2005. Physiological state of phytoplankton communities in the Southwest Atlantic sector of the Southern Ocean, as measured by fast repetition rate fluorometry. Polar Biol. 29: 44–52.

Hoppe, C. J. M., L. Holtz, S. Trimborn, B. Rost. 2015. Ocean acidification decreases the light-use efficiency in an Antarctic diatom under dynamic but not constant light. New Phytologist. 207: 159–171.

Huang, S., S. W. Steven, H. R. Harvey, K. Taylor, N. Jiao, F. Chen. 2012. Novel lineages of *Prochlorococcus* and *Synechococcus* in the global oceans. The ISME Journal, 6: 285-297.

Huete-Ortega, M., A. Calvo-Díaz, R. Graña, B. Mouriño-Carballido, E. Marañón. 2011. Effect of environmental forcing on the biomass, production and growth rate of size-fractionated phytoplankton in the central Atlantic Ocean. J. Marine Syst. 88:203-213.

Hughes, D. J. et al. 2015. Nitrogen availability drives variability of the electron requirement for carbon fixation in coastal phytoplankton communities. Keynote and Oral Papers, European Journal of Phycology, 50:sup1:22-120, DOI: 10.1080/09670262.2015.1069489

Huot, Y., M. Babin, F. Bruyant, C. Grob, M. S. Twardowski, et al. 2007a. Relationship between photosynthetic parameters and different proxies of phytoplankton biomass in the subtropical ocean. Biogeosciences, European Geosciences Union, 4(5):853-868.

Huot, Y., M. Babin, F. Bruyant, C. Grob, M. S. Twardowski, et al. 2007b. Does chlorophyll a provide the best index of phytoplankton biomass for primary productivity studies? Biogeosciences Discussions, European Geosciences Union, 4(2): 707-745.

Huot, Y. and M. Babin. 2010. *Overview of Fluorescence Protocols: Theory, Basic Concepts, and Practice*. In: Suggett, D.J., Prasil, O., and Borowitzka, M.A. (Eds). Chlorophyll-a Fluorescence in Aquatic Sciences: Methods and Applications. Springer, New York, 323p.

Irwin, A. J., Finkel, Z. V., Schofield, O. M. and Falkowski, P. G. 2006. Scaling-up from nutrient physiology to the size-structure of phytoplankton communities. J. Plankton Res. 28(5): 459-471.

Jassby, A. D., T. Platt. 1976. Mathematical formulation of the relationship between photosynthesis and light for phytoplankton. Limnol. Oceanogr. 21: 540-547.

Jeffrey, S. W. 1974. Profiles of Photosynthetic Pigments in the Ocean Using Thin-Layer Chromatography. Marine Biology, 26: 101-110.

Jeffrey, S. W, S. W. Wright and M, Zapata. 2011. *Microalgal classes and their signature pigments.* In: Roy S. et al. Phytoplankton pigments: characterization, chemotaxonomy, and applications in oceanography. p.845. Cambridge Uni Press, New York.

Key, T., A. McCarthy, D. A. Campbell, C. Six., S. Roy, Z. V. Finkel. 2010. Cell size trade-offs govern light exploitation strategies in marine phytoplankton. Environmental Microbiology. 12(1): 95–104.

Khatiwala, F. Primeau and T. Hall. 2009. Reconstruction of the history of anthropogenic CO2 concentrations in the ocean, Nature, 462.

Kiefer, D. A. and Mitchell, B. G. 1983. A simple, steady state description of phytoplankton growth based on absorption cross section and quantum efficiency. Limnol. Oceanogr. 28(4): 770-776.

Kiefer, D. A and R. A. Reynolds, 1992. *Advances in understanding phytoplankton fluorescence*. In: Falkowski P. G. and A. D. Woodhead (Eds). In: Primary Productivity and Biogeochemical Cycles in the Sea. Plenum Press, New York, 550p.

Kirk, J. T. O. 1994. Light and Photosynthesis in Aquatic Ecosystems. Cambridge University Press. 509p.

Kolber, Z. J. Zehr, P. Falkowski. 1988. Effects of Growth Irradiance and Nitrogen Limitation on Photosynthetic Energy Conversion in Photosystem II. Plant Physiol. 88:923-929.

Kolber, Z., and P. G. Falkowski. 1993. Use of active fluorescence to estimate phytoplankton photosynthesis in situ. Limnol. Oceanogr. 38: 1646-1665.

Kolber, Z. S., O. Prasil, P. G. Falkowski. 1998. Measurements of variable chlorophyll fluorescence using fast repetition rate techniques: defining methodology and experimental protocols. Biochimica et Biophysica Acta 1367: 88-106.

Kromkamp, J. C. and R. M. Forster. 2003. The use of variable fluorescence measurements in aquatic ecosystems: differences between multiple and single turnover measuring protocols and suggested terminology. Eur. J. Phycol. 38:103–112.

Lamont, T., R. G. Barlow, M. S. Kyewalyanga. 2014. Physical drivers of phytoplankton production in the southern Benguela upwelling system. Deep Sea Res. I, 90:1-16.

Lawrenz E., G. Silsbe, E. Capuzzo et al. 2013. Predicting the Electron Requirement for Carbon Fixation in Seas and Oceans. PLoSONE 8(3): e58137.

Laws, E. A. 1991.Photosynthetic quotients, new production and net community production in the open ocean. Deep-Sea Res. 138: 143–167.

Lazar, D. 1999. Chlorophyll a fluorescence induction. Biochimica et Biophysica Acta 1412:1-28.

Lencina-Avila, J. M., R. G. Ito, C. A. E. Garcia, V. M. Tavano. Sea-air carbon dioxide fluxes along 35°S in the South Atlantic Ocean. Submitted to Deep-Sea Res.

Lin, H., F. I. Kuzminov, J. Park, S. Lee, P. G. Falkowski, and M. Y. Gorbunov. 2016. The fate of photons absorbed by phytoplankton in the global ocean. Science. 351: 264–267.

Lohr, M. 2011. *Carotenoid metabolism in phytoplankton*. In: Roy S. et al. Phytoplankton pigments: characterization, chemotaxonomy, and applications in oceanography. p.845. Cambridge Uni Press, New York.

Long, S. P., S. Humpries, P.G. Falkowski. 1994. Photoinhibition of photosynthesis in nature. Annu. Rev. Plant Physial. Plant Mol. BioI. 45: 633-62

Longhurst, A., S. Sathyendranath, T. Platt, and C. Caverhill. 1995. An estimate of global primary production in the ocean from satellite radiometer data. J. Plankton Res. 17: 1245–1271.

Longhurst, A. 1998. Ecological Geography of the Sea. Elsevier Academic Press. p. 542.

López-Sandoval, D. C., T. Rodríguez-Ramos, P. Cermeño, C. Sobrino, E. Marañon. 2014. Photosynthesis and respiration in marine phytoplankton: Relationship with cell size, taxonomic affiliation, and growth phase. J. Exper. Mar. Biol. Ecol. 457: 151–159.

Lorenzen, C. J. 1966. A method for the continuous measurement of in vivo chlorophyll concentration. Deep Sea Res. Oceanogr. Abstr. 13: 223–227.

McClain, C. R., S. R. Signorini, and J.R. Christian. 2004. Subtropical gyre variability observed by ocean color, Deep-Sea Res. Part II , 51: 281-301.

MacIntyre, H. L., T. M. Kana, T. Anning, R. J. Geider. 2002. Photoacclimation of photosynthesis irradiance response curves and photosynthetic pigments in microalgae and cyanobacteria. J. Phycol. 38: 17–38.

Macintyre, H. L. and J. J. Cullen. 2005. Using Cultures to Investigate the Physiological Ecology of Microalgae. In: Andersen, R.A. Algal culturing techniques. Elsevier Acadmeic Press, Osford, UK, p. 578.

Mackey, M. D., Mackey, D. J., Higgins, H. W., Wright, S. W., 1996. CHEMTAX- a program for estimating class abundances from chemical markers: application to HPLC measurements of phytoplankton. Marine Ecology Progress Series 144, 265–283.

Marañón, E. 2015. Cell Size as a Key Determinant of Phytoplankton Metabolism and Community Structure. Annu. Rev. Mar. Sci. 7: 4.1–4.24. doi: 10.1146/annurev-marine-010814-015955.

Maranon, E. and Holligan, P. M. 1999. Photosynthetic parameters of phytoplankton from 50°N to 50°S in the Atlantic Ocean. Mar. Ecol. Pro. Ser. 176: 191-203.

Marra, J. 2002. *Approaches to the Measurement of Plankton Production*. In: Williams, P. J., Thomas, D. N., Reynolds, C.S. (Eds). Phytoplankton Productivity - Carbon Assimilation in Marine and Freshwater Ecosystems. Blackwell Science. p. 386.

Maxwell, K. & Johnson, G. N. 2000. Chlorophyll fluorescence: a pratical guide. Journal of Experimental Botany, 51: 659-668.

McGillicuddy, D. J., L. A. Anderson, N. R. Bates, T. Bibby, K. O. Buesseler, C. A. Carlson, C. S. Davis, C. Ewart, P. G. Falkowski, S. A. Goldthwait, D. A. Hansell, W. J. Jenkins, R. Johnson, V. K. Kosnyrev, J. R. Ledwell, Q. P. Li, D. A. Siegel,

and D. K. Steinberg. 2007. Eddy/Wind Interactions Stimulate Extraordinary Mid-Ocean Plankton Blooms. Science. 316: 1021–1026.

Mendes, C. R., P. Cartaxana, and V. Brotas. 2007. HPLC determination of phytoplankton and microphytobenthos pigments: comparing resolution and sensitivity of a C 18 and a C 8 method. Limnol. Oceanogr. Methods 5: 363–370.

Moore, C. M. et al. 2003. Physical controls on phytoplankton physiology and production at a shelf sea front: A fast repetition-rate fluorometer based field study. Mar. Ecol. Pro. Ser. 259: 29–45.

Moore, C. M., M. I. Lucas, R. Sanders, R. Davidson. 2005. Basin-scale variability of phytoplankton bio-optical characteristics in relation to bloom state and community structure in the Northeast Atlantic. Deep-Sea Res. I. 52: 401–419.

Moore, C. M., D. J. Suggett, A. E. Hickman, Y.-N. Kim, J. F. Tweddle, J. Sharples, R. J. Geider, and P. M. Holligan. 2006. Phytoplankton photoacclimation and photoadaptation in response to environmental gradients in a shelf sea. Limnol. Oceanogr. 51: 936–949.

Moore, C. M. et al 2008.Relative influence of nitrogen and phosphorus availability on phytoplankton physiology and productivity in the oligotrophic sub-tropical North Atlantic Ocean. Limnol. Oceanogr. 53(1):291-305.

Morel, A. and A. Bricaud. 1981. Theoretical results concerning the optics of phytoplankton, with special reference to remote sensing application. Oceanography from Space, 313-327.

Nixon, P. J. 2000. Chlororespiration. Philos. Trans. R. Soc. London Ser. B 355:1541–47

Omand, M. M., E. A. D'Asaro, C. M. Lee, M. J. Perry, N. Briggs, I. Cetinić, and A. Mahadevan. 2015. Eddy-driven subduction exports particulate organic carbon from the spring bloom. Science. 348: 222–225.

O'Reilly, J. E., S. Maritorena, B. G. Mitchell, D. A. Siegel, K. L. Carder, S. a. Garver, M. Kahru, and C. McClain. 1998. Ocean color chlorophyll algorithms for SeaWiFS. J. Geophys. Res. 103: 24937

Oxborough, K. and N. R. Baker. 2000. An evaluation of the potential triggers of photoinactivation of photosystem II in the context of a Stern–Volmer model for downregulation and the reversible radical pair equilibrium model. Phil. Trans. R. Soc. Lond. B. 355: 1489-1498.

Oxborough, K. et al. 2012. Direct estimation of functional PSII reaction center concentration and PSII electron flux on a volume basis: a new approach to the analysis of Fast Repetition Rate fluorometry (FRRf) data. Limnol. Oceanogr.: Methods. 10:142-154.

Papageorgiou, G. C. and Govindjee. 2004. Chlorophyll-a Fluorescence: A signature of Photosynthesis. Springer, Dordrecht, The Netherlands.

Parkhill, J., G. Maillet, J. J. Cullen. 2001. Fluorescence-based maximal quantum yield for PSII as a diagnostic of nutrient stress. J. Phycol. 37:517-529.

Partenski, F., J. La Roche, K. Wyman, P, Falkowski. 1997. The divinyl-chlorophyll a/b-protein complexes of two strains of the oxyphototrophic marine prokaryote Prochlorococcus – characterization and response to changes in growth irradiance. Photosynthesis Res. 51: 209–222.

Partenski, F., W. R. Hess, D. Vaulot. 1999. Prochlorococcus, a Marine Photosynthetic Prokaryote of Global Significance. Microbiology and Molecular Biology Reviews, p. 106-127.

Peltier, G. and L. Cournac. 2002. Chlororespiration. Annu. Rev. Plant Biol. 53:523–50. 10.1146/annurev.arplant.53.100301.135242

Peres, A. L. F. 2013. Efeito de diferentes massas de água nas classes de tamanho da biomassa fitoplanctônica na região de desembocadura da baía do Araçá (Canal de São Sebastião - SP) durante o verão e inverno de 2012. Master Thesis - Oceanography (Faculdade de Filosofia Ciências e Letras de Ribeirão Preto- USP).

Peterson, R. G. and L. Stramma. 1991. Upper-level circulation in the South Atlantic Ocean. Prog. Oceanogr., 26: 1–73.

Prasil O., Z. Kolber, J. A. Berry, P. G. Falkowski. 1996. Cyclic electron flow around Photosystem II in vivo. Photosynthesis Res. 48: 395-410.

Ralph, P. J., C. Wilhelm, J. Lavaud, T. Jakob, K. Petrou, and O. Prasil. 2010. Fluorescence as a Tool to Understand Changes in Photosynthetic Eletron Flow Regulation. In: Suggett, D.J., Prasil, O., and Borowitzka, M.A. (Eds). Chlorophyll-a Fluorescence in Aquatic Sciences: Methods and Applications. Springer, New York, 323p.

Rattan, K. J., W. D. Taylor, R. E. H. Smith. 2012. Nutrient status of phytoplankton across a trophic gradient in Lake Erie: evidence from new fluorescence methods. Can. J. Fish.Aquat. Sci. 111:94-111.

Regaudie-de-Gioux, A., S. Lasternas, S. Agusti, C. M. Duarte. 2014. Comparing marine primary production estimates through different methods and development of conversion equations. Frontiers in Marine Science, 1: 1-14. DOI: 10.3389/fmars.2014.00019.

Roessler, C. S. 1998. Theoretical and experimental approaches to improve the accuracy of particulate absorption coefficients derived from the quantitative filter technique. Limnol. Oceanogr. 43(7): 1649-1660.

Ryther, J. H. 1956. The Measurement of Primary Production. Limnology and Oceanography 1: 72–84.

Saba, V. S., M. A. M. Friedrichs, D. Antoine, R. A. Armstrong, I. Asanuma, M. J. Behrenfeld, A. M. Ciotti, M. Dowell, N. Hoepffner, K. J. W. Hyde, J. Ishizaka, T. Kameda, J. Marra, F. Mélin, A. Morel, J. O'Reilly, M. Scardi, W. O. Smith, T. J. Smyth, S. Tang, J. Uitz, K. Waters, and T. K. Westberry. 2011. An evaluation of ocean color model estimates of marine primary productivity in coastal and pelagic regions across the globe. Biogeosciences 8: 489–503.

Saldanha-Correa, F. P. 1993. Simulação da mistura vertical de massas de água da região de Ubatuba (SP): Efeitos sobre a produção primaária e biomassa fitoplantônica. Master Thesis–BiologicalOceanography (OceanographyInstitute- Univerisdade de São Paulo - USP).

Saldanha-Corrêa, F. M., and S. M. F. Gianesella, 2008. *Produção primária e fitoplâncton*. In: A.M.S. Pires-Vanin. (Org.). Oceanografia de um Ecossitema Subtropical: Plataforma de São Sebastião. 1st ed. São Paulo: Editora da Universidade de São Paulo- EDUSP, v. 1, p. 223-251.

Shoaf, W. T. and B. W. Lium, 1976: Improved extraction of chlorophyll a and b from algae using dimethyl sulfoxide. Limnol. Oceanogr. 21: 926-928.

Sieburth, J. M.,V. Smetacek, J. Lens. 1978. Pelagic ecosystem structure: Heterotrophic compartments of the plankton and their relationships to plankton size fractions. Limnol. Oceanogr. 23(6):1256-1263.

Silio-Calzada, A., A. Bricaud, J. uitz, B. Gentili. 2008. Estimation of new primary production in the Benguela upwelling area, using ENVISAT satellite data and a model dependent on the phytoplankton community size structure. J. Geophys. Res. 113: C11023.

Silsbe, G. M. and Kromkamp, J. C. 2012. Modeling the irradiance dependency of the quantum efficiency of photosynthesis. Limnol. Oceanogr.: Methods.10: 645-652.

Steemann-Nielsen E. 1952. The use of radio-active carbon (14C) for measuring organic production in the sea. Journal du Conseil International pour Exploration de la Mer, 18, 117–140.

Steglich, C., C. W. Mullineaux, K. Teuchner, W. R., Hess, H. Lokstein. 2003. Photophysical properties of Prochlorococcus marinus SS120 divinyl chlorophylls and phycoerythrin in vitro and in vivo. FEBS Letters, 553: 79-84.

Suggett, D. J. et al. 2003. Fast repetition rate and pulse amplitude modulation chlorophyll a fluorescence measurements for assessment of photosynthetic electron transport in marine phytoplankton. Europ. J. Phycol. 38: 371-384.

Suggett, D. J., H. L. MacIntyre, R. J. Geider. 2004. Evaluation of biophysical and optical determinations of light absorption by photosystem II in phytoplankton. Limnol. Oceanogr.: Methods. 2:316-332.

Suggett, D. J., C. M. Moore, E. Maranon, C. Omachi, R. A. Varela, J. Aiken, and P. M. Holligan. 2006. Photosynthetic electron turnover in the tropical and subtropical Atlantic Ocean. Deep Sea Research Part II: Topical Studies in Oceanography 53: 1573–1592.

Suggett, D. J., C. Moore, A. Hickman, R. Geider. 2009a. Interpretation of fast repetition rate (FRR) fluorescence: signatures of phytoplankton community structure versus physiological state. Mar. Ecol. Prog. Ser. 376: 1-19.

Suggett, D. J. et al. 2009b. Comparing electron transport with gas exchange: parameterising exchange rates between alternative photosynthetic currencies for eukaryotic phytoplankton. Aquat. Microb. Ecol.56:147–162.

Suggett, D. J., C. M. Moore, R. J. Geider. 2010. *Estimating Aquatic Productivity from Active Fluorescence Measurements*. In: Suggett, D.J., Prasil, O., and Borowitzka,

M.A. (Eds). Chlorophyll-a Fluorescence in Aquatic Sciences: Methods and Applications. Springer, New York, 323p.

Sun, J. and D. Liu. 2003. Geometric models for calculating cell biovolume and surface area for phytoplankton. J. Plankton Res. 25(11): 1331-1346.

Tassan, S., and G. M. Ferrari. 1998. Measurement of light absorption by aquatic particles retained on filters: determination of the optical pathlength amplification by the "transmittance-reflectance" method. Journal of Plankton Research 20: 1699–1709.

Takahashi, T., S. C. Sutherland, R. Wanninkhof, C. Sweeney, R. A. Feely, D. W. Chipman, B. Hales,G. Friederich, F. Chavez, C. Sabine, and others. 2009. Climatological mean and decadal change in surface ocean pCO2, and net sea-air CO2 flux over the global oceans. Deep-Sea Res. II 56(8–10): 554–577.

Thimijan, R. W. and Heins, R. D. 1983. Photometric, Radiometric and Quantum Light Units of Measure: a review of procedures for interconversion. Reprinted from Hortscience.18(6).

Tilstone, G., S. Timothy, A. Poulton, R. Hutson. 2009. Measured and remotely sensed estimates of primary production in the Atlantic Ocean from 1998 to 2005. Deep-Sea Res. II. 56: 918–930.

Uitz, J., H. Claustre, A. Morel and S. B. Hooker. 2006. Vertical distribution of phytoplankton communities in open ocean: An assessment based on surface chlorophyll. J. Geophys. Res. 111: C08005, doi:10.1029/2005JC003207.

Veldhuis, M., G., Kraay and K. Timmermans. 2001. Cell death in phytoplankton: correlation between changes in membrane permeability, photosynthetic activity, pigmentation and growth. European Journal of Phycology, 36:2, 167-177.

Vidussi, F., H. Claustre, B. B. Manca, A. Luchetta, and J. C. Marty. 2001. Phytoplankton pigment distribution in relation to upper thermocline circulation in the eastern Mediterranean Sea during winter, J. Geophys. Res., 106(C9): 19,939–19,956.

Wagner, H., Jakob, T. and Wilhelm, C. 2006. Balancing the energy flow from captured light to biomass under fluctuating light conditions. New Phytologist, 169:95-108.

Webb, W. L., M. Newton and D. Starr. 1974. Carbon Dioxide Exchange of Alnusrubra: A Mathematical. Oecologia. 17(4):281-291.

Welschmeyer, N. A. 1994. Analysis of chlorophyll a in the presence of chlorophyll b and pheopigments. Limnol. Oceanogr. 39: 1985-1992.

Williams, P. J., and N. W. Jenkinson. 1982. A transportable microprocessor-controlled precise Winkler titration suitable for field station and shipboard use. Limnol. Oceanogr. 27: 576–584.

Williams, P. J. B., D. N. Thomas, and C. S. Reynolds. 2002. Phytoplankton Productivity - Carbon Assimilation in Marine and Freshwater Ecosystems, P.J. le B. Williams, D.N. Thomas, and C.S. Reynolds [eds.]. Blackwell Science Ltd.

Wood, A. M., Everroad, R.C. and Wingard, L.M. 2005. *Measuring Growth Rates in Microalgal Cultures*. In: Andersen, R.A. Algal Culturing Techniques, Elsevier Academic Press. p. 578.

Wright, S. W. and S. W. Jeffrey. 2006. *Pigment markers for phytoplankton production.* In: Volkmann, J.K. (Ed.), Marine Organic Matter: Biomarkers, Isotopes and DNA. Spring-Verlag, Berlin, pp. 71–104.

Wright, S. W., R. L. Van den enden, I. Pearce, A. T. Davidson, F. J. Scott, K. J. Westwood. 2010. Phytoplankton community structure and stocks in the Southern Ocean (30–80°E) determined by CHEMTAX analysis of HPLC pigment signatures. Deep Sea Res II, 57: 758–778.

Wu, Y., J. Jeans, D. J. Suggett, Z. V. Finkel, D. A., Campbell. Large centric diatoms allocate more cellular nitrogen to photosynthesis to counters lower RUBISCO turnover rates. Front. Mar. Sci. 1(68):1-11.

Zapata, M., F. Rodríguez, and J. Garrido. 2000. Separation of chlorophylls and carotenoids from marine phytoplankton: a new HPLC method using a reversed phase C8 column and pyridine-containing mobile phases. Mar. Ecol. Prog. Ser. 195: 29–45.